

# Selenium Nanoparticles for Biomedical Applications: From Development and Characterization to Therapeutics

Cláudio Ferro, Helena F. Florindo,\* and Hélder A. Santos\*

**Selenium (Se) is an essential element to human health that can be obtained in nature through several sources. In the human body, it is incorporated into selenocysteine, an amino acid used to synthesize several selenoproteins, which have an active center usually dependent on the presence of Se. Although Se shows several beneficial properties in human health, it has also a narrow therapeutic window, and therefore the excessive intake of inorganic and organic Se-based compounds often leads to toxicity. Nanoparticles based on Se (SeNPs) are less toxic than inorganic and organic Se. They are both biocompatible and capable of effectively delivering combinations of payloads to specific cells following their functionalization with active targeting ligands. Herein, the main origin of Se intake, its role on the human body, and its primary biomedical applications are revised. Particular focus will be given to the main therapeutic targets that are explored for SeNPs in cancer therapies, discussing the different functionalization methodologies used to improve SeNPs stability, while enabling the extensive delivery of drug-loaded SeNP to tumor sites, thus avoiding off-target effects.**

selenoproteins, whose function often depends on the presence of Se in their active site,<sup>[5]</sup> such as reactive oxygen species (ROS) protection.<sup>[5,6]</sup> As a result, both Se deficiency and excess can lead to toxicity in humans,<sup>[7,8]</sup> being correlated with cardiovascular and inflammatory diseases, immunodeficiency and brain disorders,<sup>[9,10]</sup> type 2 diabetes,<sup>[11]</sup> fertility/reproduction complications,<sup>[7,9]</sup> thyroid autoimmune diseases, and cancer.<sup>[7,12]</sup>

Tumor cells seem to be more susceptible to the pro-oxidant and potential cytotoxic effects induced by high doses of Se. However, Se-based therapeutic compounds have a narrow therapeutic window, and therefore, have been mostly used against aggressive late-stage cancers.<sup>[5,13]</sup>

Se nanoparticles (SeNPs) present lower toxicity and higher biocompatibility than organic or inorganic Se compounds,

attracting the attention of the scientific community for their application as therapeutic and theranostic agents.<sup>[5,14–16]</sup> Herein, SeNPs are described as nanomaterials that have a main inorganic therapeutic core consisting of Se (0), that can be stabilized/functionalized with specific compounds or loaded with active drugs.<sup>[13]</sup> SeNPs led to the production of higher levels of ROS than those obtained following the treatment of cancer cells with selenite, therefore presenting better antitumor properties than the Se salts.<sup>[5,17]</sup> In addition, SeNPs present versatile physical properties, such as the possibility of forming different shapes depending on the chemicals or solvents used for their preparation.<sup>[18,19]</sup>

The methods most frequently employed for SeNP synthesis include the use of chemical agents and biological organisms (both plants, fungi, or bacteria) to reduce oxidized forms of Se to its elemental form, biosynthesis or green synthesis, in addition to physical approaches, such as pulsed laser ablation (PLA).<sup>[16,20]</sup> However, bare SeNPs chemically synthesized are highly unstable, aggregating, and precipitating in aqueous solutions, which translates into their lower bioactivity.<sup>[21–23]</sup> Several approaches have been explored for decorating and/or functionalizing SeNPs in order to improve formulation stability and targeted therapeutic effect. Several substances have been used to modify SeNP surface, such as amino acids,<sup>[23]</sup> peptides<sup>[24]</sup> and proteins,<sup>[25]</sup> chitosan and other polysaccharides,<sup>[21,26–28]</sup> folic acid (FA),<sup>[29,30]</sup> and hyaluronic acid (HA),<sup>[29,30]</sup> among others<sup>[13,31]</sup> discussed in more detail in the next sections of this review.

SeNPs have been studied for the treatment of several diseases, such as diabetes, Alzheimer's disease (AD)<sup>[32]</sup> and inflammation-related diseases,<sup>[13]</sup> such as rheumatoid arthritis.<sup>[33]</sup> Additionally,


## 1. Introduction

Selenium (Se), initially discovered by Jons Jacob Berzelius, is a chemical element essential to human health.<sup>[1–3]</sup> The twenty-first amino acid, selenocysteine (Sec),<sup>[4]</sup> is used to produce

C. Ferro, Prof. H. A. Santos  
Drug Research Program  
Division of Pharmaceutical Chemistry and Technology  
Faculty of Pharmacy  
University of Helsinki  
Helsinki FI-00014, Finland  
E-mail: helder.santos@helsinki.fi

C. Ferro, Prof. H. F. Florindo  
Research Institute for Medicines  
iMed.Ulisboa  
Faculty of Pharmacy  
Universidade de Lisboa  
Lisbon 1649-003, Portugal  
E-mail: hflorindo@ff.ulisboa.pt

Prof. H. A. Santos  
Helsinki Institute of Life Science (HiLIFE)  
University of Helsinki  
Helsinki FI-00014, Finland

 The ORCID identification number(s) for the author(s) of this article can be found under <https://doi.org/10.1002/adhm.202100598>

© 2021 The Authors. Advanced Healthcare Materials published by Wiley-VCH GmbH. This is an open access article under the terms of the Creative Commons Attribution License, which permits use, distribution and reproduction in any medium, provided the original work is properly cited.

DOI: 10.1002/adhm.202100598

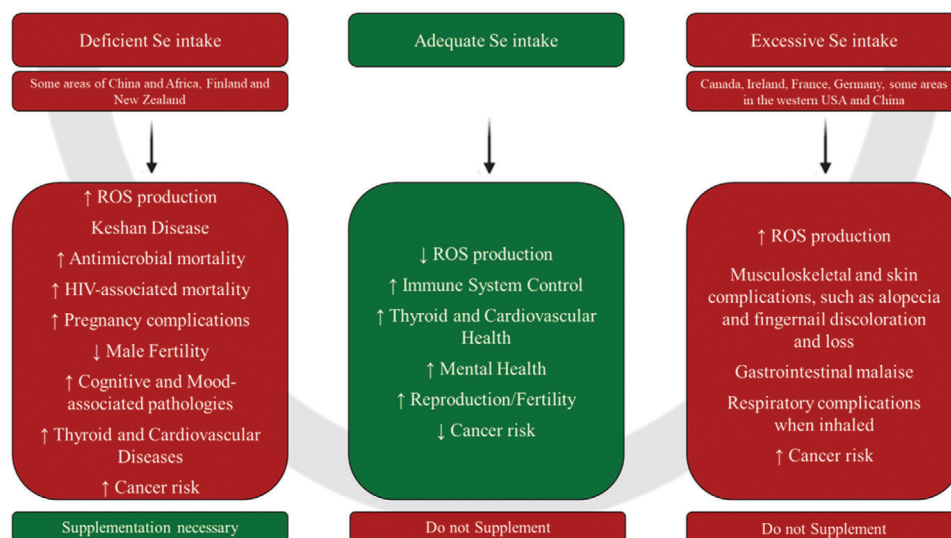


**Figure 1.** U-shaped relationship between Se levels and human health. Adapted with permission.<sup>[7]</sup> Copyright 2020, SpringerLink.

they are being explored as a protector against potential toxic agents, such as chromium, cadmium, and chemotherapeutic agents, which side effects can be very harmful.<sup>[13]</sup> Also, by triggering ROS overproduction, SeNPs induce caspase-3 activation and the PARP cleavage, thereby leading to mitochondria-mediated apoptosis.<sup>[34–36]</sup>

SeNPs have shown an increasing potential as major therapeutic platforms, especially in anticancer therapy,<sup>[13]</sup> including in combination with well-known chemotherapeutic agents like 5-Fluorouracil (5-Fu),<sup>[13,37]</sup> doxorubicin (DOX)<sup>[38]</sup> and irinotecan,<sup>[39]</sup> as well as with oligonucleotides like small interfering RNA (siRNA),<sup>[31,40]</sup> exhibiting synergistic anticancer activity and overcoming multidrug resistance.<sup>[13,41]</sup>

The main aim of this review is to present and discuss in detail the effect of Se function in human body, and the current methodologies used for SeNPs production, physical and antioxidant properties highlighting the advantages of these nanocarriers compared to Se compounds. We further address the main mechanisms behind the SeNPs major therapeutic applications, with special focus toward cancer therapy.

## 2. Selenium Compounds and Their Physiological Effects

Se is essential for human health, being involved in several physiological functions (**Figure 1**), such as modulation of immune system activity and ROS control. Therefore, the Se daily intake should be monitored.<sup>[2,42]</sup> The recommended daily allowance (RDA) is 60 µg/day for women, 70 µg d<sup>-1</sup> for men,<sup>[3]</sup> 75 µg d<sup>-1</sup> for lactating women, and 65 µg d<sup>-1</sup> for pregnant women according to the European Food Safety Authority.<sup>[43,44]</sup> Approximately 20 µg d<sup>-1</sup> is the minimum quantity of Se required to prevent a dilated cardiomyopathy, i.e., Keshan disease in adults,<sup>[3]</sup> and its tolerable upper intake level for adults is set at 400 µg d<sup>-1</sup>,<sup>[42,45]</sup> being pro-oxidant and cytotoxic at higher doses.<sup>[5]</sup>

The main form of Se in human diets is selenomethionine (SeMet), the Se analog of the amino acid methionine.<sup>[4,46]</sup> Once

ingested, SeMet is absorbed and enters the methionine pool in the body.<sup>[4,42]</sup> Inorganic Se, especially selenite and selenate, is usually used for Se supplementation.<sup>[4]</sup> Once in the human body, Se is mostly used for the production of selenoproteins, which are essential to human health due to their antioxidant effect, and role in controlling thyroid hormone metabolism, protein folding, redox signaling, among other functions.<sup>[43]</sup>

Se has demonstrated antitumor, antiviral, antibacterial, and antifungal properties,<sup>[3]</sup> decreasing the risk of tuberculosis in HIV infected patients,<sup>[7,47]</sup> and is well correlated to cancer prevention.<sup>[7,11]</sup> In addition, Se has been demonstrated to affect neurological, thyroid, and cardiovascular function.<sup>[10,43]</sup> Also, adequate Se intake plays an important role in the immune system, by increasing T-cell proliferation and NK cell activity against pathogens and cancer cells, and enhancing vaccine efficacy,<sup>[47]</sup> while reducing the risk of diseases related to severe and chronic inflammation, such as rheumatoid arthritis.<sup>[47,48]</sup> Se has shown to protect against heavy metals and radiation toxicity<sup>[49,50]</sup> and alcoholism-induced cirrhosis,<sup>[10]</sup> since it enhances DNA stability and stabilizes ROS production, as well as decreases the hepatic and renal side effects of the chemotherapeutic drugs, cisplatin, and cyclophosphamide.<sup>[2]</sup>

### 2.1. Selenium Bioavailability, Metabolism, and Physiological Functions

Se bioavailability depends on the food ingested,<sup>[12,42]</sup> being higher in animal products than in vegetables. Se content in fish is also elevated, although it can be highly influenced by its source and animal species, as well as by the presence of heavy metal contaminants, such as mercury, which bind to Se to form insoluble inorganic molecules.<sup>[42]</sup> SeMet is present in both plants and animals, while selenocysteine mainly exists in animal products.<sup>[4]</sup> SeMet more efficiently enhance Se status, since it is directly integrated into proteins, even though it is necessary for its decomposition into an inorganic precursor to enter the Se pool.<sup>[4,9]</sup>

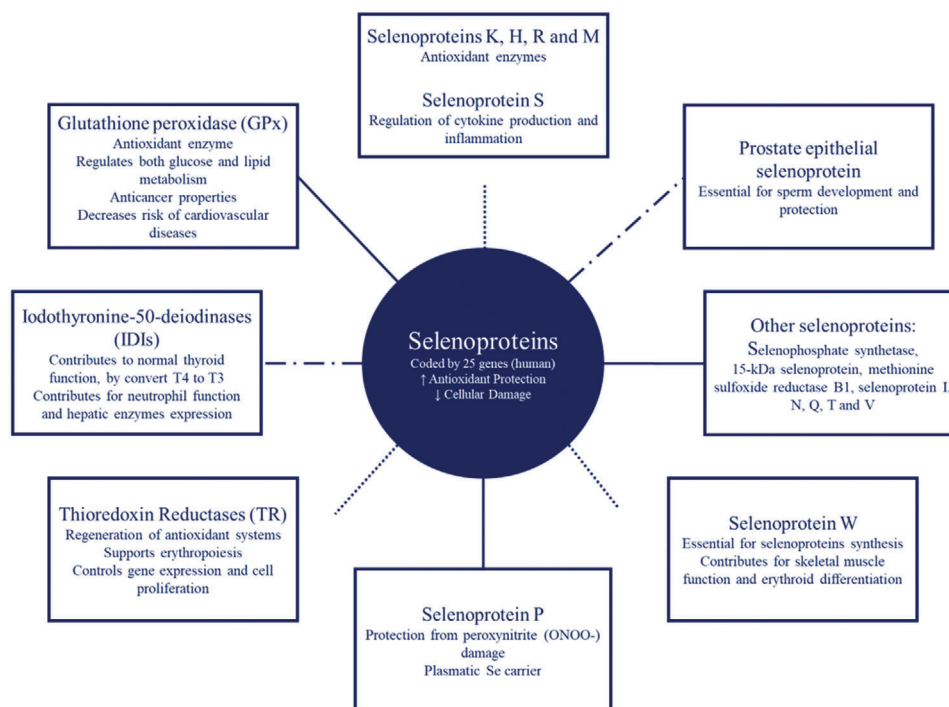


**Figure 2.** Brief description of selenoproteins function in human body.

Several Se forms present an absorption rate of 70–90% under normal physiologic conditions, except for selenite, with an absorption lower than 60%. Se bioavailability is also affected by ethanol and sulfur agents, in addition to heavy metals other than mercury, such as zinc and cadmium.<sup>[42,51]</sup> Moreover, food processing can also influence Se bioavailability, since increased temperatures improve protein digestibility, and enhance Se release and bioavailability. The total fat, protein, carbohydrates, and fiber within the food ingested can also influence the Se bioavailability due to additive, antagonistic, or synergistic interactions with Se.<sup>[42,51]</sup> The total Se quantity in the human body ranges from 10 to 20 mg, mainly as selenocysteine, contributing half of that amount in the skeletal muscles. Although, the organs in which Se is found to be more concentrated are the kidneys, testis, and liver, where it is mostly used by the immune system, erythrocytes, and platelets.<sup>[42]</sup> Several pathways of Se metabolism may occur, according to its form. The inorganic forms are reduced to selenite, while the organic forms are cleaved by  $\beta$ -lyase, and both will be further used for selenoprotein synthesis.<sup>[52,53]</sup>

In intestinal mucosal cells, selenite is taken by red blood cells and reduced by glutathione (GSH) and NADPH-dependent reductases. Alternatively, selenite can be also used as a substrate for the thioredoxin system.<sup>[4,10,42,49,52]</sup> However, selenite may not be immediately subjected to GSH reduction, rather leaving the bloodstream to be excreted in urine or to be metabolized in the liver to selenide, is then used for the production of selenoproteins or methylated compounds.<sup>[52]</sup> Main roles and properties are summarized in **Figure 2**. The organic forms, such as SeMet, the main form of Se present in the human diet,<sup>[4,10,42]</sup> enter the methionine pool and are randomly inserted into proteins at methionine positions, being transported to the liver.<sup>[4]</sup> The liver is the main organ

responsible for Se metabolism, being responsible for most of the selenoproteins synthesis and the regulation of Se metabolite excretion. Se excretion occurs mainly through urine, but Se is also substantially excreted via feces.<sup>[42]</sup> Once fecal excretion becomes saturated, Se excess detoxification is activated, and dimethylselenide is excreted through respiration, in addition to enhanced urinary excretion.<sup>[4,10]</sup>

## 2.2. Se Potential Therapeutic Impact

Since Se has anti-inflammatory and immunomodulatory actions, Se supplementation has been studied for the treatment of several inflammatory diseases, such as asthma,<sup>[1,10]</sup> chronic lymphedema,<sup>[50]</sup> rheumatoid arthritis, and Crohn's disease.<sup>[10]</sup> Kamer et al. demonstrated that children with a food allergy presented Se levels lower than children without any allergy, which resulted in reduced values of glutathione peroxidase (GPx) and superoxide dismutase (SOD), which suggests the role of Se in the pathogenesis of food allergies.<sup>[54]</sup>

Se compounds can also be toxic, depending on their chemical composition, dose, and exposure time.<sup>[55]</sup> However, Se has been studied as a cancer prevention agent, as several Se-based compounds have shown to decrease ROS production, and prevent DNA damage and gene dysfunction induced by the excessive oxidative stress.<sup>[10,56,57]</sup> Se has also been studied for cancer treatment as a radiotherapy and chemotherapeutic adjuvant since malignant cells are more susceptible to Se pro-oxidant effects than healthy cells.<sup>[5,49]</sup>

Se deficiency has been correlated with several viral, bacterial, and parasitic infections, which further demonstrates Se impact

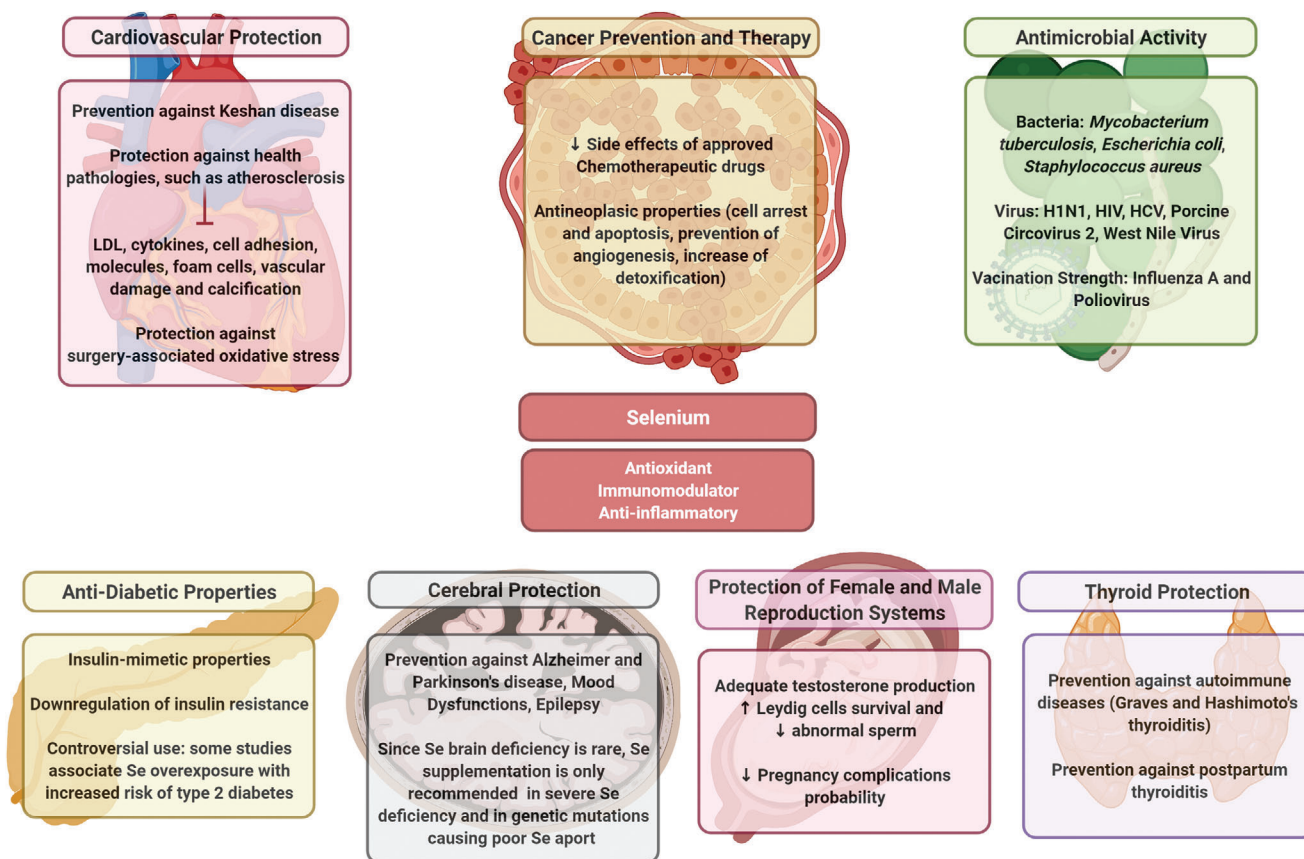


**Figure 3.** Main Se medicinal properties. Figure created with Biorender.

on immune system function.<sup>[45,47,58]</sup> Examples of these diseases include Keshan disease,<sup>[9,58]</sup> influenza A, H1N1, HIV infection, and infection by other viruses, such as hepatitis C virus (HCV), Porcine Circovirus 2, and West Nile virus.<sup>[9]</sup> Se supplementation has been shown to be beneficial for the treatment of several infections caused by several bacterial, such as *Helicobacter pylori*, *Escherichia coli*,<sup>[45]</sup> methicillin-resistant *Staphylococcus aureus* (MRSA) and *Mycobacterium tuberculosis*,<sup>[45]</sup> especially as a concomitant opportunistic infection in HIV patients.<sup>[47]</sup> Se supplementation has been also related to antiparasitic properties against *Trypanosoma cruzi* and *Heligmosomoides bakeri*,<sup>[47]</sup> besides improving the immune responses for influenza A and poliovirus vaccination.<sup>[45]</sup>

Several studies have shown the potential role of Se and selenoproteins in protecting the cardiovascular system against oxidative damage and excessive platelet aggregation, ultimately preventing several cardiovascular pathologies, such as atherosclerosis, hypertension, heart hypertrophy, and consequent congestive failure.<sup>[9,10,59]</sup>

These Se-related antioxidant properties have been associated with type 2 diabetes prevention,<sup>[10,60]</sup> due to the modulatory action of selenoproteins in the insulin signaling cascade. Selenoprotein P was shown to diminish pancreatic insulin production, and thioredoxin reductases (TR) indirectly reduce insulin resistance. Therefore, this Se insulin-mimetic property supports Se supplementation benefits. However, other studies have also asso-

ciated Se supplementation and overexposure, or selenoproteins overexpression, with higher risk for type 2 diabetes,<sup>[60,61]</sup> and therefore the role of Se in diabetes not yet clear.<sup>[60]</sup>

Since the thyroid is the human organ with the highest concentration of Se,<sup>[46,62]</sup> Se supplementation has also shown beneficial properties on the course of autoimmune thyroiditis and other thyroid pathologies, such as Grave's hyperthyroidism, and chronic autoimmune Hashimoto's thyroiditis. Se has been associated with thyroid protection from oxidative stress, especially due to GPx3 activity,<sup>[46,62]</sup> as well as with metabolism regulation of thyroid hormones and increased efficiency of IDIs,<sup>[10]</sup> contributing to the conversion of T4 into T3. Se supplementation has also shown benefits for the treatment of hyperthyroidism-related pathologies, such as mild Graves' orbitopathy, improving the quality of life and slowing the disease progression in patients treated with levothyroxine.<sup>[63]</sup>

Since Se is also present in higher concentrations in gray matter regions and in the glandular sections,<sup>[10]</sup> participating in several neurotransmission and dopaminergic pathways,<sup>[64]</sup> this element has been studied as a biomarker for several neurological diseases, such as epilepsy, Alzheimer disease, and Parkinson's disease.<sup>[10]</sup> Se antioxidant neuroprotective function, impact on the regulation of cytoskeleton assembly, as well as the ability to bind to several neurotoxic metals and attenuate A $\beta$  deposition and tau proteins hyperphosphorylation,<sup>[64–66]</sup> constitute some of the factors that have been identified as possible causes for the role of

**Table 1.** Comparison between the main SeNPs production methods.

Production method	Main materials	SeNPs characteristics	Advantages	Disadvantages
Biosynthesis	Reduction of inorganic Se form (e.g., selenite or selenate) by a bioorganism (e.g., bacteria, fungi, protozoan, plant extracts.)	Dependent on the bioorganism used for SeNP preparation	<ul style="list-style-type: none"> <li>• SeNPs already capped and stabilized with biocompounds specific of the bioorganism used</li> <li>• Environment friendly</li> </ul>	<ul style="list-style-type: none"> <li>• Several parameters and steps to be optimized in the SeNPs biosynthesis</li> </ul>
Chemical reduction	Reduction of inorganic Se form (e.g., selenite or selenate) using a reducing chemical agent (e.g., ascorbic acid, GCH) and another compound as a stabilizing agent	Dependent on the stabilizing agent (bare SeNPs are not stable and precipitate within a few days)	<ul style="list-style-type: none"> <li>• Simple process, without need of bioorganism incubation or a technologic instrument</li> </ul>	<ul style="list-style-type: none"> <li>• Least environment friendly method, since it often uses harsh chemicals</li> </ul>
Physical synthesis	Use of physical-based methods (e.g., heating, laser ablation) to induce changes in inorganic Se compounds and produce SeNPs, in the presence of a stabilizing agent	Dependent on the stabilizing agent and the gamma ray doses applied. Possibility of production of ultrasmall SeNPs	<ul style="list-style-type: none"> <li>• Rapid and uniform production</li> <li>• Rapid reaction time</li> <li>• Increased reaction rates</li> <li>• Less energy spent, therefore a more economical method</li> <li>• Environment friendly</li> </ul>	<ul style="list-style-type: none"> <li>• Necessity of specific instruments</li> </ul>

Se in Alzheimer disease development. More recently, Vicente-zurdo et al. studied the metal-chelating potential of several Se species, such as SeMet, Sec, Se-methylselenocysteine and Se(VI), concluding that although Cu(II) and Fe(II) interacted with all Se species, Zn(II) only interacted with SeMet. However, these Se species have shown to increase the A $\beta$  fibrils width at the same degree as the neurotoxic metals studied.<sup>[64]</sup> In addition, several selenoproteins were shown to protect dopaminergic neurons, reinforcing the beneficial property of Se against Parkinson's disease.<sup>[67,68]</sup> Se levels have also been correlated with mood alterations, depression, and aggressive behavior.<sup>[9]</sup> However, since brain Se levels are rarely low, and excessive Se levels may also be prejudicial, its application in neuronal disorders may only be advantageous for patients with severe Se deficiency and/or with mutations in genes related with Se delivery or selenoproteins production.<sup>[67]</sup>

Se potential role in pregnancy<sup>[44]</sup> and reproduction,<sup>[69]</sup> as well as in male fertility<sup>[70]</sup> has also been recently revealed. Low levels of plasmatic Se have been connected to miscarriage episodes, and other pregnancy-associated complications, such as preeclampsia, preterm labor, and gestational diabetes.<sup>[44]</sup> Moreover, Se has proven to be an intracellular antioxidant in Leydig cells<sup>[70,71]</sup> and to neutralize the H<sub>2</sub>O<sub>2</sub> produced during testosterone biosynthesis.<sup>[50]</sup> Se supplementation seems to have an important role in spermatogenesis, as it was shown to decrease the quantity of abnormal sperm in mice, and enhance the viability of Sertoli cells and the expression of essential protein components due to its antioxidant properties.<sup>[70,72]</sup> The main Se medicinal properties are summarized in **Figure 3**.

### 3. Preparation and Characterization Methods of Se Nanoparticles (SeNPs)

#### 3.1. SeNP Production Methods

SeNPs can be synthesized by chemical, physical, and biosynthesis methods (**Table 1**).<sup>[14,20,73]</sup> Chemical methods require the use of agents to induce the catalytic reduction of ionic Se, commonly

involving high temperatures, acidic pH, and dangerous chemicals, which makes this method unsafe in several situations.<sup>[14,74]</sup> Physical methods that are less used than the chemical methodologies, include photo-thermal-assisted synthesis approaches, electrodeposition techniques, PLA, and microwave synthesis.<sup>[20]</sup> The biosynthesis of SeNPs, also referred to as green chemistry, consists in the use of bacteria, fungi, yeasts, algae, and plants as catalyst for SeNPs production,<sup>[73]</sup> resulting in inexpensive, nontoxic and ecofriendly SeNPs.<sup>[14,75]</sup> Biosynthesis methods present several advantages when compared to physical and chemical methods, such as inexistence of extreme conditions,<sup>[34]</sup> fast growth rate of the microorganisms used, low cost, common culture procedures,<sup>[76,77]</sup> low toxicity and ecofriendly,<sup>[74,78]</sup> and unique spectroscopic characteristics.<sup>[77]</sup>

##### 3.1.1. Biosynthesis of SeNPs

Biosynthesis methods reduce selenate or selenite to elemental Se by compounds existing in bioorganisms, such as phenols, flavonoids amines, alcohols, proteins, and aldehydes, resulting in specific red SeNPs.<sup>[14,16,34,79]</sup> Although, biogenic SeNPs are more frequently produced by prokaryotic cells,<sup>[14,77]</sup> such as anaerobic,<sup>[78]</sup> aerobic,<sup>[75,80]</sup> and anoxic bacteria,<sup>[14]</sup> both fungi,<sup>[81]</sup> protozoan,<sup>[82]</sup> and plant extracts<sup>[74,83,84]</sup> have been used as well. The latter is easily manipulated, converting selenate (SeO<sub>4</sub><sup>2-</sup>) into red SeNPs, due to the action of selenate reductases, which first reduce selenate to selenite (SeO<sub>3</sub><sup>2-</sup>), which will be subsequently reduced to elemental Se in the periplasm, by selenite reductases, such as nitrite, nitrate, and sulfite reductase.<sup>[14,77]</sup> Thiols, including GSH, cysteine, and cystine, and protein-bound thiols, such as phytochelatins and metallothioneins, have been involved in the SeNPs biosynthesis. Usually, GSH donates an electron to selenite, producing selenodiglutathione (GS-Se-SG) and superoxide anion (O<sub>2</sub><sup>•-</sup>). GS-Se-GS, due to the activity of NADPH and GSH reductase/TR, forms selenopersulfide (GS-Se<sup>-</sup>), which breaks into reduced GSH and elemental Se<sup>0</sup>, being the O<sub>2</sub><sup>-</sup> degraded by antioxidant enzymes.<sup>[34,77,85]</sup> Macromolecules, such

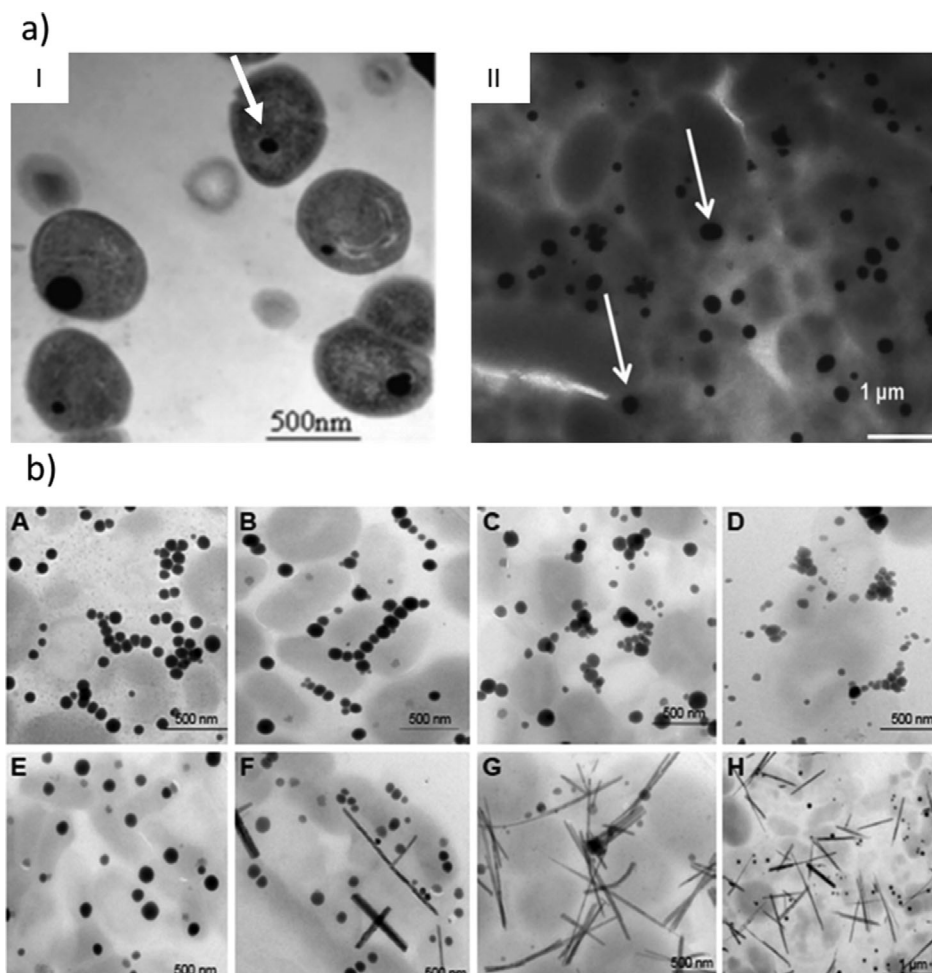


**Figure 4.** a) TEM images of Se nanostructures produced by both a-I) gram-positive *L. lactis* and a-II) gram-negative bacteria *P. putida* KT2440. Reproduced with permission.<sup>[78]</sup> Copyright 2019, Frontiers, and Reproduced with permission.<sup>[85]</sup> Copyright 2016, Nature, respectively. b) *Acinetobacter* sp. SW30 produces different Se nanostructures according to the concentration of  $\text{Na}_2\text{SO}_3$ : A)  $0.3 \times 10^{-3}$  M; B)  $0.5 \times 10^{-3}$  M; C)  $1.0 \times 10^{-3}$  M; D)  $1.5 \times 10^{-3}$  M; E)  $2.0 \times 10^{-3}$  M; F)  $2.5 \times 10^{-3}$  M; G)  $3.0 \times 10^{-3}$  M; and H)  $4.0 \times 10^{-3}$  M. Reproduced with permission.<sup>[89]</sup> Copyright 2017, Dovepress.

as proteins, enzymes, cellular residues, and even membrane phospholipids, may surround the SeNPs produced by biosynthesis, which is indicated by the presence of C, O, P, and S in elemental analysis assays.<sup>[78,82,86]</sup>

Both gram-positive and gram-negative bacteria have been used to produce SeNPs (Figure 4a), such as *Idiomarina* sp. PR58-8,<sup>[34]</sup> *E. coli* ATCC 35 218,<sup>[76]</sup> *Stenotrophomonas maltophilia*, *Bacillus mycoides*,<sup>[86]</sup> *Lactococcus lactis*,<sup>[78]</sup> *Enterococcus faecalis*,<sup>[87]</sup> *Ralstonia eutropha*,<sup>[88]</sup> *Acinetobacter* sp. SW30,<sup>[89]</sup> *Bacillus pumilus* sp. BAB-3706,<sup>[90]</sup> *Pseudomonas putida* KT2440,<sup>[85]</sup> *Azospirillum brasilense*,<sup>[91]</sup> *Bacillus licheniformis*,<sup>[35]</sup> *Vibrio natriegens*,<sup>[92]</sup> *Rhodococcus aetherivorans*,<sup>[80]</sup> *Pseudomonas alcaliphila*,<sup>[93]</sup> *Alcaligenes faecalis*,<sup>[94]</sup> *Pseudomonas stutzeri*<sup>[95]</sup> and, more recently, *Bacillus amyloliquefaciens* SRB04, which has been shown to produce SeNPs smaller than 50 nm.<sup>[75]</sup>

The mechanisms behind bacterial SeNPs biosynthesis are divided into three steps: 1) transport of Se oxyanions into the cell, mainly by sulfate permeases; 2) reduction of these compounds by bacteria proteins, producing the red amorphous  $\text{Se}^0$ , followed by its release from the cell; 3) assembly of elementary  $\text{Se}^0$  into

SeNPs by continuous reduction of Se oxyanions to  $\text{Se}^0$ ,<sup>[77,93]</sup> and 4) isolation of SeNPs from the bacteria by both centrifugation and filtration methods.<sup>[91]</sup>

To optimize the biosynthesis of SeNPs, it is important to control several parameters, such as the: 1) bacterial culture temperature and rotation;<sup>[88]</sup> 2) incubation time and the Se salt concentration;<sup>[14,89]</sup> 3) culture growth pH;<sup>[95]</sup> 4) Se minimum inhibitory concentration (MIC) for the microorganism; 5) several growth kinetics indicators, like specific growth rate, doubling time and lag time, the selenite/selenate uptake rate;<sup>[14,34,80,85]</sup> and 6) microorganism reducing potential.<sup>[76,80]</sup> For example, Wadhvani et al. produced SeNPs using *Acinetobacter* sp. SW30, and demonstrated that using  $0.3 \times 10^{-3}$  to  $2.0 \times 10^{-3}$  M  $\text{Na}_2\text{SO}_3$  resulted in spherical SeNPs, while concentrations of  $3.0 \times 10^{-3}$  M  $\text{Na}_2\text{SeO}_3$  and higher produce rod-like SeNPs (Figure 4b).<sup>[89]</sup> Presentato et al. have also shown that the bioconversion in *R. aetherivorans* BCP1 exposed for the first time to  $\text{SeO}_3^{2-}$  was inferior to the one obtained in *R. aetherivorans* BCP1 reinoculated in fresh medium and reused.<sup>[80]</sup> In addition, the bacterial medium culture can influence the characteristics of biogenic

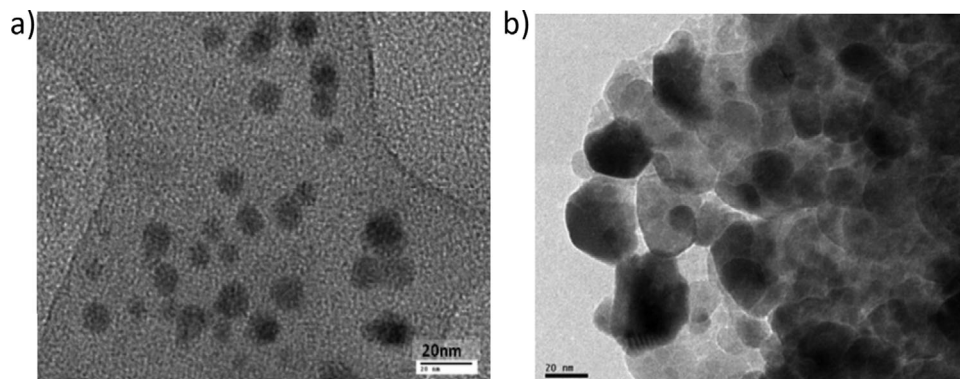


**Figure 5.** TEM images of Se nanostructures produced using plant extracts: a) *V. vinifera* extract. Reproduced with permission.<sup>[83]</sup> Copyright 2014, Molecules. b) *E. officinalis* extract. Reproduced with permission.<sup>[74]</sup> Copyright 2019, PMC.

SeNPs. For example, Rajkumar et al. verified that the use of banana peel extracts a medium constituent for *P. stutzeri* led to biogenic SeNPs more stable than those obtained while using the commercial media. The amorphous SeNPs presented a size of 75–200 nm and Fourier transform infrared (FTIR) assays indicated the existence of functional groups responsible for the reduction and stability of SeNPs.<sup>[95]</sup>

Protozoan, such as *Tetrahymena thermophila*, were also used for the synthesis of SeNPs. *T. thermophila* showed optimal production with  $150 \times 10^{-6}$  M selenite, producing amorphous SeNPs with a size ranging from 50 to 500 nm due to the reducing action of GHS.<sup>[82]</sup> Faramarzi et al. used *Saccharomyces cerevisiae* to produce SeNPs, employing amounts of sodium selenite ranging from 5.0 to 25  $\mu$ g. It was observed that *S. cerevisiae* growth increased with higher amounts of sodium selenite, which affected the physical and antioxidant characteristics of SeNPs, since the use of the 5.0  $\mu$ g selenite originated SeNPs with the smallest size (75 nm) and also with the highest antioxidant activity. However, intakes of 25  $\mu$ g selenite originated more uniform SeNPs.<sup>[81]</sup>

Plant extracts also demonstrated potential for SeNPs biosynthesis. For example, *Vitis vinifera* fruit extract has shown to reduce selenious acid, producing elemental Se. Sharma et al. indicated that the biopolymer lignin, due to its phenolic group, is responsible for the reduction and stabilization of SeNPs (Figure 5a).<sup>[83]</sup> Fruit extracts of *Emblica officinalis* also reduced sodium selenite into elemental Se due to their high content of phenolics (gallic acid), flavonoids (catechin), and tannins (tannic acid) (Figure 5b).<sup>[74]</sup> *Capsicum annum L.* extract has also been shown to reduce Se ions into amorphous elemental Se, controlling its nucleation and growth. Transmission electron microscopy (TEM) images revealed different SeNP shapes, according to the pH of the reaction environment.<sup>[84]</sup>

The use of plant extracts is preferable to the use of fungi and bacteria, since those are widely available and safer to manipulate, requiring mild conditions and less damaging solvents, in addition of offering more effective and faster production of SeNPs. In fact, the reduction of Se salts usually occurs in one step, allowing for an effective control of SeNP size and shape.<sup>[36]</sup> Moreover, a specific plant can be used for SeNPs production due to its beneficial properties. For example, Qamar et al. used *Trachyspermum ammi* seed extract, since this plant exhibits anti-inflammatory, antioxidant, immunomodulatory, antimicrobial, antifilarial, an-

thelmintic, and gastroprotective abilities due to the presence of thymol,<sup>[96]</sup> to produce biogenic SeNPs with an average size of 40 nm.

It is believed that in the future, SeNPs can be extracted using biomineralization, since this method can produce the purest product.<sup>[20]</sup> Biosynthesized SeNPs have also already been stabilized and functionalized, being capped with biocompounds. However, since specific microorganisms have been used to produce SeNPs with different characteristics, more studies are required to match the microorganism to the corresponding capping biomolecules and therapeutic activity.<sup>[74,77]</sup> This is important, since polysaccharide capping is preferred to coating with phenolics or proteins, since the latter are susceptible to enzymatic degradation, while phenolics are auto-oxidized and aggregate in the stomach's acidic environment.<sup>[36]</sup>

### 3.1.2. Chemical Reduction Synthesis of SeNPs

Several Se reducing compounds can be used to produce SeNPs, such as sodium selenite,<sup>[97,98]</sup> selenious acid<sup>[22,99]</sup> and Se dioxide.<sup>[100]</sup> However, Kumar et al. used Se powder and sodium sulfite at a ratio of 1:4 in an aqueous solution, which was kept under stirring at 70 °C for 9 h, leading to a transparent sodium selenosulfate solution. The carboxylic group of the reducing agents acetic acid, pyruvic acid, and benzoic acid led to the SeNPs synthesis.<sup>[101]</sup> Other reducing agents have been used, such as GSH<sup>[102,103]</sup> and sodium borohydride,<sup>[104–106]</sup> although the most environmental friendly and most common reducing agent used is ascorbic acid.<sup>[15,97,107]</sup> Zeng et al. optimized the reaction conditions and the ratios between ascorbic acid and selenite acid, describing a temperature of 25 °C, a reaction time of 2 h and an ascorbic acid: Se molar ratio of 4:1 as optimal conditions. Theoretically, ascorbic acid would reduce Se in a stoichiometry of 2:1; however, the excess of reducing agent provided a more efficient reducing environment and prevented the SeNPs oxidation, thereby leading to smaller SeNPs.<sup>[97,107]</sup> Recently, an antioxidant agent named phycocyanin, extracted from *Spirulina*, was also used to reduce sodium selenite in order to produce SeNPs.<sup>[108]</sup> The agitation submitted during the SeNPs formation also influenced the SeNPs size.<sup>[97]</sup>

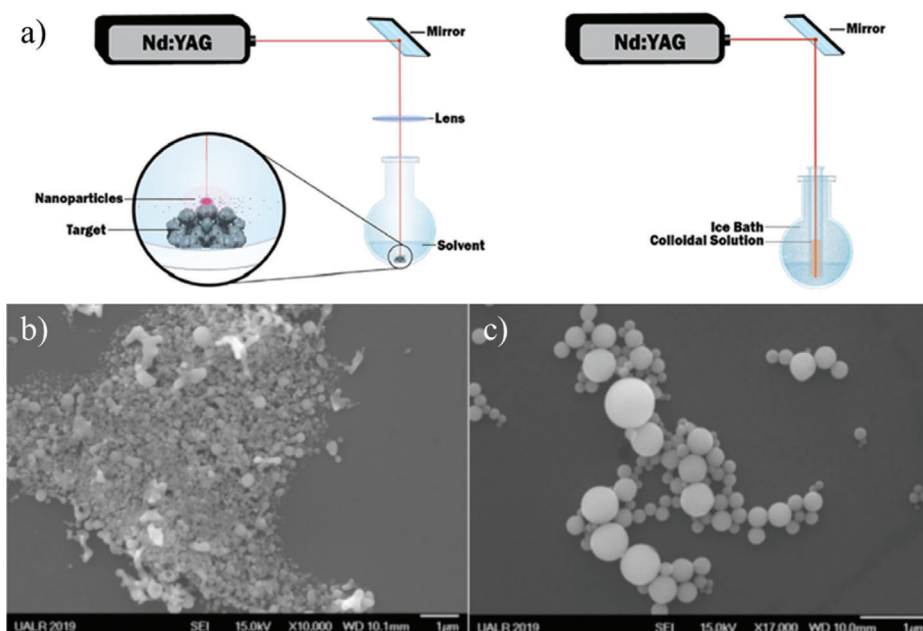


**Figure 6.** a) Schematic of SeNPs production using PLA method. b) SEM image of the SeNPs produced by the initial 3000 Hz irradiation. c) SEM image of the SeNPs produced by two sets of 3000 Hz irradiation, with a more delineated spherical shape than the SeNPs produced by only one irradiation set. Reproduced with permission.<sup>[115]</sup> Copyright 2020, American Chemical Society.

Also, Ma et al. produced a block copolymer with diselenide containing polyurethane (PUSeSe), with one water-insoluble diselenide part and another part of soluble polyethylene glycol (PEG) via polymerization of toluene diisocyanate. These diselenide-containing polymers were amphiphilic and, therefore, could self-assemble into micellar structures of 76 nm in an aqueous environment. Also, the block copolymer presented both oxidation and reduction responsive behavior, being sensitive to external redox behaviors, and consequently, with potential for production of drug delivery systems<sup>[109]</sup>

### 3.1.3. Physical Synthesis of SeNPs

Physical methods include PLA, hydrothermal treatments, microwave irradiation sonochemical processes, and physical evaporation.<sup>[20,79]</sup> Microwave synthesis of SeNPs consists in a traditional laboratory heating technique that uses Se salts in an aqueous solution. It presents several advantages, such as rapid and uniform heating, rapid reaction time, enhanced reaction rates, and less energy spent.<sup>[110]</sup> Mellinas et al. used microwave heating to produce trigonal and amorphous SeNPs with *Theobroma cacao* L. bean shell extract as a stabilizer, with a size of 1–3 nm, that was stable for 55 d at 4 °C.<sup>[111]</sup>

Ultrasmall SeNPs conjugated with PEG were produced by a hydrothermal process, by dissolving gray Se powder in PEG solution at 210–220 °C for 15–20 min, without the need for any reducing reagent, therefore being a more accessible and ecological method.<sup>[112]</sup> More recently, gamma irradiation was also used to produce SeNPs, as the radiolysis of aqueous solutions reduces metal ions<sup>[113,114]</sup> by creating solvated electrons, which then reduce the metallic ions into metal atoms that combine and form aggregates. Therefore, the SeNPs physicochemical properties de-

pendent not only on the capping agent, but also on the gamma-ray doses applied. For example, El-Batal et al. used gamma ray doses ranging from 0 to 100 kGy to produce various types of SeNPs capped by chitosan, sodium alginate, citrus pectin, and biogenic SeNPs using *Pleurotus ostreatus* aqueous extract of fermented powdered fenugreek seeds.<sup>[113]</sup>

Another popular physical method for SeNPs production is the PLA in liquids, which creates SeNPs with sizes between 5 to 120 nm.<sup>[115]</sup> This method uses liquid phased PLA in deionized water that turns Se pellets into colloidal solutions, where the electrical charge prevents the SeNPs from agglomerating by creating an electrical charge at its surface.<sup>[20,115]</sup> PLA has the advantages of being ecologically friendly and an economical method,<sup>[115]</sup> in addition to not requiring the use of chemical reagents, thereby avoiding the existence of contaminating by-products. These SeNPs are also easily collected as in the colloidal solution their stability is elevated.<sup>[20,116]</sup> PLA method also conserves the stoichiometry of the material and the sizes of the SeNPs are easily controlled according to the laser parameters used, e.g., fluence, wavelength, pulse duration, and ambient gas conditions like pressure and flow parameters.<sup>[116]</sup>

PLA method was used to produce antibacterial SeNPs. A Q-switched Nd:YAG laser with a wavelength of 1064 nm was used to irradiate the solution of 2 nm Se pellets immersed in deionized water, with the pulse frequency analyzed varying from 100 to 5000 Hz, and the pulse duration time from 70 to 200 ns according to the repetition rate. The laser was redirected by a mirror at a 45° and was focused by an 83 mm focal length lens to irradiate from the top of the SeNPs, creating a high-temperature plasma. After 5 min under radiation, the particles were irradiated to reduce their size, and then subjected to an ice bath to prevent agglomeration, while a second irradiation was employed (Figure 6a). However, when the frequency values surpassed 3000 Hz, the



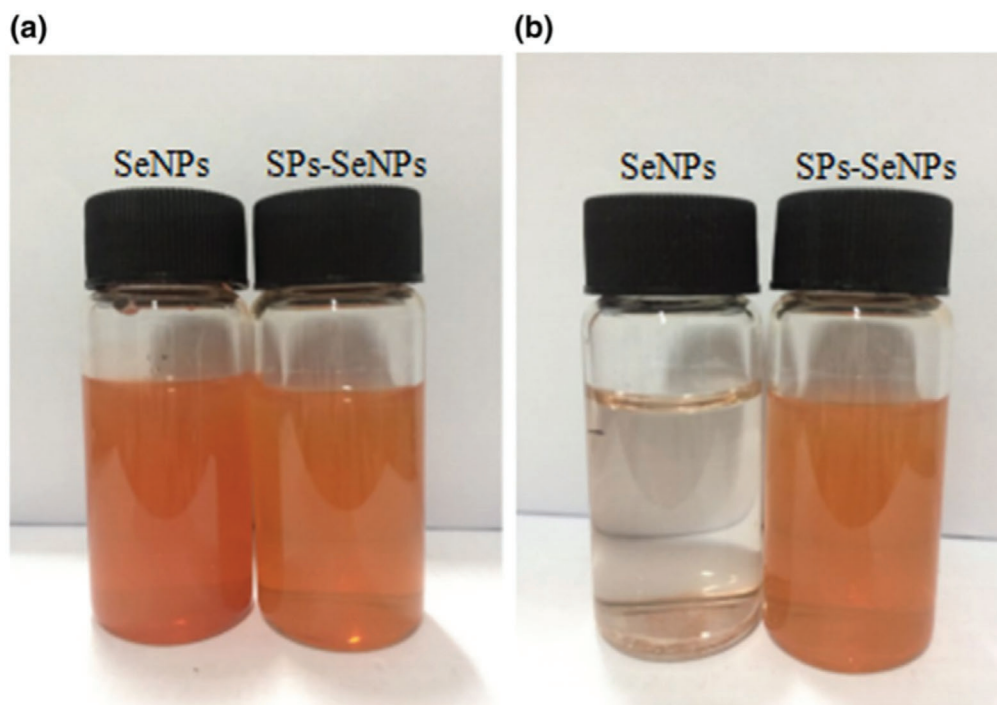


**Figure 7.** Effect of stabilizers on the size and stability of SeNPs: although the solutions of bare SeNPs (b) and SeNPs stabilized with *Spirulina platensis* polysaccharide (a) initially appear homogenous, after 90 d, only the SeNPs capped with the polysaccharides remain stable, while the bare SeNPs precipitated. Reproduced with permission.<sup>[117]</sup> Copyright 2020, Wiley-VCH GmbH.

production of SeNPs decreased, since the pulsed beam hit the cavitation bubble. After the cavitation bubble collapsed, the SeNPs were released into the solvent. In order to avoid the cavitation bubble and increase the production of SeNPs, the repetition rate chosen was 3000 Hz. The second set of irradiation helped to stabilize and to diminish the size of the SeNPs, producing SeNPs with a size and zeta potential values of  $43 \pm 20$  nm and  $+66 \pm 3$  mV, respectively (Figure 6b,c).<sup>[115]</sup>

Guisbiers et al. also used the PLA method to produce antibacterial SeNPs. The neodymium-doped yttrium aluminum garnet NT342B laser was used with a pulse duration of 3.6 nanoseconds, a frequency of 20 Hz and a wavelength within the ultraviolet spectrum, 355 nm, for 15 min, producing stable SeNPs with a size and zeta-potential of  $115 \pm 38$  nm and  $-45.6$  mV, respectively.<sup>[116]</sup>

### 3.2. SeNP Stabilization and Functionalization Approaches

Since bare SeNPs produced by chemical synthesis are unstable in aqueous solutions (Figure 7-b), leading to aggregates of stable gray/black Se, <sup>[15,106,117]</sup> stabilizers are usually added to preserve SeNPs size and bioactivity.<sup>[40,23]</sup> In fact, small changes in the SeNPs size may have an effect on their antioxidant activities, for example, by promoting Se accumulation and GSH S-transferase activity in vivo.<sup>[15]</sup> Several compounds have been used to stabilize the SeNPs, such as aminoacids,<sup>[23]</sup> bovine serum albumin (BSA),<sup>[97,103]</sup> polysaccharides (Figure 7-a) like chitosan<sup>[15,27]</sup> and gum arabic,<sup>[15,22,106]</sup> and polymers as poly(lactic-co-glycolic acid) (PLGA).<sup>[102]</sup>

SeNPs have shown potential to target specific cancer cells, by passive targeting based on the fact that the tumor environment is more acidic than the environment existing in healthy tissues.<sup>[36]</sup> However, the active targeting, achieved through SeNPs functionalization with ligands that bind to receptors overexpressed in cancer cells, is more successful in delivering compounds to the site of interest, avoiding healthy tissues, thereby increasing the therapeutic efficacy and reducing the toxicity.<sup>[118]</sup> SeNPs active targeting was demonstrated to be successful using folic acid,<sup>[100]</sup> transferrin (Tfr),<sup>[119]</sup> and HA.<sup>[120,121]</sup>

#### 3.2.1. Chitosan

Chitosan is the N-deacetylated form of chitin found in crustaceans, insects, and fungi.<sup>[99]</sup> Although, Chitosan is not soluble in aqueous or alkali solutions, and therefore acetic acid is often added for its dissolution.<sup>[15,26,107]</sup> This polysaccharide has been used in biomedical applications, including for oral delivery, due to its low toxicity, good bioavailability, and positive charge,<sup>[27,122]</sup> which enhances drug bioadhesion,<sup>[99]</sup> while avoiding pepsin and pancreatin degradation.<sup>[99,122]</sup> Moreover, chitosan enables the drug release in the acidic tumor environments, as well as within the lysosomes and endosomes, being capable of enhancing the passive targeting of NPs.<sup>[40]</sup> Therefore, several studies have demonstrated the potential application of chitosan as a SeNPs stabilizing agent, and its antioxidant<sup>[26]</sup> and antitumor effect, while addressing the effect of the chitosan molecular weight (high vs low) in the morphology and properties of SeNPs.<sup>[21,27,99]</sup>

**Table 2.** Physicochemical differences between SeNPs capped with low and high molecular weight chitosan.

Process studied	Type of chitosan used for SeNPs capping		
	High molecular weight	Low molecular weight	
Storage	Particle size improved with time, being stable for 180 d: indicated for long-term storage	Presented some aggregation, being stable for 30 d	
Heating	Results in opaque solutions, due to the breakage of hydrogen bonds between chitosan and the SeNPs Stayed below 200 nm and formed rod-like structures when temperature reached 95 °C	400 nm aggregates at 70 °C	
Freeze-drying	Maintenance of the spherical shape, being well-dispersed in water, although with size increase	Possible flocculated morphology, with aggregation	
Freeze-thawing	Loss of stability, due to breakage of hydrogen bonds		
Antioxidant capacity	Effects	Both showed better radical scavenging activity for ABTS than for DPPH	
		Higher antioxidant capacity, due to its loosened structure	Decreased antioxidant capacity
	Heating	Decreased both the ABTS and DPPH free radical scavenging activity	Increased both the ABTS and DPPH free radical scavenging activity (improved Se release ratio)
	Freeze-thawing	Did not affect the antioxidant capacity	
	Rehydration	Improved the antioxidant capacity	
Antibacterial activity	Effects	Antibacterial properties against <i>S. aureus</i> , however without inhibition effects towards <i>E. coli</i>	
	Heating	Only affected by 95 °C temperatures	Heating above 70 °C decreased the antibacterial activity
	Rehydration	Without significant effect	Decreased the antibacterial activity

SeNPs reacted with the lateral groups  $\text{NH}_2$  and  $\text{CH}_2\text{OH}$  of the chitosan, forming Se–O bonds, while the positive  $\text{NH}_3^+$  groups are present on the outer surface, enhancing its stability in aqueous solutions.<sup>[21,22,99]</sup> Although bare SeNPs presented a slightly negative zeta-potential in aqueous solutions due to the existence of trace elements  $\text{HSe}^-$  and  $\text{Se}^{2-}$  on the surface of the SeNPs, chitosan–SeNPs were clearly positive and stable, because of the existence of amino groups, that are protonated under acidic conditions.<sup>[99,123]</sup> While chitosan(l)–SeNPs appeared as uniform small spheres of 20–50 nm, chitosan(h)–SeNPs formed irregular aggregates, cross-linking effects obtained due to the use of high molecular weight macromolecular chitosan. Chitosan(l)–SeNPs maintained their structure for 30 d, after which they started to degrade leading to larger spherical aggregates,<sup>[27,99,122]</sup> probably due to the reduction of the absolute  $\zeta$ -potential over time.<sup>[15]</sup> Zhang et al. demonstrated that chitosan–SeNPs release in gastric (pH 1.2), intestinal (pH 7.4), and sweat (pH 6.3) environments is almost insignificant, supporting the high stability provided by chitosan. Chitosan(h)–SeNPs demonstrated to have a release rate higher than chitosan(l)–SeNPs in all media, probably due to the lower network impediment provided by the compact structure of chitosan(h)–SeNPs.<sup>[99]</sup> Chen et al. also studied the impact of molecular weight of chitosan on the properties of chitosan–SeNPs, using  $\text{I}^-$  as a surface regulating agent. These studies demonstrated that the chitosan concentration positively affected the chitosan–SeNPs size due to the decrease of the distance between chitosan molecules, enhancing the intermolecular hydrogen bond forces, which results in increased crosslinking effects.<sup>[27]</sup> However, chitosan(h)–SeNPs presented higher cellu-

lar uptake by cancer cells lines than normal cell lines, probably due to the higher amount of  $-\text{NH}_3^+$  groups, which permits an enhanced electrostatic attraction between the positively charged chitosan(h)–SeNPs and the phosphoryl groups of phospholipids in the cancer cell membrane, that are more negatively charged than normal cell membranes.<sup>[21,22]</sup>

Also, Song et al. analyzed the physicochemical characteristic of Chitosan–SeNPs produced using both high and low molecular weight chitosan, as summarized in **Table 2**.<sup>[124]</sup>

Chitosan–SeNPs exhibited higher radicals scavenging activity in 2,2'-azino-bis(3-ethylbenzothiazoline-6-sulfonic acid) (ABTS) than in 2,2-diphenyl-1-picrylhydrazyl (DPPH) and lipid peroxidation assays, which indicated that chitosan–SeNPs presented higher solubility in water phase than in lipid phase solvents, showing more propensity to react by electron transfer based reaction than hydrogen atom transfer reaction.<sup>[122]</sup> Chitosan(h)–SeNPs scavenging activity for  $\text{ABTS}^{\cdot+}$  radical cation and superoxide anion radical ( $\text{O}_2^{\cdot-}$ ) was the highest compared to SeNPs stabilized by medium and low molecular weight chitosan (**Figure 8**).<sup>[27,124]</sup> The antioxidant activity of chitosan–SeNPs was demonstrated in vitro, by inhibiting ROS production in a dose-dependent manner and enhancing the viability of BABLC-3T3 cell lines. In vivo, the chitosan–SeNPs enhanced the GPx activity and reduced the lipofuscin levels in mice subjected to UV radiation during 15 d.<sup>[122]</sup>

Chitosan–SeNPs have also presented antitumor properties against hepatic cancer cell lines, especially the chitosan(h)–SeNPs,<sup>[21,27]</sup> promoting ROS generation and mitochondria dysfunction.<sup>[21]</sup> These nanosystems also had the ability to load

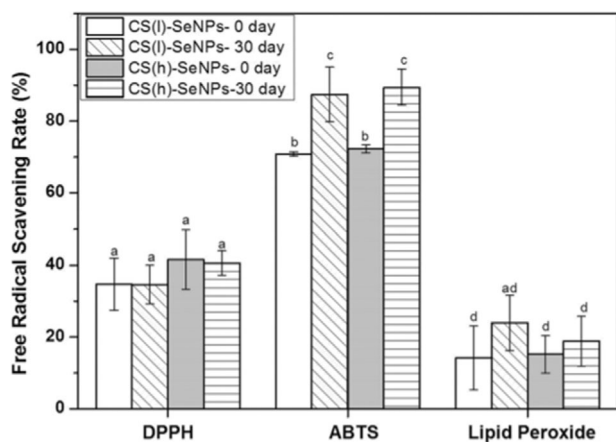


**Figure 8.** Antioxidant properties of chitosan–SeNPs. Overall, chitosan(h)–SeNPs has higher radical scavenging properties than chitosan(l)–SeNPs; however, all chitosan–SeNPs presented higher radicals scavenging activity in ABTS than in DPPH and lipid peroxidation assays. Reproduced with permission.<sup>[122]</sup> Copyright 2017, BMC.

several anticancer drugs, such as DOX, providing a selective drug release in acidic endosomes and lysosomes.<sup>[41,125]</sup> Chitosan–SeNPs have been also explored as mRNA carriers for cancer therapy,<sup>[126]</sup> as antidiabetic compounds,<sup>[107]</sup> and as a biocompatible material for cardiac tissue engineering.<sup>[127]</sup>

More recently, a spray-drying technique was studied to increase the stability of SeNPs, by adding a new layer of chitosan to the already formed Chitosan–SeNPs, producing microspheres (SeNPs-M) that remained stable for 60 days.<sup>[15]</sup> SeNPs were purified by ultrafiltration in which soluble compounds crossed the filtration membrane, while SeNPs-M were entrapped and separated.<sup>[15,128]</sup> SeNPs-M presented toxicity lower than selenite, with a LD<sub>50</sub> value of 18–20 fold, and increased mice growth and the levels of antioxidant enzymes in dosages considered toxic for selenite administration.<sup>[15,123]</sup> SeNPs-M were studied as antioxidant agents for the scavenging of hepatic radicals caused by alcohol overconsumption.<sup>[123,128]</sup>

Ionic gelation was also studied to increase the stability of Chitosan–SeNPs. In this technique, chitosan–SeNPs were embedded into a sodium citrate solution with moderate stirring, and a crosslinking gelation occurred, resulting in a chitosan/citrate gel. Afterwards, the gel was removed, and a spray-drying technique was applied to obtain solid red SeNPs-C/C, which were stable for 60 d (Figure 9a). Although SeNPs-C were completely dissolved in pH 2.0–2.5, suggesting its release in the stomach, SeNPs-C were not soluble in pH above 3.0, due to the non-ionization of the citrate at these pH values (Figure 9b,c). SeNPs-C/C were stable in 60 °C in relative humidity for 10 d (stress conditions) and in 40 °C, in the dark for 6 months, reaching the standard stability required for food storage and transportation. Furthermore, in the presence of 1/11-1/4 of the selenite toxicity, SeNPs-C presented antioxidant and protective effects against D-galactose (D-gal)-induced aging in mice, decreasing the growth suppression caused by D-gal and diminishing liver damage, by increasing the level of antioxidant enzymes.<sup>[26]</sup>

### 3.2.2. Folic Acid (FA)

FA has been widely studied as a ligand for the functionalization of NPs for cancer treatment, as the folate receptor is frequently overexpressed in several cancer types.<sup>[129]</sup> Thereby active targeting using FA has shown to increase NP uptake by cancer cells through the receptor-mediated endocytosis,<sup>[130,131]</sup> improving the overall antitumor effect of these carriers while avoiding off-target effects in healthy cells.<sup>[100]</sup> SeNPs functionalized with FA (FA-SeNPs) were studied for breast<sup>[100,131]</sup> and hepatocellular cancer treatment.<sup>[130]</sup> FA-SeNPs were produced by chemical reaction, by ionic or polar-polar interaction between the –NH<sub>2</sub> and –COOH groups of the FA, and the hydroxyl groups on the SeNPs, via carbonyl bonds.<sup>[100,129]</sup> Active targeting using FA was studied using an excess of FA to inhibit the cellular uptake of FA-SeNPs, demonstrating that the FA molecules on the surface of SeNPs were available to specifically target cancer cells.<sup>[130,131]</sup>

### 3.2.3. Hyaluronic Acid (HA)

HA is a linear, negatively charged polysaccharide containing two alternating units of d-glucuronic acid and N-acetyl-d-glucosamine.<sup>[30]</sup> As a result of its diverse sources, biocompatibility, biodegradability, nontoxicity, nonimmunogenicity, and abundance of functional groups (–COOH and –OH), HA has been used for several pharmaceutical applications, such as for the targeted delivery of antitumor drugs<sup>[29,30,120]</sup> by specifically binding the CD44 receptors present in cancer cells.<sup>[29,120]</sup> The HA receptor CD44 is abundant in several cancer cells, such as HepG2 (human liver carcinoma cells), HeLa (cervical adenocarcinoma cancer cells), and A549 cells (lung carcinoma cells). Thereby, antitumor potential of HA–SeNPs has been studied, in which HA not only stabilized, but functionalized the SeNPs toward cancer cells.<sup>[30]</sup>

HA hydrogels have also shown potential for the delivery of SeNPs for seborrheic dermatitis treatment, as a hydrogel containing ketoconazole NPs and SeNPs, by employing the cross-linking method. HA protects SeNPs from aggregation and preserving their colloidal arrangement, resulting in a hydrogel with potential to treat topical fungal infections.<sup>[132]</sup>

### 3.2.4. Other Polymers

Several other polymers have been used to stabilize SeNPs, such as polyvinyl alcohol (PVA). Kumar et al. studied the anticancer properties of SeNPs against Dalton's lymphoma cells, using PVA as a stabilizer agent, concluding that the concentration of PVA did not affect the size and shape of the SeNPs.<sup>[101]</sup> The precipitation of SeNPs in poly-L-lactic acid (PLLA) produced an antitumor material against osteosarcoma cells, while promoting bone regeneration. PLLA was coated with SeNPs, by adding GSH and sodium selenite to PLLA, and NaOH to alkalize the medium and precipitate the SeNPs onto the PLLA.<sup>[133]</sup>

PEG is an amphiphilic molecule soluble in both water and in several organic solvents,<sup>[134]</sup> and it has been widely explored as a stabilizer.<sup>[134,135]</sup> PEG is FDA approved for injectable, topical, rectal, and nasal formulations.<sup>[40,112,136]</sup> Its popularity is mainly

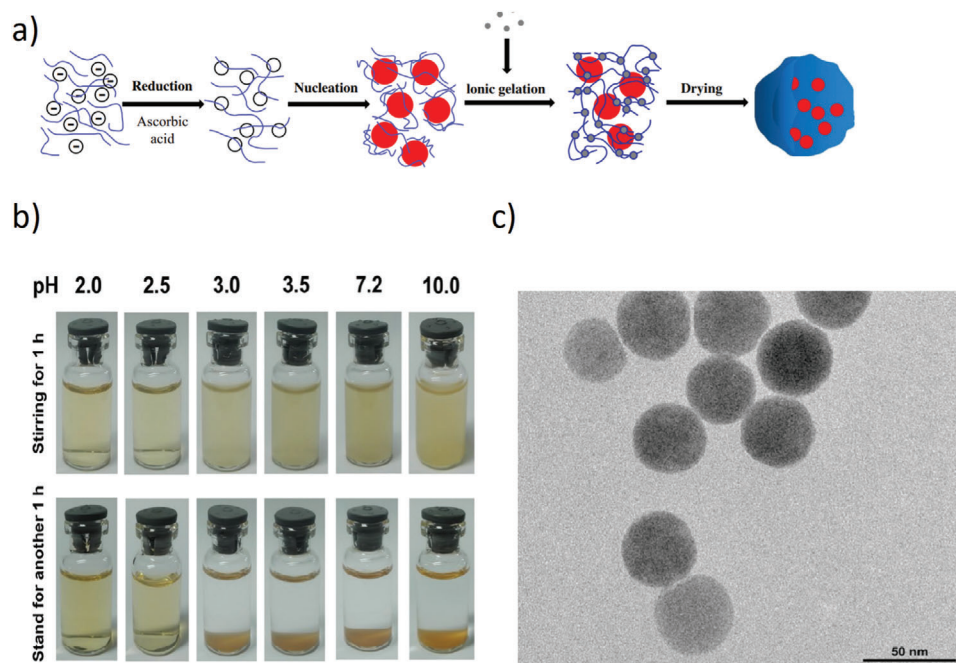


**Figure 9.** Effect of the ionic gelation process on Chitosan-SeNPs. a) Representative scheme of process of SeNPs-C/C preparation. b) SeNPs-C/C dissolution according to the solution (SeNPs-C/C are not soluble at pH equal or above 3). and c) TEM image of SeNPs-C/C dissolved in pH 2.5 solution for 8 h. Reproduced with permission.<sup>[126]</sup> Copyright 2017, BMC.

due to its favorable characteristics, such as overcoming several physicochemical instabilities,<sup>[134]</sup> high safety and stability at high temperatures, decreased nanoparticle clearance by the mononuclear phagocytic system, while preventing protein aggregation and enzymatic degradation, which increase NPs accumulation in the tumor site due to the enhanced permeability and retention (EPR) effect. In addition, PEG chains are used for NP functionalization by enabling the binding of specific targeting antibodies and other compounds identified by the cancer cells. Accordingly, PEG-SeNPs presented potential for the treatment of hepatic<sup>[112,134]</sup> and lung cancer.<sup>[137]</sup> During the production of PEG-stabilized SeNPs at high temperatures, its oxygen atom is sp<sup>3</sup> hybridized and forms two carbon-oxygen covalent bonds and two lone-pair electrons, which coordinate with the empty 4d orbitals of each Se atom. Thereby, PEG has not only enabled the atomic clusterization of gray Se, but also controlled its size, preventing SeNPs aggregation and reversion to its gray as the temperature decreases.<sup>[112]</sup>

The cationic polymer polyethylenimine (PEI) has been shown to enhance NP stability, in addition to having immunostimulatory properties, via Toll-like receptor (TLR) activation,<sup>[136]</sup> as well as enabling the delivery of nucleic acids due to the electrostatic interactions established between PEI ammonium groups and the phosphate groups of DNA. Jalalian et al. used PEI linked to PEG (PEI-PEG) to deliver SeNPs loaded with epirubicin and functionalized with aptamers. The amine groups of PEI were activated with sulfosuccinimidyl 4-(N-maleimidomethyl) cyclohexane-1-carboxylate and covalently bound to the thiol group of PEG, providing a biocompatible environment for aptamer attachment.<sup>[136]</sup>

Selmani et al. studied the stabilization of SeNPs using four different polymers: polyvinylpyrrolidone (PVP), poly-L-lysine (PLL),

polyacrylic acid (PAA), and sodium bis(2-ethylhexyl) sulfosuccinate (AOT) (**Figure 10**). TEM analysis has shown that PLL-SeNPs tended to aggregate and form clusters, while the stabilization using the other polymers resulted in spherical SeNPs with an average size ranging between 70 and 80 nm. The coating of SeNPs with the negatively charged PAA or AOT resulted in SeNPs with a negative zeta-potential, while a positive charge was obtained following their coating with PLL, as expected. However, in spite of the positively charged PVP, PVP-SeNPs presented negative zeta-potential values, which can be explained by the attachment of selenite on the surface of the particles.<sup>[138]</sup>

### 3.2.5. Other Polysaccharides

Other polysaccharides have been chosen to stabilize SeNPs due to their low toxicity, good water solubility, great amount of hydroxyl groups, complex branch structures, and high surface area, which enhances their connection to SeNPs and cell membranes.<sup>[139]</sup> For example, gum arabic is an extensively used polysaccharide in the food and pharmaceutical industry, and has allowed the production of stabilized SeNPs (**Figure 11a-I**), which presented smaller sizes, and thus, stronger oxidant scavenging activity than those Se-based NP produced in the absence of this polymer, probably due to the stronger interaction established between the SeNPs surface and Gum Arabic terminal hydroxyl groups. This stability is further enhanced under acid conditions (pH 2–4), resulting in smaller SeNPs, which indicates that the hydrogen ions compacted SeNP structure. However, under pH 4, their size barely changed, which indicates that SeNP's higher stability in aqueous

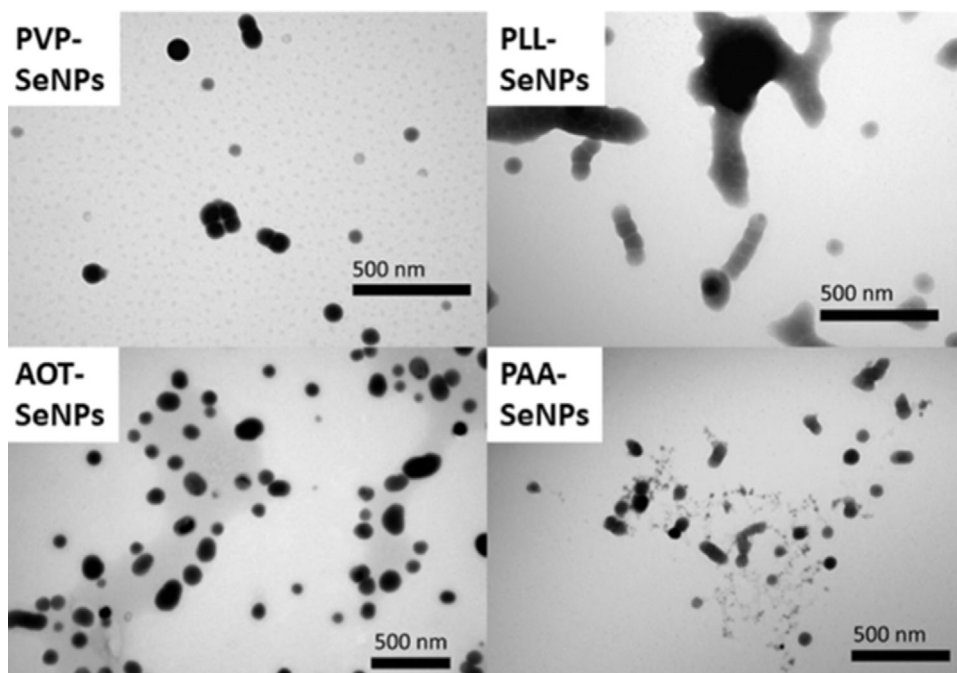


**Figure 10.** TEM images of SeNPs stabilized with several polymers (PVP, PLL, AOT, and PAA). Reproduced with permission.<sup>[138]</sup> Copyright 2020, Elsevier.

solutions may be due to the highly branched structure of arabinogalactan present in gum arabic.<sup>[106]</sup>

Several other polysaccharides used to stabilize SeNPs were obtained from fungi, especially mushrooms.<sup>[28,140–142]</sup> Mushroom polysaccharides have shown immunomodulatory and antitumor activities, being used in chemotherapy in Asia for many years.<sup>[28]</sup> For example, Cai et al. used polysaccharides from *Lignosus rhinocetis* to stabilize SeNPs, producing amorphous SeNPs with an average diameter of 50 nm, by both using the chemical reduction and, after dialysis and freeze-drying, ultrasound technique, with the goal to decrease SeNPs size and increase their stability. Moreover, SeNPs subjected to ultrasound exhibited the strongest antioxidant activity in both DPPH and ABTS radical-scavenging assays, by increasing the ratio surface area: volume, offering more reacting sites with free radicals.<sup>[140]</sup>

Zeng et al. stabilized SeNPs with polysaccharides from the fungi species *Pleurotus tuber-regium* (PTR), *Polyporus rhinoceros*, *Coriolus versicolor*, and *Ganoderma lucidum*. All these SeNPs were stable for 13 weeks and the FTIR spectroscopy analysis indicated the bind of the polysaccharide —OH and —NH groups to the SeNPs surface. The stabilization using polysaccharides from PTR resulted in smaller SeNPs (around 12.5 nm), with high anticancer potential, especially against gastric adenocarcinoma, while having low cytotoxicity against normal cells.<sup>[28]</sup> Huang et al. also produced SeNPs stabilized with PTR polysaccharides, producing 30 nm SeNPs that were also stable for 13 weeks (Figure 11a-IV).<sup>[141]</sup>

The *Catathelasma ventricosum* is an edible mushroom from southwest China, known for its protective effects on liver, kidney, and pancreas tissues. Polysaccharides obtained from this mushroom have been used for the chemical synthesis of spherical SeNPs, stabilized by the amino, hydroxyl, or carboxyl groups of this polysaccharide (Figure 11a-II), while bare SeNPs aggre-

gated as clusters (Figure 11b-II).<sup>[142]</sup> *Cordyceps sinensis* polysaccharide was also used for SeNPs stabilization (Figure 11a-III), due to its high viscosity. SeNPs conjugation with *Cordyceps sinensis* polysaccharides was accomplished by the formation of electrostatic bonds between the polysaccharide's —OH groups and SeNPs (C—O···Se), creating amorphous SeNPs more stable than those prepared without the polysaccharide (Figure 11b-III). The optimal Se:polysaccharide ratio for SeNPs production was 1:1, demonstrating better radical scavenging activity on superoxide anion radical and ABTS radical cation assays than the polysaccharides themselves or SeNPs produced with lower Se:polysaccharide ratios. However, when the quantity of Se increases beyond this ratio, the SeNPs tends to become more unstable.<sup>[143]</sup> *Polyporus umbellatus* (PUP) polysaccharides also decreased the diameter of SeNPs, producing negatively charged PUP-SeNPs with an average size of  $82.5 \pm 0.7$  nm (Figure 11a-VII), which were stable for 84 d at 4 °C in dark conditions.<sup>[144]</sup>

A water soluble 1,6- $\alpha$ -D-glucan from *Castanea mollissima* was also studied for SeNP stabilization due to its large number of hydroxyl groups, producing homogenous and monodispersed spherical SeNPs. The diameter of these SeNPs decreases with the increase of 1,6- $\alpha$ -D-glucan concentration until  $5 \text{ mg mL}^{-1}$  ( $53.7 \pm 4.0$  nm), although a net structure was formed at a  $10 \text{ mg mL}^{-1}$  concentration. More recently, Zhang et al. used polysaccharides extracted from *Spirulina platensis* to produce stabilized and uniform SeNPs with an average diameter of  $73.42 \pm 0.69$  nm. The optimal conditions included a polysaccharide solution concentration of  $100 \text{ mg L}^{-1}$ , an ascorbic acid:sodium selenite concentration ratio of 3:1 and a reaction time of 6 h. The hydroxyl groups of the polysaccharides coated the SeNPs, conferring a negative charge to the SeNPs, which remained stable for 75 d at 4 °C. Also, the produced SeNPs have shown lower cytotoxicity when compared with sodium selenite.<sup>[117]</sup>

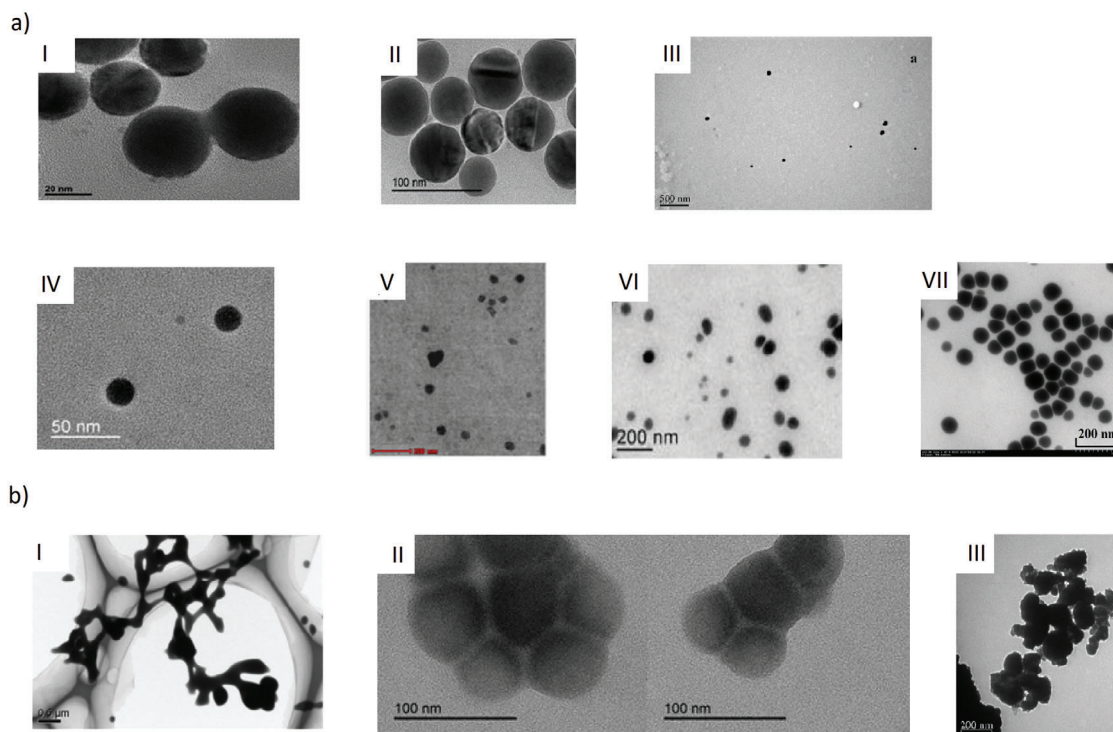


**Figure 11.** a) SeNPs stabilized with several polysaccharides: (I) Gum Arabic; (II) *Catathelasma ventricosum* polysaccharides; (III) *Cordyceps sinensis* polysaccharides; (IV) PTR polysaccharides; (V) *Castanea mollissima* polysaccharides; (VI) PEC; and (VII) *Polyporus umbellatus* polysaccharide. Reproduced with permission.<sup>[106]</sup> Copyright 2014, Elsevier. Reproduced with permission.<sup>[142]</sup> Copyright 2018, Elsevier. Reproduced with permission.<sup>[143]</sup> Copyright 2017, Elsevier. Reproduced with permission.<sup>[141]</sup> Copyright 2018, Royal Society of Chemistry. Reproduced with permission.<sup>[148]</sup> Copyright 2019, Elsevier. Reproduced with permission.<sup>[145]</sup> Copyright 2018, Elsevier. Reproduced with permission.<sup>[144]</sup> Copyright, Elsevier, respectively. b) Images of SeNPs without stabilization. Reproduced with permission.<sup>[106]</sup> Copyright 2014, Elsevier. Reproduced with permission.<sup>[142]</sup> Copyright 2018, Elsevier and reproduced with permission.<sup>[143]</sup> Copyright 2017, Elsevier, respectively.

Qiu et al. stabilized SeNPs with pectin (PEC), a polysaccharide used as a thickening and antioxidant agent in the food industry, composed by an anionic heteropolysaccharide complex derived from sequences of (1→4)- $\alpha$ -D-galacturonosyl units and their methyl esters interrupted by (1→2)- $\alpha$ -L-rhamanopyranosyl units. Spherical amorphous PEC-SeNPs were produced (Figure 11a-VI) using an optimized Se/PEG ratio of 1:2, since a lower ratio resulted in formation of large clusters and higher ratios produced heterogenous PEC-SeNPs, because the amount of PEC was less than the required to decorate and stabilize SeNPs. Also, the antioxidant properties of PEC-SeNPs decreased when the ratio increased to 4:3. PEC bound to the SeNPs surface by hydrogen bonds (Se—O—H), forming PEC-SeNPs exhibited stability in acidic solutions for 30 d; however, while the size of PEC-SeNPs did not change, their absolute zeta-potential decrease overtime due to the protonation of COO<sup>-</sup> groups of PEC under acidic conditions. PEC-SeNPs demonstrated enhanced antioxidant activities in both DPPH radical scavenging and Trolox equivalent antioxidant capacity (TEAC) assays.<sup>[145]</sup>

Stabilization of SeNPs was also studied using cationic pullulan, a water-soluble nonionic polysaccharide, which presents several advantages, such as low-toxicity and biocompatibility, linked to FA, using chemical synthesis and cysteine as reducing agent, producing Se microflowers, whose conformation seemed to be dependent on the amount of cysteine used. These also presented antitumor properties by serving as DOX carriers, enhanc-

ing its antiproliferative effect toward cancer cells, while reducing their cytotoxicity against normal cells.<sup>[19]</sup> Also, Yu et al. stabilized SeNPs with galactose (GA), producing GA-SeNPs used for DOX loading, forming nanostructures stable for 16 d, with therapeutic potential against hepatocellular carcinoma.<sup>[146]</sup> Also, some polysaccharides have been chosen for SeNPs production due to their medicinal applications, with the goal of studying a potential synergy between the two compounds. For example, a water-soluble  $\beta$ -(1,3)-D-glucan (BFP) with a triple-helix conformation, isolated from the fruits of a black Chinese fungus known for its anticancer activity, was used to produce BFP nanotubes to which SeNPs were embedded, producing BFP-Se, with an average diameter of 118 nm. The BFP nanotubes interacted with SeNPs through its hydroxyl group, producing structures with high stability in water and with strong anticancer properties.<sup>[147]</sup>

### 3.2.6. Peptides and Other Compounds

Several other compounds have been used for stabilization and functionalization of SeNPs. For example, Feng et al. studied the decorated potential of the aminoacids valine (Val), aspartic acid (Asp), and lysine (Lys) to produce smaller, more negatively charged, and stable SeNPs. The aminoacids conjugated with SeNPs through their —NH<sub>3</sub><sup>+</sup> groups, producing uniform spherical SeNPs with exception of Asp conjugation, which resulted

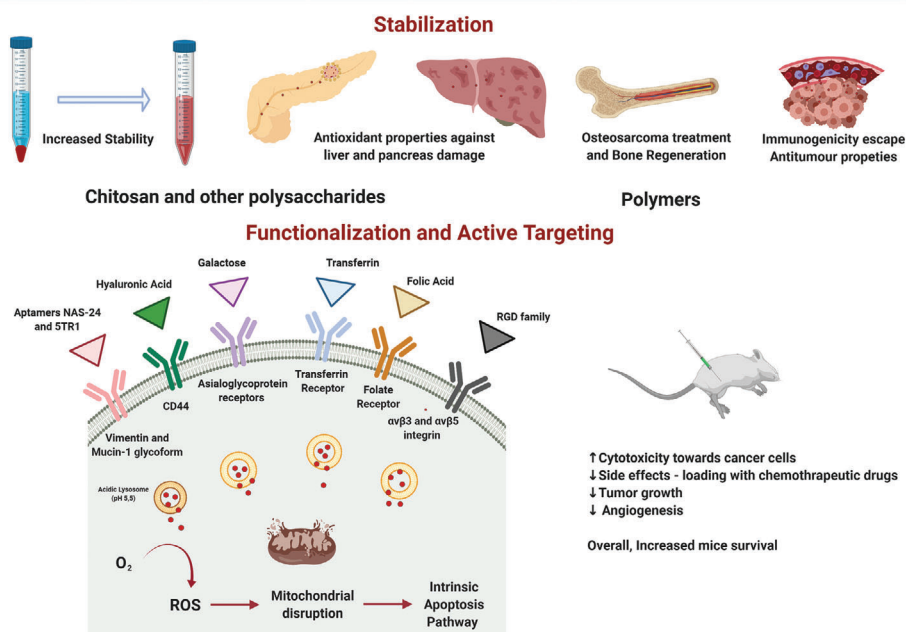


**Figure 12.** Main compounds used in SeNPs functionalization. Figure created with Biorender.

in irregular SeNPs. Lys conjugation produced more stable SeNPs, because Lys offers more two  $\text{NH}_3^+$  groups than Val and Asp to bind to SeNPs.

Peptides have also been used in SeNPs functionalization due to their ability to enhance cellular delivery via noncovalent binding and as a result of the existence of a wide range of aminoacids with several physicochemical properties.<sup>[149]</sup> For example, Shirazi et al. stabilized SeNPs with a peptide synthesized by Fmoc/tBu-based solid-phase chemistry, composed of four arginine, five tryptophan, and one cysteine being that tryptophan is the aminoacid with the highest reducing efficiency, arginine increased the reducing activity and cysteine facilitated the SeNPs stabilization through S—Se bonds. The stabilized SeNPs displayed an enhanced uptake in several cancer cell lines, by the interaction of tryptophan and arginine with the lipid bilayer's hydrophobic groups and the negatively charged phospholipids, causing deformation of the exterior phospholipid monolayer and internalization of the nanosystem by caveolae-mediated and macro pinocytosis pathways. Thereby, this nanosystem has shown synergic activities with several antitumor drugs, enhancing their antiproliferative effects.<sup>[149]</sup> A synthetic peptide composed by 12 aminoacid denominated GE11 is another peptide used for SeNPs functionalization. Pi et al. functionalized SeNPs with GE11 by EDC chemistry, in which the  $-\text{NH}_2$  groups of the loaded SeNPs covalently bound to the  $-\text{COOH}$  groups of GE11. The functionalized nanosystem was loaded with oridonin to study its antiproliferative properties against esophageal cancer.<sup>[150]</sup> RGD, a peptide composed by the sequence Arg-Gly-Asp, has also been used to functionalize SeNPs, due to its unique ability to recognize  $\alpha v \beta 3$  and  $\alpha v \beta 5$  integrins on target cells (Figure 12).<sup>[24]</sup> A similar peptide, RGDfC, constituted by Arg-Gly-Asp-d-Phe-Cys has also been used due to its ability to specifically target  $\alpha v \beta 3$  integrin, commonly expressed in several types of cancer cells,<sup>[151]</sup> resulting in

nanosystems that remain stable for 16 d. RGDfC-SeNPs are also able to load the chemotherapeutic drug DOX, resulting in efficient antitumor nanosystems.<sup>[152]</sup>

Proteins have also been used for SeNP stabilization and functionalization. Zhang et al. analyzed the properties of SeNPs stabilized with  $\beta$ -lactoglobulin ( $\beta\text{Ig}$ ), the most abundant whey protein in cow's milk, which comprises a lot of properties such as strong affinity for several cellular molecules, such as retinol, vitamin D, fatty acids, phenolic compounds, and cholesterol. The stabilization resulted in amorphous red SeNPs with a size of 40 nm, stable in 4 °C for at least 30 d, although their size increased to 80 nm when stored at room temperature. The conjugation was initiated by the electrostatic attraction of the selenium precursor,  $\text{HSeO}_3^-$  and the protonated amino groups on  $\beta\text{Ig}$ , at a pH of around 3.5. Afterward,  $\text{HSeO}_3^-$  was reduced to  $\text{Se}^0$ , which agglomerated, forming a Se nucleus that continuously grown, with  $\beta$ -lactoglobulin bound through its hydrophobic groups.  $\beta\text{Ig}$ -SeNPs were stable at pH 2.5–3.5 and 6.5–8.5, however was unstable at 4–6, near the  $\beta\text{Ig}$  isoelectric point (5.1), resulting in lower absolute zeta-potential and aggregation. IgB-SeNPs was also shown to reduce the toxicity when compared with selenite.<sup>[25]</sup> Tfr was also studied to functionalize SeNPs for antineoplastic applications, since its receptor is usually overexpressed in cancer cells compared with normal cells (Figure 12). Tfr-SeNPs have shown potential to deliver DOX to several cancer cells, in a four-layer structure, wherein Tfr is covalently linked to the  $\text{NH}_3^+$  groups of chitosan.<sup>[119]</sup>

Chung et al. demonstrated BSA has the potential to stabilize SeNPs, producing SeNPs with a size below 50 nm when the ratio Se salt:ascorbic acid (reducing agent used) was 1:4 or below, that were then studied as antibacterial agents against of *S. aureus* infections.<sup>[97]</sup> BSA contains three homologous domains in their tertiary structure, and its cysteine residues create 17

disulfide bonds to construct a double-loop bridging pattern. Kalishwaralal et al. demonstrated that once exposed to 121 °C, these disulfide bonds break, exposing —SH groups, which can be used for reduction of Se (IV) to Se (0). Interestingly, when the same reaction was attempted using other proteins such as lipase and protease, red SeNPs were not produced, probably due to the lack of —SH groups.<sup>[153]</sup>

Other compounds, such as ferulic acid (Fer), a substance derived from *Ferula foetida*, that is known for its notable antithrombotic, hypolipidemic, and anti-inflammatory applications, was used to decorate SeNPs, producing uniform spherical Fer-SeNPs with an average diameter of 105 nm. It was observed that Fer's absorption peak corresponding to the —OH group shifted from 3436 to 3396 cm<sup>-1</sup> during SeNPs preparation, suggesting that the SeNPs surface interacts with Fer molecules through their hydroxyl groups. These Fer-SeNPs were studied for their anticancer properties.<sup>[31]</sup>

The stabilization of SeNPs using mesoporous silica (MS) originated nanosystems with prolonged release of both silica and Se.<sup>[154,155]</sup> Chen et al. demonstrated that Se interacted with mesoporous silica NPs (MSNPs), forming 3p BE shifts, being the silicon in the form of SiO<sub>2</sub>.<sup>[155]</sup> The release of Se was higher in acidic pH 5.5 than in physiologic pH 7.4.<sup>[155]</sup> The use of MS to stabilize SeNPs has shown to have both antibacterial<sup>[155]</sup> and anticancer potential.<sup>[154]</sup>

Furthermore, genetic material was also used for SeNPs functionalization. Aptamers, such as NAS-24, are short single-stranded DNA or RNA sequences that can specifically target several molecules overexpressed in cancer cells. For example, both aptamers NAS-24 and ETR1 were used to functionalized SeNPs (Figure 12) loaded with epirubicin for antiproliferative studies in breast cancer and hepatocellular carcinoma cells. NAS-24 not only targets vimentin, a filament protein that modulates cell migration and adhesion, and apoptosis, being a prospective biomarker for metastasis. Furthermore, NAS-24 possesses a guanine-cytosine group, which is an ideal region to bind to anthracyclines, such as epirubicin. 5TR1 aptamer can bind to the mucin-1 glycoform, which is overexpressed in several cancers, such as breast cancer, despite it not being present in hepatocellular carcinoma cells. Therefore, the use of these aptamers to functionalize SeNPs enhanced their uptake in cancer cells by inducing receptor-mediated endocytosis.<sup>[136]</sup>

### 3.3. Main Properties and Advantages of SeNPs

SeNPs present better biocompatibility and efficacy than inorganic and organic Se, as well as the opportunity to functionalize the surface with several compounds that may influence their physicochemical properties and pharmacokinetics.<sup>[5,20]</sup> Therefore, SeNPs functionalization can influence their toxicity, surface charge, and surface hydrophobicity, which are considered crucial for their therapeutic activity.<sup>[20]</sup>

#### 3.3.1. Physical Properties of SeNPs

Properties of SeNPs depend on the method used for their preparation<sup>[79]</sup> and on the compounds used for its

stabilization/functionalization.<sup>[40,156]</sup> SeNPs characteristics like shape, size, and structure, are influenced by several parameters during their preparation and storage, such as concentration, temperature, nature of biomolecules, and pH of the reaction mixture. For example, spherical SeNPs have been proved to have high biological applications, while Se nanowires have high photoconductivity.<sup>[79]</sup> Overall, SeNPs are produced by reducing Se oxyanions into elemental Se, leading to solutions with color ranging from pink, orange, and red,<sup>[89,101,138]</sup> due to the excitations of the SeNPs surface plasmon resonance formed in the reaction mixture,<sup>[153]</sup> presenting a maximum absorption at 200–400 nm.<sup>[134]</sup> Therefore, SeNPs photoelectron spectroscopy pattern includes the distinctive Se 3d peak around 54–56 eV, as well as the Se 3p3, Se 3p1 and Se 3s peaks,<sup>[155,157]</sup> confirming the formation of its zero-valent oxidation state, although usually accompanied by the peak correspondent to a residual Se(IV), around 56–60 eV.<sup>[26,123,157,158]</sup> Also, using X-ray diffraction analysis, several studies identified a hexagonal ring lattice,<sup>[159–162]</sup> or a trigonal phase.<sup>[163–166]</sup> The formation of SeNPs with a hexagonal ring structure does not appear to be related to the production method or the shape of the SeNPs produced, since this type of crystal arrangement occurs in both biosynthesized<sup>[159–161]</sup> and chemically synthesized SeNPs,<sup>[19]</sup> and with Se nanostructures with rod-like,<sup>[161]</sup> spherical<sup>[160]</sup> and flower-like shape.<sup>[19]</sup> On the other hand, the formation of trigonal SeNPs seems to be more related to SeNPs physical synthesis methods.<sup>[163–166]</sup>

In general, the charge of SeNPs is negative,<sup>[37,138,121]</sup> however surface modification with positive charged compounds such as chitosan can also flip the charge of SeNPs to positive.<sup>[123,121]</sup> Also, the coating with different enantiomers can produce SeNPs with different characteristics.<sup>[108,167]</sup> For example, Hung et al. produced chiral SeNPs using the L-, D-, and DL- forms of GSH. While the L-GSH-SeNPs and D-GSH-SeNPs were well dispersed and had average sizes of 126.7 and 142.6 nm, respectively, the DL-GSH-SeNPs easily aggregated. Also, the  $\zeta$ -potential of L-GSH-SeNPs and D-GSH-SeNPs were highly negative (-29.5 and -25.3 mV, respectively), suggesting the existence of a strong repulsion among the SeNPs produced using the single chiral nanosystem, while DL-GSH-SeNPs were almost neutral (-9.1 mV). Furthermore, in vivo assays in mice using <sup>64</sup>Cu-radiolabeling positron emission tomography (PET) demonstrated that the chiral SeNPs presented different pharmacokinetics mechanisms. For example, L-GSH-SeNPs accumulation in the liver, spleen, and intestines was significantly higher than D-GSH-SeNPs accumulation, while DL-GSH-SeNPs and D-GSH-SeNPs escaped liver uptake and presented a faster renal clearance than its L-counterpart. Indeed, DL-GSH-SeNPs presented a stronger renal presence than the D-counterpart, specifically due to its neutral charge and steric conformation, that enabled a better electrostatic interaction with kidney and reduced the opsonization by the phagocytic system.<sup>[108]</sup>

It has been demonstrated that NPs tend to destabilize and create precipitates when exposed to solutions with higher ionic strengths, mostly due to the density of the electrical double layer and the screening effect of the ions present in the solution. Selmani et al. demonstrated that the stability of SeNPs depends on the surface coating, studying the modifications of SeNPs stabilized with PVP, PLL, PAA, and AOT in CaCl<sub>2</sub> and NaCl solutions. SeNPs were shown to have less stability and started to



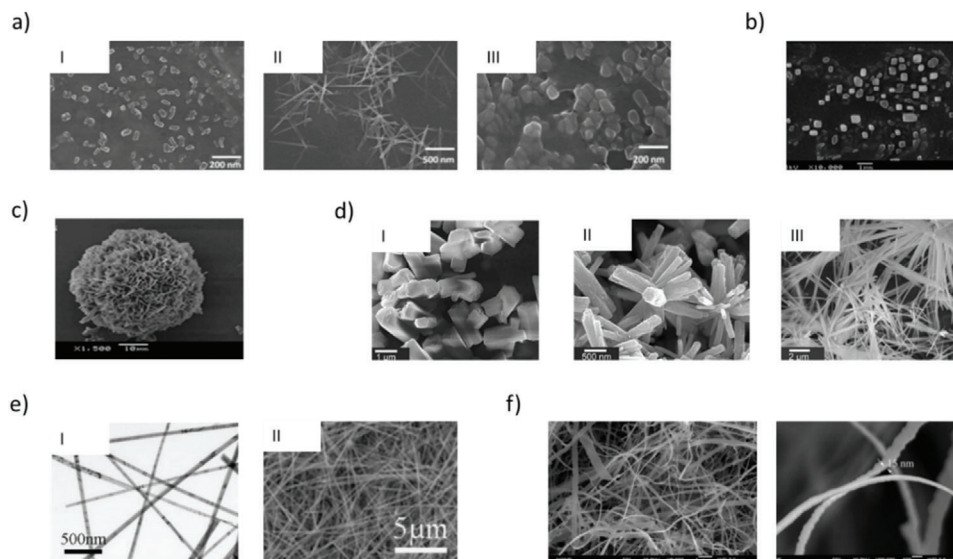


**Figure 13.** SeNPs shape can be influenced by a) their coating agents and b) the interactions among them; c) the Se reducing agent; d) the solvents used and the storage conditions; e) the reaction temperature; and f) the production method itself. Reproduced with permission.<sup>[156]</sup> Copyright 2018, Elsevier. Reproduced with permission.<sup>[169]</sup> Copyright 2016, Elsevier. Reproduced with permission.<sup>h</sup> Copyright 2018, Elsevier. Reproduced with permission.<sup>[18]</sup> Copyright 2014, Elsevier. Reproduced with permission.<sup>[166]</sup> Copyright 2010, Elsevier. Reproduced with permission.<sup>[165]</sup> Copyright 2004, Elsevier, respectively.

aggregate in  $\text{CaCl}_2$  solutions, since divalent cations have more potential to decrease the electrostatic aggregation barrier than monovalent ones, therefore decreasing more efficiently the absolute zeta-potential. PLL coating offered the least cationic protection in both NaCl and  $\text{CaCl}_2$  solutions, with formation of PLL-SeNPs precipitates ranging from few hundreds until few thousands nm in low concentration of NaCl and  $\text{CaCl}_2$ . After 24 h of incubation, PAA-SeNPs were shown to be unstable at the highest  $\text{CaCl}_2$  concentration used ( $30 \times 10^{-3}$  M), although the size distribution increased in several NaCl solutions. AOT-SeNPs presented the smallest size and were, therefore, more stable. Therefore, SeNPs depend on its size, coatings, and storage medium.<sup>[138]</sup>

The study of other physical characteristics like the wetting properties of SeNPs was also studied by Tran et al. on titanium (Ti) hydrophilic implants. SeNPs formed air pockets that increased the contact angles and implants' roughness, which contradicts Wenzel theory that affirmed that lower contact angles exist on rougher hydrophilic surfaces. Therefore Tran et al. proposed a new model to explain the wetting properties of the SeNP coated Ti implants with a possible application for the development of new nanomaterials with therapeutic applications.<sup>[168]</sup>

As already indicated, SeNPs can also present several shapes, according to the stabilizer agent used and the preparation conditions.<sup>[18,156]</sup> Overall, spherical SeNPs have been used for biological and medicinal purposes,<sup>[16,20]</sup> but reports have also described methods to produce SeNPs with other shapes, such as cubic-like,<sup>[169]</sup> nanorods,<sup>[93,156]</sup> nanowires and nanotubes,<sup>[166]</sup> nanoribbons,<sup>[165]</sup> nanoneedles,<sup>[18,156]</sup> and "flower-like" assemblies.<sup>[18,19]</sup>

Chaudhary et al. demonstrated that SeNPs shape can be influenced by their coating, using Brij-58, sodium dodecyl sulfate (SDS) and hexadecyl trimethyl ammonium bromide (CTAB) sur-

factants as stabilizer agents. For example, Brij-58-SeNPs had rectangular and square morphology (Figure 13a-I), SDS-SeNPs exhibited squared shape forms trapped in spiny needle shaped structures (Figure 13a-II), and CTAB-SeNPs were spherical, however had the tendency to form rod shapes (Figure 13a-III).<sup>[156]</sup>

Moreover, SeNPs shape can also be influenced by the type of interactions existing among the stabilizer molecules. Luesakul et al. produced cubic SeNPs (Figure 13b) using FA, gallic acid, and synthetic *N,N,N*-trimethyl chitosan. The cubic form was created due to hydrogen bonding and  $\pi$ - $\pi$  stacking of the phenyl ring of gallic and FA among the neighboring particles.<sup>[169]</sup> The reducing agent used during the chemical production of SeNPs can also influence their morphology. The use of L-cysteine as a reducing agent, made it possible to produce Se microflowers (Figure 13c), when cationic pullulan and FA were used as coating agents and DOX was used as loading drug. However, both  $\text{Na}_2\text{SeO}_3$  to cysteine concentration ratios and the concentration of cationic pullulan and FA were determinant for the production of microflowers. These structures mainly appeared at  $\text{Na}_2\text{SeO}_3$  to cysteine concentration ratios from 1:1.6 to 1:2 and cationic pullulan and FA concentrations of 0.45% (w/v). During the chemical process, the mercapto group of L-cysteine oxidized into its disulfide derivative, which may play a crucial role in formation of the hexagonal plated sheets formed among the stabilizer agents via intermolecular interactions, such as electrostatic interaction,  $\pi$ - $\pi$  interactions, hydrogen bonding, and van der Waals forces.<sup>[19]</sup>

The shape of SeNPs is also dependent on the conditions of preparation and storage. Kumar et al. produced spherical SeNPs using hydroquinone as reducing agent, but after alkalization using NaOH and further incubation at 40 °C, the SeNPs color switched from red to black, with formation of Se hexagonal crystals (Figure 13d-I). Following the addition of ethanol, SeNPs morphology changed into rod-like SeNPs that aggregated

into “flower-like” assemblies (Figure 13d-II). The addition of cyclohexane gradually changed SeNPs from spherical to needle-like forms (Figure 13d-III).<sup>[18]</sup> The temperature used for SeNPs preparation also had an impact on the conformation of SeNPs. Chen et al. produced trigonal Se (t-Se) nanowires in absolute ethanol at room temperature (Figure 13e-I), while t-Se nanotubes were achieved at 85 °C in aqueous solution (Figure 13e-I).<sup>[166]</sup> t-Se was also used to produce nanoribbons (Figure 13f) that consisted of beads in linear aggregates, using a vapor-liquid process, producing nanostructures that may be used to fabricate nanoscale optoelectronic tools.<sup>[165]</sup> Hageman et al. have also manipulated SeNPs shape using changes in temperature and pH, in which amorphous SeNPs were observed at 20 °C and pH 7, at 30 °C and pH 7, at 40 °C and pH 7 and also at 20 °C and pH 6, while acicular crystalline hexagonal SeNPs and rosettes were detected at 50 °C and pH  $\geq 7$ , at 40 °C and pH  $> 7$ , or at 30 °C and pH  $\geq 8$ .<sup>[170]</sup>

### 3.3.2. Toxicity of SeNPs

SeNPs have presented lower toxicity than inorganic and organic Se,<sup>[5,13,36]</sup> which indicates that reducing inorganic Se ions into elemental Se is a promising environmentally friendly technique to remove Se from industrial water.<sup>[170]</sup> However, it is also important to establish SeNPs toxicity and their effects on nature and in the human body, since its optimal concentration largely depends on the species, the development stage, and other environmental factors. Overall, SeNPs toxicity is related to it increasing ROS generation and cell membrane disruption.<sup>[36,138,171]</sup> Kalishwaralal et al. have studied the effects of SeNPs on Zebrafish embryos, a species that share 85% of human genome, demonstrating that although no evident mortality appeared at lower concentrations (5–10  $\mu\text{g mL}^{-1}$ ), exposure to high concentrations (20–25  $\mu\text{g mL}^{-1}$ ) resulted in a considerable percentage of mortality, with abnormalities appearing, such as cardiac malfunction (blood congestion at the cardiac inflow tract and resultant pericardial edema and decrease of heart rate) and tail malfunction.<sup>[153]</sup>

Although SeNPs capped with a polysaccharide-protein complex derived from *Pleurotus tuberregium*, improved the growth of tilapia, showing potential as an aquatic feed additive,<sup>[172]</sup> other recent studies have shown the dose-dependent aquatic toxicity of SeNPs using the freshwater crustacean *Daphnia magna* and marine bacterium *Vibrio fischeri* as standard organisms, using SeNPs stabilized with AOT; PAA, PVP, and PLL. All coated SeNPs caused a 50% reduction in the bioluminescence of *V. fischeri* and, although after 4 h of incubation the most toxic SeNPs were those coated with PVP and PAA, with a minimum biocidal concentration (MBC) of 50 mg Se L<sup>-1</sup>, while the SeNPs coated with AOT and PLL presented MBC values of 100 mg Se L<sup>-1</sup>, after 24 h there were not any statistically significant differences between the toxicities of the several SeNPs tested. Regarding *D. magna*, PAA-SeNPs were demonstrated to have the higher toxicity, similar to selenite, and PVP-SeNPs, although presented the highest percentage of free Se ions, were the least toxic, since these SeNPs more likely to agglomerate. Overall, all SeNPs could be classified as harmful to both species, according to the Directive 93/67/EEC (CEC1996) of the European Commission for the hazard classification of substances.<sup>[138]</sup>

Further studies concerning SeNPs toxicity were realized in plant and algal cells. SeNPs were shown to have genotoxicity potential in *Allium cepa* root meristems, demonstrating that bare SeNPs are more toxic than stabilized SeNPs and that the stabilizer agent also influences SeNPs' toxicity. Genotoxic effects of SeNPs included laggard, sticky, and clumped chromosomes, disturbed metaphase chromosomes, binucleated cells, and formation of chromosomal bridges (Figure 14a). SeNPs were also shown to decrease the chlorophyll content in *Chlorella sp.*, by blocking the electron transfer in photocenters, and affected the seed germination ability of *Vigna radiate* seeds, dimerizing its roots length (Figure 14b).<sup>[156]</sup>

More recent studies show that SeNPs supplementation promotes *Capsicum annum L.* growth in low dosages of 0.5 and 1 mg L<sup>-1</sup>, while dosages of 10 and 30 mg L<sup>-1</sup> induced malfunction in leaf and root development, with malfunctions on the vascular conducting tissues due to DNA hypermethylation and potential to induce epigenetic modifications. Also, while intake of low Se dosages promoted nitrate reductase activity, high Se intakes were associated with increased proline concentration.<sup>[171]</sup> SeNPs toxicity was also studied in mammalian cells like rat dermal fibroblasts, showing an inhibitory concentration (IC<sub>50</sub>) value of 46.5  $\mu\text{g mL}^{-1}$ . However, concentrations up until 31 mg mL<sup>-1</sup> induced an increase of the number of live cells, which indicates that the SeNPs can be beneficial or toxic, depending on the concentration used.<sup>[5,98]</sup> Further studies demonstrated the pharmacokinetics and the in vivo toxicity of SeNPs in rats. SeNPs have been dissolved and oxidized into inorganic oxoanions and Se (IV) by both microbial and chemical activities in the gastrointestinal tract.<sup>[173]</sup> Analysis of the rat organs demonstrated that the highest concentrations of Se were detected mainly in the liver and kidney.<sup>[173,174]</sup> Therefore, it is not surprising that the weight of these organs increased after SeNPs intake. However, viscera indices of the heart, testicle, and thymus decreased significantly in higher concentrations of SeNPs (8.0 mg Se per kg body weight). Kidney and liver are the main metabolizing organs of SeNPs, being able to metabolize lower concentrations of Se. The natural GSH reductive pathway showed limited activity, and higher concentrations of SeNPs led to the exhaustion of GSH reduction, and unstable GSSeSG or selenopersulfide intermediates were formed, inducing Se oxidative damage and toxicity.<sup>[173]</sup> While lower intakes of SeNPs (0.2 and 0.4 mg Se kg<sup>-1</sup>) resulted in increased body weight, higher intakes (2.0–8.0 mg Se kg<sup>-1</sup>) resulted in decreased body weight, which suggests SeNPs toxicity. Histologic assays confirmed SeNPs toxicity at higher dosages, showing hepatocyte necrosis and degeneration, morphological changes in the kidneys with signs of glomerulonephritis, and renal tubule necrobiosis, signs of hemorrhage in lungs, and thymus and testis atrophy, which translated into immunosuppression and reduced spermatogenesis, respectively.<sup>[174]</sup> Plasmatic selenoprotein P levels were used as a blood biomarker to compare the range of bioavailability and incorporation of Se provided by both selenite and SeNPs. While dosages of Se (IV) ranging from 0.05 to 0.5 mg Se per kg body weight increased Selenoprotein P levels compared to control, only the SeNPs dosage of 0.5 mg Se per kg body weight increased selenoprotein P levels. However, since the plasmatic levels were not considerably different for the highest dose SeNPs group compared with Se (IV), and it was concluded that both Se forms

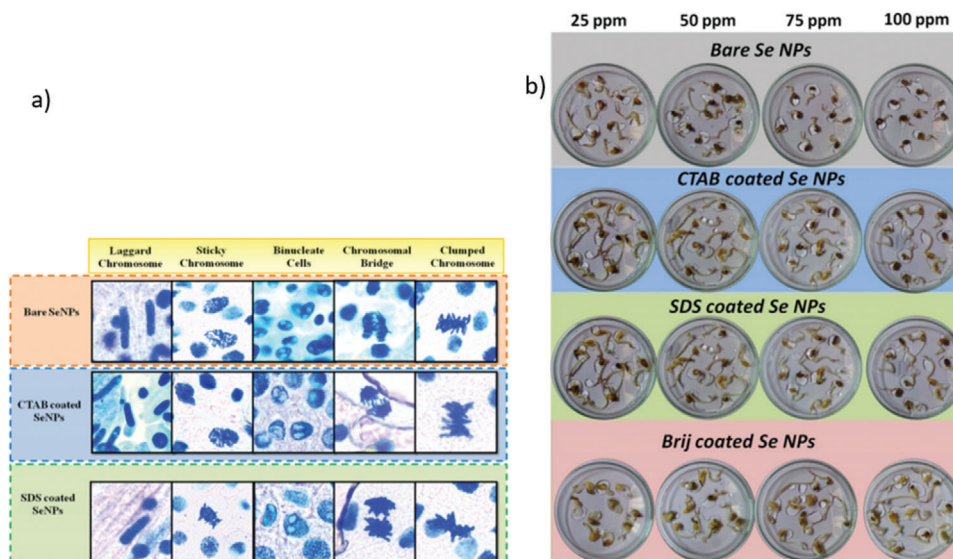


**Figure 14.** SeNPs toxic effects on *Allium cepa* root meristems. a) Chromosomal aberrations in *Allium cepa* root tip cells after SeNPs treatment. b) Influence of SeNPs concentration on *A. cepa* germination percentage, root growth, and seed germination index. Reproduced with permission.<sup>[156]</sup> Copyright 2018, Elsevier.

displayed equal bioavailability, the same conclusion was valid for the liver, plasma, and kidney Se. Se (IV) was more efficient than SeNPs in enhancing liver and kidneys TR levels. Regarding Se excretion, Se<sup>0</sup> in feces was higher in rats receiving SeNPs than those receiving Se (IV), indicating a lower absorption of Se<sup>0</sup>NPs. Se excretion in urine as Se-methylseleno-N-acetyl-galactosamine and the trimethylselenonium-ion was mainly increased for the higher dosages of both Se forms. It appears that Se is mainly excreted in the urine in the form of Se-methylseleno-N-acetyl-galactosamine.<sup>[173]</sup> Ultimately, it was demonstrated that SeNPs potential may directly link to human DNA, affecting its structure into a coiled and twisted form, leading to DNA damage.<sup>[156]</sup>

#### 4. SeNPs for Pharmaceutical Applications

SeNPs have been demonstrating several therapeutic applications due to its antioxidant or pro-oxidant effects, depending on the dose and duration of treatment.<sup>[175]</sup> SeNPs offer many therapeutic advantages compared to the ionized Se forms, such as better bioavailability and low toxicity, which can be extremely important since Se is a chemical element that, although essential to human life, presents a very narrow therapeutic window between the beneficial and the toxic effect.<sup>[122,175–178]</sup> Overall, SeNPs have shown potential in the treatment of several diseases, such as cancer, diabetes, inflammatory-related diseases, and by directly exercising their effect or by being incorporated in selenoproteins.<sup>[175]</sup> SeNPs have the possibility to be delivered by several routes, such as oral and intravenous administration, depending on the desired therapeutic application.<sup>[39]</sup>

SeNPs have been used nonfunctionalized or conjugated with other chemical compounds, whether for stabilization of the SeNPs or to direct them toward a specific target.<sup>[175]</sup> SeNPs have demonstrated that they inhibit at concentrations of 1 ppm both antibiotic-resistant gram-positive and gram-negative bacteria strains.<sup>[115]</sup> SeNPs larvicidal potential was also demon-

strated against the larvae of a dengue fever-causing vector *Aedes aegypti*.<sup>[179]</sup> SeNPs have shown potential against diabetes, having been proposed for insulin oral delivery, due to its antioxidant activity, protecting the pancreas against streptozotocin (STZ) side effects.<sup>[13]</sup> SeNPs have also shown potential against Huntington's disease, a disease characterized by neuronal degeneration, diminishing the patients' physical and mental skills overtime. SeNPs, in a dose-dependent way, reduced neuronal death in HA759 mutated nematodes, by decreasing the protein aggregation corresponded to the HTT gene mutations and the amount of ROS and by downregulating histone deacetylase mRNA, decreasing the axonal degradation and reacting better towards stimuli.<sup>[176]</sup> SeNPs have also been shown to reduce the viability of immortal keratinocyte cell lines, with IC<sub>50</sub> values lower than 4 μg mL<sup>-1</sup> by promoting the appearance of ROS and loss of mitochondrial membrane potential, enhancing of amount of proapoptotic proteins, such as tumor necrosis factor alfa (TNF-α) and Bax and downregulating anti-apoptotic proteins like Bcl-2, c-Jun, c-MET, p-44/42 MAPK, and MMP-7, leading to cell cycle arrest at Sub G1 phase and apoptosis by autophagy. This cytotoxic property of SeNPs can be useful in the treatment of skin diseases related to keratinocytes hyperproliferation, such as psoriasis, vitiligo, skin fibrosis, and melanoma.<sup>[180]</sup>

However, most of the studies concerning SeNPs therapeutic effects regard its anticancer properties, since Se has less probability to be pro-oxidant and to cause DNA damage in healthy cells than in cancer cells. Se has been shown to induce apoptosis in cancer cells, by ROS production and activation of several caspases, inducing cell arrest, chromatin condensation and DNA fragmentation, loss of cellular adhesion, inducing apoptosis through mitochondrial pathways and formation of apoptotic bodies. SeNPs were functionalized with compounds whose receptors are more abundant in cancer cells than in normal cells, such as FA, adenosine triphosphate (ATP) and sialic acid to preferably target cancer cells. SeNPs were also studied in

**Table 3.** Antidiabetic effects of SeNPs presented in several studies.

Treatment after STZ induced diabetes <sup>a)</sup>	Wt	Glycemia	Antioxidant potential	Cholesterol, LDL-C, triglyceride	HDL	Concentration	Type of study	Refs.
STZ only	↓	↑	↓	↑	↓	–	In vivo study	[107]
Chitosan-SeNPs	↑	↓	↑	↓	↑	2.0 mg Kg <sup>-1</sup>	In vivo study	[107]
RTFP-SeNPs	–	–	↑	–	–	2.0 mg mL <sup>-1</sup>	In vitro study	[182]
CVP-SeNPs	↑	↓	↑	↓	↑	0.5 mg Se kg <sup>-1</sup>	In vivo study	[142]
MPE-SeNPs	–	–	↑	–	–	900 µg d <sup>-1</sup>	In vivo study	[181]
Glucose-PVP-SeNPs	↑	↓	↑	–	–	–	In vitro study	[178]
Metformin-SeNPs combination therapy	↑	↓	↑	↓	↑	0.4 mg kg <sup>-1</sup> SeNPs-metformin	In vivo study	[177]
	↑	↓	↑	↓	↑	500 mg/Kg bw/day metformin and Chitosan-SeNPs 2 mg Se/Kg/day (8 weeks treatment)	In vivo study	[183]

<sup>a)</sup> CVP, Polysaccharides from *Catathelasma ventricosum*; HDL, high-density lipoproteins; LDL-C, low density lipoprotein-cholesterol; MPE, *Pueraria lobate* extracts; RTFP, polysaccharide extracted from *Rosa roxburghi* fruit; STZ, streptozotocin; Wt, animal weight.

combination with others chemotherapeutic agents such as DOX, 5-Fu, adriamycin, irinotecan, and cisplatin enhancing their activity and protecting the normal cells against their side effects (e.g., cisplatin nephrotoxicity and anastrozole osteoporosis).<sup>[13]</sup>

#### 4.1. Diabetes

There are several hypoglycaemic medicines currently available for diabetes treatment, such as biguanides and sulfonylureas, however, these medicines have several side effects like hypoglycemia, gastrointestinal distress, liver, and pancreatic damage. Se has already been shown to be an effective antioxidant to combat several biomarkers relative to diabetes, acting like insulin in STZ-induced diabetic mice, by having similar hypoglycaemic effects,<sup>[178,181]</sup> and promoting antioxidant activities by being the major active compound in several antioxidant proteins such as GPx.<sup>[107]</sup>

Several experiments have studied the potential of SeNPs as a tool to be used in diabetes therapy (Table 3), showing their antiapoptotic potential, by influencing HSP70, SIRT1, and Bcl-2 production.<sup>[13]</sup> Overall, in vivo studies used STZ to trigger diabetes in mice/rats animal models, by destroying their pancreatic islet  $\beta$ -cells, diminishing the insulin body concentration and increasing their blood glucose levels.<sup>[142,177]</sup> Several other studies have demonstrated the antidiabetic potential of SeNPs functionalized with negative charged antidiabetic polysaccharides<sup>[142,181,182]</sup> or with combination therapy with known antidiabetic drugs.<sup>[177]</sup> However, nonfunctionalized SeNPs also had antidiabetic properties on their own. Chitosan-SeNPs proved to have antidiabetic effects at the concentration of 2.0 mg kg<sup>-1</sup>, by increasing the body weight and controlling the glycemia on STZ-treated mice. Both concentrations of 0.5 and 4 mg kg<sup>-1</sup> had the poorest antidiabetic activities, which suggested the existence of a therapeutic window. The antidiabetic effect of these SeNPs was proved to be a result of their antioxidant activities, by increasing the activity of several enzymes like GPx, catalase (CAT), and SOD, which led to a decrease of LDL-C, triglyceride,

and total cholesterol levels and an increase of HDL levels, showing these NPs as possible antidiabetic supplements.<sup>[107]</sup>

Functionalization of SeNPs with several polysaccharides, such as RTFP-3, collected from *Rosa roxburghi* fruit, have also potential synergistic antidiabetic properties. RTFP-3 is a known antioxidant and  $\alpha$ -glucosidase inhibitor and its use as a functionalizing agent resulted in stable SeNPs with excellent antidiabetic effects. The resulting SeNPs exhibited great antioxidant properties in both DPPH and ABTS radical scavenging activity assays, and in the oxygen radical absorbance capacity (ORAC) assay. Also, the viability of islet  $\beta$ -cells incubated with H<sub>2</sub>O<sub>2</sub> was improved with the administration of RTFP-SeNPs, by decreasing the mitochondria oxidative stress, via downregulation of UCP-2 expression, a protein associated with the reduction of the mitochondrial membrane potential and, and thereby reducing the caspase activation (caspases-8/-9 and 3). Therefore, RTFP-SeNPs have shown to reverse the cell arrest at G1 phase caused by H<sub>2</sub>O<sub>2</sub>, increasing mainly the cells in the S phase.<sup>[182]</sup>

SeNPs have been demonstrated to have synergistic antidiabetic effects when functionalized with polysaccharides from *Catathelasma ventricosum* (CVP). CVP-SeNPs recovered the body weight and decreased the blood sugar in mice treated with STZ, especially at the concentration of 0.5 mg Se kg<sup>-1</sup>. CVP-SeNPs decreased the oxidative stress produced by the diabetes-derived hyperglycemia, by increasing the activity of antioxidant enzymes, such as GPx and SOD, and diminishing the activity of malondialdehyde (MDA), an organic compound that produces oxidative stress. In addition, the levels of cholesterol, LDL-C, and triglyceride, increasing the HDL. These SeNPs also exhibited a synergistic effect with vitamin E towards the previous parameters.<sup>[142]</sup>

SeNPs were also functionalized for oral delivery with *Pueraria lobate* extracts (MPE), which are traditionally used in diabetes treatment, due to their potential to stimulate insulin excretion, inhibit  $\alpha$ -glucosidase and enhance glucose use. About 900 µg d<sup>-1</sup> of MPE-SeNPs were administered daily to rats (human equivalent to 150 µg d<sup>-1</sup>). MPE decreased the SeNPs first-pass effect, enhancing their oral bioavailability and increased its transport toward liver, through the portal vein, as well as showing the ability

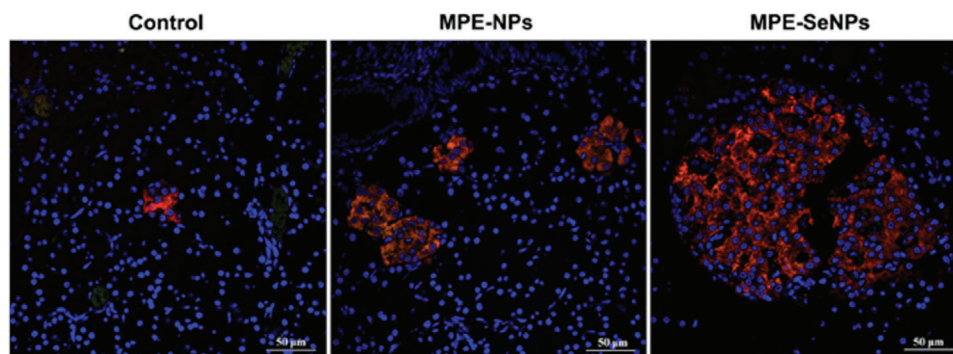


**Figure 15.** Fluorescent histomorphologies of the pancreatic islet of diabetic rats treated with MPE-NPs and MPE-SeNPs for 2 weeks. Cy3-conjugated antibody was used to specifically label insulin, and DAPI was used for nuclei labeling. After SeNPs treatment, a dramatic increase of the insulin secreted cells was observed. Reproduced with permission.<sup>[181]</sup> Copyright 2019, Springer Nature.

to sustain their release. MPE-SeNPs have been shown to enter the cells through several pathways, such as clathrin- and caveolin-mediated endocytosis. Similar to previous studies, MPE-SeNPs have been shown to have antioxidant activities, protecting islet  $\beta$  cells in oxidant environments (Figure 15).<sup>[181]</sup>

El-Borady et al. studied SeNPs antidiabetic potential when capped with glucose and PVP. The SeNPs demonstrated caused weight loss and a decline in food consumption, and to revert the increase of glucose levels in mice in which diabetes was STZ-induced. The SeNPs also decrease the levels of ROS, while increasing the levels of the antioxidant enzymes GSH and GPx, restoring the atrophic islets of Langerhans to their normal shape, and protecting the pancreatic tissues from oxidative damage. Interestingly, it was observed that the plasmatic levels of insulin in the SeNPs-control group were dramatically reduced when compared to the control group, which can be explained by the fact that Se itself has insulin-like properties.<sup>[178]</sup>

SeNPs have also shown to have a synergistic effect when combined with metformin.<sup>[177,183]</sup> The therapeutic combination showed synergic effects, increasing ROS scavenging, and controlling the weight and blood sugar better than the SeNPs or metformin alone, increasing the serum levels of insulin and the viability/activity of islet  $\beta$  cells, and enhancing liver and kidney functions. This combination therapy reduced triglycerides levels and increased high density lipoproteins (HDL) levels, better than the therapeutics used in monotherapy. This combination therapy has also shown to decrease the inflammation STZ-induced, by reducing the protein level of p65- NF- $\kappa$ B and COX-2, decreasing the expression of several cytokines and interleukins related to hepatic inflammation and damage. This combination also seemed to activate pIRS-1, pAKT, pGSK, and pAMPK pathways, enhancing insulin sensitivity and action.<sup>[177]</sup> More recently, Mohamed et al. also studied the synergy between metformin and SeNPs against diabetes induced by a high-fat diet and in STZ in rats, demonstrating that the concomitant treatment of metformin and SeNPs for 8 weeks not only prevented body weight loss and the increase in the fasting blood glucose levels, while controlling the insulin levels, but also restored the levels of hepatic enzymes associated with liver injury to that of healthy rats. Furthermore, the simultaneous administration of SeNPs and metformin regulated the lipid profile, reducing dyslipidemia in diabetes-induced rats, ameliorated the activity of several enzymatic antioxidants (CAT

and SOD), and stabilized the gene expression of proapoptotic proteins (caspase-3, Bax, Fas, Fas-L), while up-regulating Bcl-2 expression. The combination therapy also improved the pattern of cardiac injury markers, reducing the levels of troponin I and creatin kinase -MB isoenzyme. Histology studies demonstrated that, although STZ induced both cardiomyopathy and liver damage, the combined therapy reduced the cardiac and hepatic lesions to almost normal.<sup>[183]</sup>

#### 4.2. Alzheimer's Disease

Studies indicate that high concentrations of metal ions, such as  $\text{Cu}^{2+}$ ,  $\text{Zn}^{2+}$ ,  $\text{Fe}^{2+}$  bind and trigger the aggregation of  $A\beta$ , as well as contribute to the formation of cytotoxic ROS.<sup>[184]</sup> Therefore, therapeutics against Alzheimer's disease have focused on reducing these oxidant species and protecting the immune system.<sup>[185]</sup> However, the blood-brain barrier (BBB) is an obstacle for drug delivery, since more than 98% of low molecular weight drugs cannot cross it and alternatives, such as intracranial injection, have the risk of causing more neurotoxicity and physical damage.<sup>[186]</sup>

SeNPs have been shown to reduce  $A\beta$  aggregation and induce their disaggregation, in addition to acting as an antioxidant in the brain, either directly or by being part of GPx, several studies have functionalized them with specific molecules, such as sialic acid and epigallocatechin-3-gallate, a component of green tea, to enhance their permeability toward the BBB.<sup>[32,187]</sup> SeNPs have also been studied together with other compounds that also shown properties against Alzheimer's disease, such as resveratrol (Res),<sup>[188]</sup> curcumin (Cur),<sup>[184]</sup> chiral D-penicillamine (DPen),<sup>[167]</sup> and chlorogenic acid (CGA) (Figure 17).<sup>[64,185]</sup>

Res has already shown potential against Alzheimer's disease due to its antioxidant and neuroprotective properties, neutralizing the  $A\beta$  aggregation and its oxidative effects. Res-SeNPs have been shown to specifically bind to  $A\beta$  by N-donors existing in the aminoacids, creating a Se-N bond, increasing the Res inhibition on  $\text{Cu}^{2+}$ -induced  $A\beta$  aggregation (Figure 16a). Res-SeNPs have also been shown to decrease cell membrane damage, which Res is not capable of doing by itself. Res-SeNPs are not only harmless to neuroblastic cells (PC12 cells), but also have decreased their  $A\beta$ -induced apoptosis, protecting them from

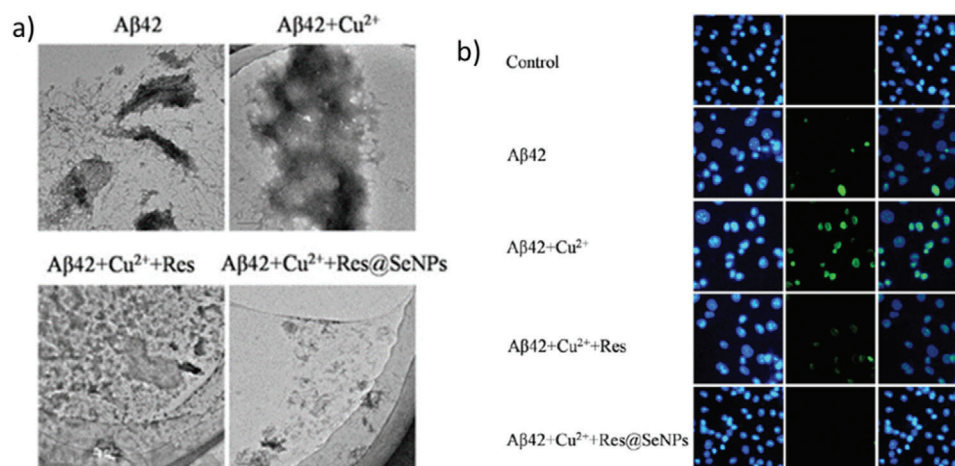


**Figure 16.** Res-SeNPs effect on Cu<sup>2+</sup>-induced Aβ<sub>42</sub> aggregation. a) While Aβ<sub>42</sub> monomers in 3 d incubation formed well-delineated aggregates, especially in presence of Cu<sup>2+</sup>, Res-SeNPs inhibits the formation of these aggregates; and b) A TUNEL-DAPI costaining assay, Res-SeNPs demonstrated to inhibit Aβ<sub>42</sub>-Cu<sup>2+</sup> complexes, while decreasing DNA fragmentation (stained in green) in PC12 cells. Reproduced with permission.<sup>[188]</sup> Copyright 2018, Wiley-VCH GmbH.

oxidant stress, showing a possible synergism between SeNPs and Res (Figure 16b).<sup>[188]</sup>

Cur, another natural compound, derived from *Curcuma longa*, has shown potential synergism with SeNPs against Alzheimer's disease. PLGA-stabilized Cur-SeNPs have displayed good viability for kidney, lung, liver, and heart cell lines. These NPs were able to cross the BBB and bound to Aβ, having antioxidant, anti-inflammatory anti-Aβ, and Anti-Tau hyperphosphorylation properties. It was shown that Cur binds Aβ by hydrophobic interactions at the Aβ nonpolar regions, developing their antioxidant and anti-inflammatory activity along with Se.<sup>[184]</sup> Pen has two enantiomers, LPen and DPen, and in spite of the low neuroprotective effect of the first enantiomer, the second one showed high potential to inhibit ion-induced Aβ and to enhance the memory. Pen-SeNPs were produced through formation of Se-S links, being that DPen-SeNPs were far more efficient in preventing Aβ formation and improving mice memory than the SeNPs formulated with the other enantiomer. LPen-SeNPs have been shown to be neurotoxic, mainly due to the L-enantiomer, while the D-enantiomer were much less toxic when functionalizing SeNPs, especially at low concentrations (less than 20 μg mL<sup>-1</sup>).<sup>[167]</sup>

SeNPs conjugation with CGA, an anti-inflammatory, antioxidant, and neuroprotective compound, has also been studied for Alzheimer's disease. CGA-SeNPs have been shown to reduce Aβ-generated ROS in a dose-dependent way, inhibiting their neurotoxicity and, therefore, decreasing the apoptosis rate, being also able to bind on the Aβ proteins N-donors, forming a Se-N bond, blocking their aggregation, which was translated in a synergic effect between CGA and SeNPs.<sup>[185]</sup> CGA-SeNPs have also demonstrated that they interact with several potential neurotoxic metals, such as Cu(II), possibly due to its reactive aromatic -OH groups. CGA-SeNPs also demonstrated to have better antioxidant capacity than chitosan-SeNPs and several inorganic and organic selenium species. However, Vicente-Zurdo et al. noticed that, while CGA-SeNPs did not inhibit Aβ aggregation and in the fibril length, chitosan-SeNPs prevented Aβ aggregation and diminished both the number and fibril width in the presence of

Zn(II), Fe(II), and Cu(II). Furthermore, chitosan-SeNPs also decline the Fe(II)-induced Aβ aggregation.<sup>[64]</sup>

More recently, Gao et al. produced SeNPs conjugated with chondroitin sulfate (CS), an extracellular matrix compound with anti-inflammatory, antioxidant, and neuroprotection activities, involved in neurogenesis, axon growth, synaptic plasticity, and neuron regeneration in the form of CS proteoglycan. Negatively charged CS-SeNPs were produced using L-cysteine as reducing agent at a CS/L-cys/Na<sub>2</sub>SeO<sub>3</sub> ratio of 2:2:1, with the formation of C-O...Se and C-N...Se bonds responsible for the high stability of the nanosystem. CS-SeNPs showed an improved inhibitory effect on Aβ<sub>1-42</sub> formation and aggregation into toxic Aβ<sub>1-42</sub> fibrils when compared to SeNPs and CS alone, decreasing β-sheet fibril formation in congo red assays. In vitro studies using a neural cell line (SH-SY5Y cells) indicated that CS-SeNPs inhibit Aβ fibrillation and reduced Aβ<sub>1-42</sub>-induced cytotoxicity. Also, CS-SeNPs protected the neural actin cytoskeleton from okadaic acid-induced instability, while reducing the amount of ROS and MDA produced by Aβ<sub>1-42</sub>, while increasing GPx levels, thereby decreasing the oxidative damage in neural cells. Furthermore, CS-SeNPs were shown to decrease tau protein hyperphosphorylation at Ser396 and Ser404 by controlling GSK3β activity, and overall decelerate the progression of AD.<sup>[189]</sup>

The functionalization of SeNPs toward Aβ has also been studied (Figure 17), by targeting two peptides, LPFFD and TGN in a 1:1ratio, stabilizing these NPs with chitosan. The positive-charge SeNPs produced could overcome the BBB and strongly recognize the β-sheet structures of the Aβ, blocking their aggregation. These two peptides have different effects in SeNPs efficacy. TGN enhances the amount of SeNPs crossing the BBB, also having a synergistic effect with Chitosan. LPFFD increases the linkage between SeNPs and Aβ through hydrophobic interactions, in addition to the electrostatic ones between the negative charged Aβ and the positive charged chitosan, inhibiting Aβ formation and the corresponding ROS, and improving neuro cell viability.<sup>[186]</sup> Vicente-Zurdo et al. compared the neuroprotective properties of several Se compounds with SeNPs stabilized with chitosan and

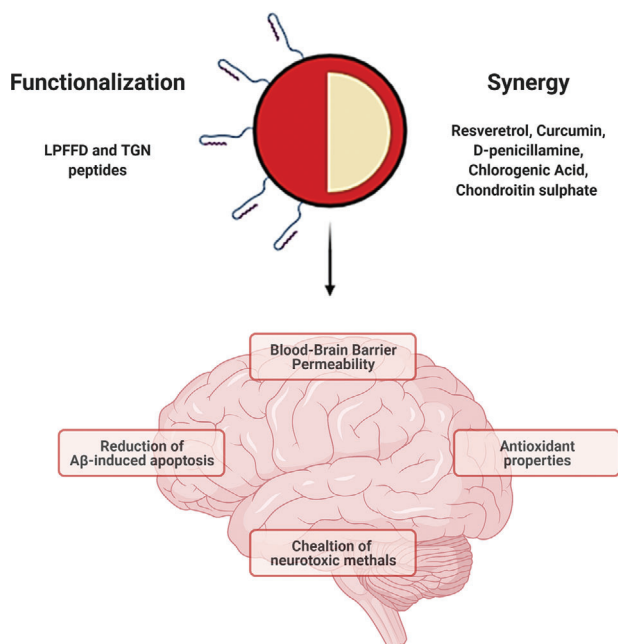


**Figure 17.** Mechanisms behind the SeNPs action against AD. Figure created with Biorender.

CGA, a substance known to promote brain activity, as well as having cardioprotective, anti-inflammatory, antiobesity, and antioxidant properties. The GCA-SeNPs not only demonstrated to form chelates with several neurotoxic metals and to have better antioxidant properties compared to chitosan-SeNPs, but also prevented metal-induced  $A\beta$  aggregation and disaggregated the  $A\beta$  fibrils formed, unlike the others Se compounds studied.<sup>[64]</sup>

Therefore, SeNPs have been demonstrated to have potential for Alzheimer's disease treatment, not only due to their antioxidant properties, but also by loading and functionalization with other potential therapeutic compounds, which have synergic therapeutic potential (Figure 17).

### 4.3. Anti-Inflammatory and Antioxidant Applications

SeNPs have been shown to have anti-inflammatory and antioxidant properties, exhibiting immunomodulatory and organ-protective properties.<sup>[190,191]</sup> For example, studies indicated that SeNPs protected the male reproductive system from aflatoxin B1 toxicity, decreasing the number of aberrant spermatozoa and the DNA fragmentation induced by aflatoxin B1, while increasing sperm count, motility and viability and fertilization in mice. Furthermore, histological studies demonstrated that SeNPs improved the structural architecture of testis, reducing the atrophy caused by aflatoxin B1 in the seminiferous tubules, although without full recovery.<sup>[72]</sup>

SeNPs also reduced radiation and carrageenan-induced inflammation in rats, decreasing several inflammation indicators, such as several cytokines ( $TNF-\alpha$  and  $IL-1\beta$ ),  $PGE_2$ , ROS, and thiobarbitone acid reactive substances, a by-product of lipid peroxidation, decreasing the number of leukocytes, monocytes and granulocytes, the exudate volume and associated pain. SeNPs demonstrated not only anti-inflammatory activity, but also anti-

hyperalgesia, by modulating peripheral pain mediators, without exerting any effect in the central nervous system. SeNPs immunomodulatory potential was also described, being able to prevent monocyte differentiation into macrophages, as well as diminish L-selectin expression through a metalloproteinase-dependent mechanism, preventing neutrophil migration and lymphocytes adhesion to endothelial cells.<sup>[191]</sup> SeNPs also show antioxidant potential, by directly diminishing the level of several oxidant species, and by increasing GPx levels,<sup>[42,78]</sup> which scavenge  $H_2O_2$  and lipid and phospholipidic hydroperoxides, turning them into water and alcohols, respectively.<sup>[42]</sup> Additionally, SeNPs loaded with CAT and functionalized with FA and HA are shown to target activated macrophages associated with rheumatoid arthritis and atherosclerosis via CD44 and FR- $\beta$  receptors which are higher expressed in these cells. Therefore, SeNPs specifically destroyed proinflammatory-activated macrophages responsible for producing high levels of  $H_2O_2$ , without affecting non-activated macrophages.<sup>[190]</sup> More recently, Huang et al. produced SeNPs using L-GSH, D-GSH, and DL-GSH, demonstrating that SeNPs chirality may influence their antioxidant properties. L-GSH-SeNPs presented higher antioxidant capacity than D-GSH-SeNPs, decreasing the oxidative effect and derived cytotoxic of palmitic acid in INS-1E cells (insulinoma cell line). Since L-GSH-SeNPs strongly adhere to INS-1E cells, resulting in a higher uptake compared to its L- and DL-counterpart, they also presented better ROS scavenging properties, preventing mitochondrial fragmentation and reducing caspase-8 and caspase-9 activities.<sup>[108]</sup> SeNPs also prevent neurotoxicity associated with cypermethrin, a substance used to control household insects. This substance can modify the sodium ion channels function, leading to motor deficit problems, which translated into an increased number of crossed squares, stops, and immobility duration in rats. However, Ali et al. verified ameliorating of these symptoms associated with cypermethrin neurotoxicity when SeNPs were administered at the dosage of  $2.5 \text{ mg Kg}^{-1}$ , three times a week for 21 d. SeNPs improved liver parameters, attenuated the decrease of gamma-aminobutyric acid levels in the brain tissue, reducing the levels of several inflammatory cytokines and oxidant compounds, such as MDA, while raising GSH levels. Also, histological studies demonstrated that SeNPs were able to decrease cypermethrin cytotoxicity on pyramidal cells, with a decline in faint shrunken cells with pyknotic nuclei and reducing the number of congested blood vessels in the cerebral cortex and pia mater.<sup>[192]</sup> Overall, SeNPs are a powerful tool that can be used for the treatment of diseases with a pathology based on inflammatory and oxidant compounds.<sup>[33,190]</sup>

Rheumatoid arthritis (RA) is a chronic disease characterized by several joint inflammations and tissue damage promoted by increased ROS production.<sup>[193]</sup> SeNPs, unlike selenite, have shown good cellular viability, while decreasing paw size and cartilage degradation better than approved corticosteroids in Wistar rats with induced RA. Inflammation biomarkers, such as C-reactive protein,  $PGE_2$ ,  $TNF-\alpha$ ,  $IL-1\beta$ ,  $IL-6$ , and MCP-1, although elevated in RA-induced rats, decrease after treatment with SeNPs. Also, the levels of antioxidant enzymes, usually decreased in RA, were restored in both liver, kidney, and spleen.<sup>[33,193]</sup> However, different SeNPs doses were proposed: while Malhotra et al. have shown results with  $250 \text{ }\mu\text{g per kg body weight}$ ,<sup>[193]</sup> Ren et al. proposes an intake of  $500 \text{ }\mu\text{g per kg body weight}$  as the daily therapeutic

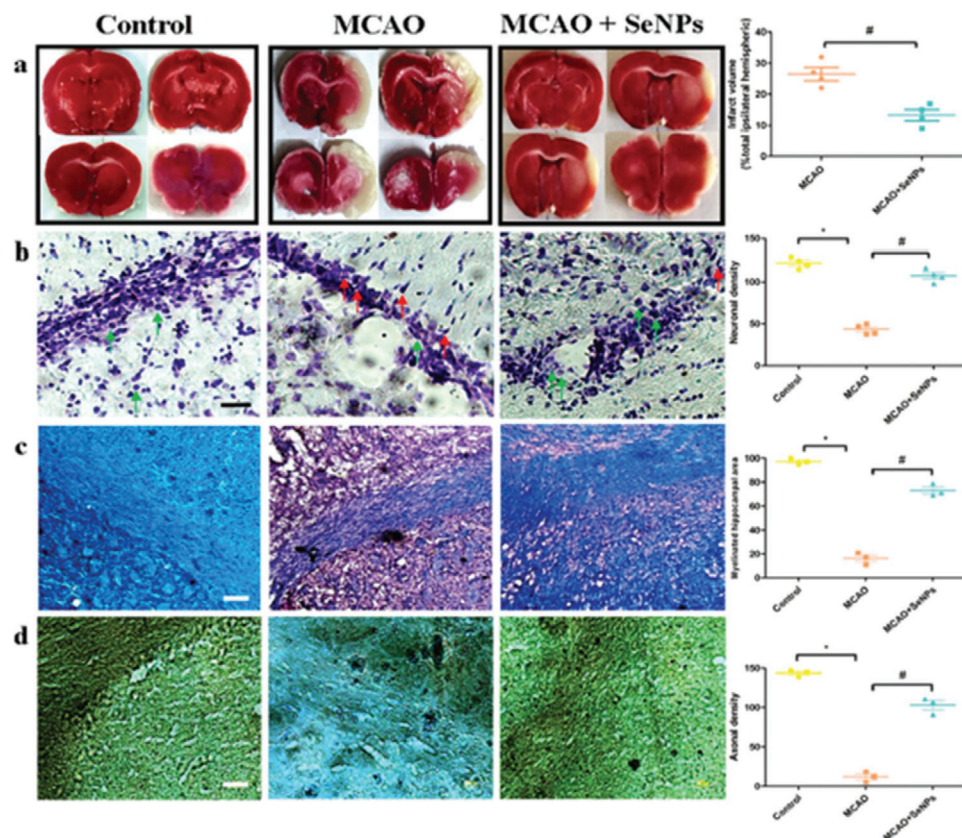


**Figure 18.** SeNPs protecting role against stroke. a) TTC staining indicating that treatment with OX26-PEG-SeNPs represents a decrease of infarct volume compared with MCAO group (non-infarcted brain areas are red while the infarcted ones appeared as white). b) Nissl staining of hippocampal CA1 subregion demonstrating that OX26-PEG-SeNPs augmented neuronal survival under oxidative stress (Green arrows indicate normal cells while red arrows indicate necrotic ones). c) LFB staining of hippocampal CA1 subregion demonstrated that OX26-PEG-SeNPs reversed the decreased of myelinated hippocampal area observed with MCAO (blue, myelinated fibers; pink, neutrophils; and purple, nerve cells); and d) Bielschowsky's silver staining of hippocampal CA1 subregion revealed that OX26-PEG-SeNPs preserved the number of axons compared MCAO groups (axons, black). Reproduced with permission.<sup>[135]</sup> Copyright 2019, Nature.

dosage in RA-induced rats.<sup>[33]</sup> Combination therapy of SeNPs and tripterine was also studied. Tripterine is a substance that has shown antioxidant, anti-inflammation, and immunoregulation potential, and its combination with SeNPs show synergic effects in reducing inflammation and joint swelling, as well as decreasing NO and cytokine levels in vitro. Therefore, the combination of these two compounds demonstrated potential properties for treatment of RA.<sup>[194]</sup> The potential of biogenic SeNPs produced using *Trachyspermum ammi* seed extract against RA was also studied. Although the produced SeNPs increased the urea levels in mice, these SeNPs successfully reduced paw edema and swelling, while restoring liver alkaline phosphatase levels. The biogenic SeNPs also shown high antioxidant activity, especially at concentrations of 5 mg kg<sup>-1</sup> of SeNPs (when compared to 10 mg kg<sup>-1</sup> of SeNPs), as well as decreased synovial hyperplasia and lymphocytic cellular infiltration in histopathological analysis of the damaged areas around the paw tissue.<sup>[196]</sup> As a result of its anti-inflammatory and antioxidant properties, SeNPs also demonstrated potential for the treatment of cardiovascular diseases, such as coronary disease, stroke, and peripheral artery disease.<sup>[195]</sup> Epidemiologic studies correlated low plasmatic levels of Se and respective selenoproteins to cardiomyopathies.<sup>[127]</sup>

50 µg kg<sup>-1</sup> of SeNPs has shown potential to reduce atherosclerosis, by decreasing triglycerides, enhancing HDL levels, and reducing the number of lesions in the vascular smooth muscle cells of ApoE<sup>-/-</sup> mice subjected to a hypercholesteremic diet. SeNPs mechanism of action was demonstrated to be related to the reduction of the mRNA expression of 3-hydroxy-3-methylglutaryl coenzyme A reductase, an enzyme responsible for cholesterol biosynthesis, and the enhancing of the enzyme cholesterol 7 alpha-hydroxylase, responsible for converting cholesterol into bile acid. Additionally, the enhancing of selenoprotein levels by SeNPs consumption shown to have an important role in decreasing the oxidative stress that enhances vascular injury risk and reduced the damages in the liver and kidney caused by the hypercaloric diet.<sup>[195]</sup>

In addition, PEG-SeNPs were also used for stroke therapy, using an anti-Tfr receptor monoclonal antibody (OX26) as a functionalizing agent. OX26-PEG-SeNPs revealed to have a role in protecting neuronal cells against stroke, reducing the cellular swelling caused by abnormal entry of Na<sup>+</sup> ions. SeNPs were able to reduce the infarction volumes in Wistar rats subjected to middle cerebral artery occlusion (MCAO) (Figure 18a) and at the same time, decrease the number of necrotic cells



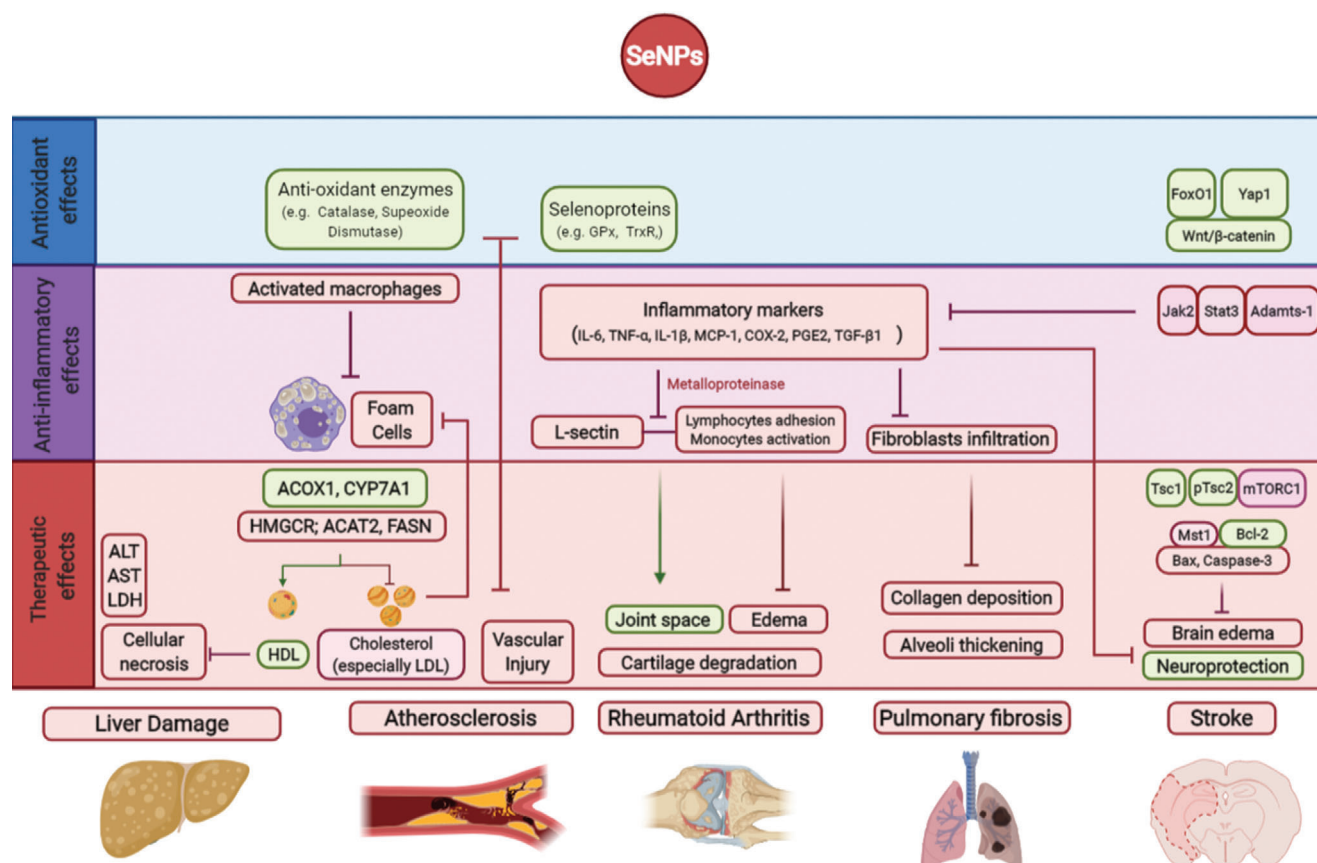
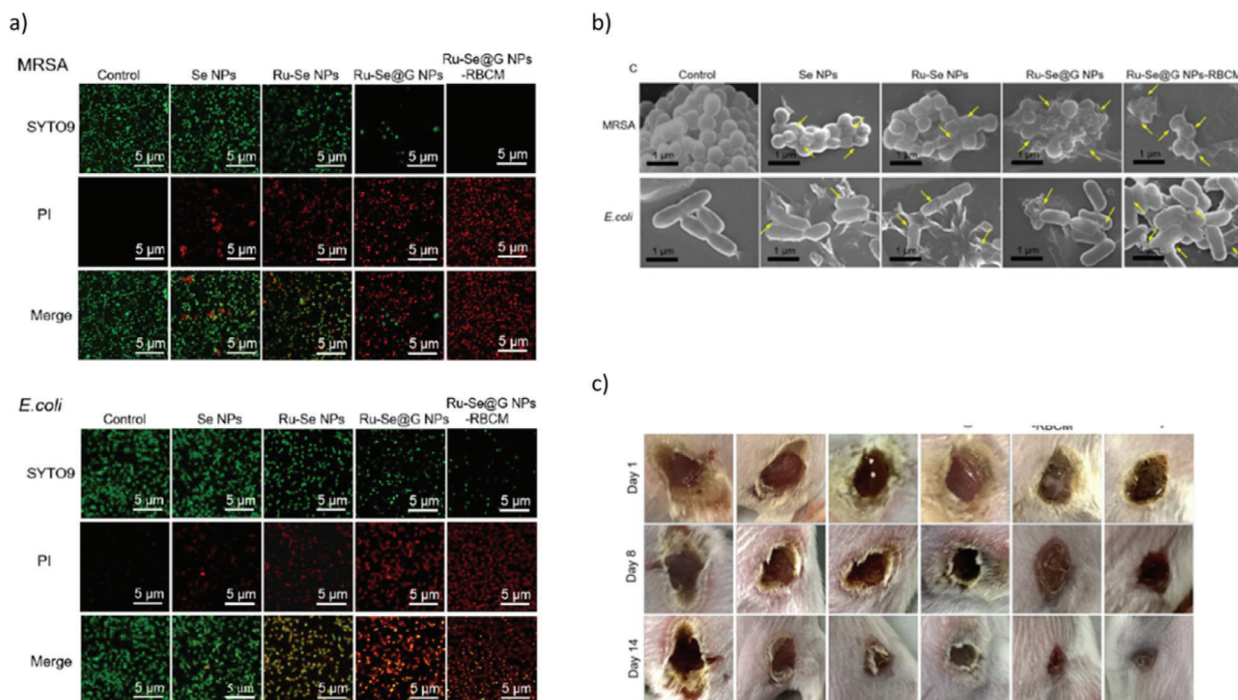


Figure 19. Anti-inflammatory therapeutic applications and mechanisms of SeNPs. Figure created with Biorender.

(Figure 18b), while increasing the myelinated areas (Figure 18c) and negate the loss of axons in hippocampus region caused by the artery occlusion (Figure 18d). The molecular mechanisms behind SeNPs neuroprotective action seem to be related to several cellular signaling pathways that control neuronal metabolic state (TSC1/TSC2, p-mTOR, mTORC1), antioxidant (FoxO1,  $\beta$ -catenin/Wnt, Yap1) and inflammatory system (jak2/stat3, Adams-1), autophagy and apoptotic cell death (Mst1, ULK1, Bax, Caspase-3 and Bcl-2), and the maintenance of the hippocampal neurons (rictor/mTORC2).<sup>[135]</sup> Interestingly, chitosan-SeNPs film also shows potential for cardiac repair, enhancing the electrical conductivity of myocardial cells, and enhancing the tensile strength and elasticity of the natural myocardium. The SeNPs used for this purpose had rough surfaces, which decreased the possibility of immune reactions and implant rejections after transplantation. These properties make Chitosan-SeNPs film a suitable tool to be used to produce electrical conductivity in the cardiac patches.<sup>[127]</sup>

SeNPs have also exhibited *in vivo* anti-inflammatory protective properties for liver<sup>[128,196]</sup> and lungs.<sup>[197]</sup> SeNPs supplementation display Se liver retention abilities, increasing selenoproteins' activity and their antioxidant potential, improving liver biomarkers: alanine aminotransferase (ALT), aspartate aminotransferase (AST), and lactate dehydrogenase (LDH), and diminishing the liver damage induced by concanavalin-A.<sup>[128]</sup> Furthermore, SeNPs also demonstrated the ability to protect against

hexavalent chromium hepatotoxicity, by reducing the amount of free radicals, and downregulating the mRNA expressions of fatty acid synthase (essential for *de novo* lipogenesis) and upregulating the mRNA expression level of acyl-coenzyme A oxidase 1 (limits fatty acid  $\beta$ -oxidation), protecting against the anomalous fatty acid metabolism, promoted by chromium.<sup>[196]</sup> Also, SeNPs demonstrated anti-inflammatory properties against pulmonary fibrosis only in early stages of the disease, due to its ability to reduce the levels of cytokines, such as TGF- $\beta$ 1 and TNF- $\alpha$ . In addition, SeNPs diminished interstitial collagen deposition, reversed the thickening of alveolar septal provoked by pulmonary fibrosis and controlled the infiltration of inflammatory cells, such as fibroblasts, improving the lung histological structure.<sup>[197]</sup> More recently, Lesnichaya et al. diminished carbon tetrachloride hepatic damage, reducing the levels of lipid peroxidation products and the hepatic enzymes ALT and AST, probably due to the antioxidant effect of Se due to its role in the biosynthesis of several antioxidant enzymes. However, they also verified that, in healthy mice, the administration of an excessive amount of SeNPs resulted in dysfunction of the excretion system, with increased urea, AST, and MDA levels. Also, SeNPs excessive administration may augment ROS levels due to its interaction with GSH.<sup>[198]</sup> Overall, SeNPs have potential to treat several inflammation-related diseases across the body, such as cardiopathies, RA and pulmonary fibrosis (Figure 19).



**Figure 20.** In vitro and in vivo studies concerning the antibacterial properties of Ru-Se@GNPs-RBCM: a) Fluorescence microscopic observation (LIVE/DEAD) indicating that the complex has a synergic bacterial activity, with only a small percentage of cells alive (green) and a large number of dead cells (red) compared to SeNPs or Ru-SeNPs. b) SEM images translating the effect of the Se-Ru nanocomplex on the bacteria cells after 2 h incubation, causing shrinking of the cell walls, rupture and morphology alteration; and c) Photos of mice wound area infected with MRSA and treated with SeNPs, Ru-SeNPs, Ru-Se@G NPs, Ru-Se@G NPs-RBCMs, and vancomycin, using untreated mice as control groups, in which it is observed the potential of the nanosystem in the healing and treatment of the infected injury. Reproduced with permission.<sup>[202]</sup> Copyright 2019, American Chemical Society.

#### 4.4. Antimicrobial Applications

SeNPs also demonstrated antimicrobial applications against bacteria, fungi, and viral infection (Figure 20).<sup>[13]</sup> Bacterial infections are a critical problem of worldwide healthcare due to resistances caused by continuous overuse of highly concentrated antibiotics,<sup>[155]</sup> and, although several NPs shown antibacterial properties,<sup>[105,199]</sup> several metalloids and metal-based NPs, such as silver NPs, also demonstrated several side effects during administration of high dosages or prolonged therapy.<sup>[105,155,200]</sup> Unlike other metals, Se is an essential element in the human body and SeNPs have been shown to have bactericidal effects mainly against MRSA at 1 ppm, however were less effective against *E. coli*, probably due to the negative nature of its outer membrane, which repulse the also negative SeNPs.<sup>[157,199]</sup> Antibacterial activity of the SeNPs is negatively correlated to its size, being that 81 nm SeNPs were found to be more effective against MRSA (inhibitory capability of 25 μg mL<sup>-1</sup>) than 124 nm SeNPs (inhibitory capability of 140 μg mL<sup>-1</sup>).<sup>[199]</sup> Chung et al. produced BSA-stabilized SeNPs with a size less than 40 nm with antibacterial properties against *S. aureus*. The SeNPs produced accomplished IC<sub>50</sub> values much lower than those for the human dermal fibroblasts, which translated into a promising safety window for its use as an antibacterial agent.<sup>[97]</sup>

Also, SeNPs at 0.5 mg Se mL<sup>-1</sup> inhibited MRSA adherence by more than 60% on glass and catheter surface (polystyrene surface), demonstrated their potential against biofilms formed in

medical devices.<sup>[201]</sup> Furthermore, biosynthesized SeNPs also inhibited fungi biofilms, without affecting the viability of human cells, such as fibroblasts and dendritic cells.<sup>[86]</sup>

Functionalization of SeNPs was also studied in order to develop better targeting towards bacteria cells.<sup>[105,155,202]</sup> The incorporation of Se into Se-MSNPs was attempted. Se-MSNPs showed better antibacterial activity than bare SeNPs for MRSA, although being ineffective against *E. coli*.<sup>[155]</sup> In another study, SeNPs were also functionalized with quercetin and acetylcholine, showing a synergic effect against both *E. coli* and MRSA at 25 μg mL<sup>-1</sup>, not only killing them but also inhibiting their cellular division. Quercetin is itself a bactericidal molecule, and acetylcholine was used to enhance bacterial permeability to SeNPs.<sup>[105]</sup> In more recent studies, SeNPs were loaded with Ruthenium (Ru) and, afterwards, were encapsulated into bacteria-sensitive gelatin NPs, coated by red blood cell membranes (RBCM), developing a multilayer nanosystem with a size of approximately 152 nm with antibacterial properties against gram positive and negative strains (Figure 21a). Synergic antibacterial effects were achieved in vivo: 1) RBCMs had a camouflage effect from the phagocytosis of macrophages and increased the nanosystem's internalization by bacteria; 2) The nanocore absorbed the bacterial exotoxins, neutralizing their virulence, and gelatin is degraded into aminoacids by bacterial gelatinases, inducing Ru-SeNPs release; 3) Ru enabled monitoring the treatment through fluorescence signal, besides having additional bacterial effect; and 4) SeNPs attack the bacterial cells, increasing the amount

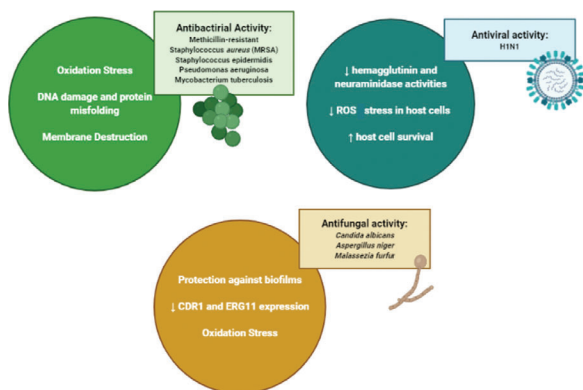


**Figure 21.** Antimicrobial activity of SeNPs and the associated pathways. Figure created with Biorender.

of cellular ROS and triggering bacterial lysis (Figure 21b). In vitro assays show the antibacterial potential of these NPs against MRSA, *Staphylococcus epidermidis* and *P. aeruginosa*, although with less effect on *E. coli*. In vivo studies in mice demonstrated that these SeNPs not only escape the immune system, and attack bacterial cells, but also accelerate skin tissue repair (Figure 21c). They were quickly metabolized, having only a residual concentration within the liver and kidney (organs responsible for their metabolism), not presenting any toxicity at therapeutic dosages ( $2 \text{ mg kg}^{-1}$ ).<sup>[202]</sup> Overall the antibacterial potential of SeNPs seems to be due to: metabolic dysfunction due to decreasing of ATP concentrations;<sup>[199]</sup> increase of the intracellular concentration of ROS, causing oxidation stress,<sup>[105,155,199,202]</sup> which results in a loss of bacterial resistance to SeNPs;<sup>[105,202]</sup> inhibition of protein synthesis and DNA mutation and damage;<sup>[105,155,200]</sup> depolarization and destruction of the bacterial membrane.<sup>[105,155,199,202]</sup> A nanohybrid containing SeNPs and lysozyme, a biomolecule that has a defensive role in the immune system against gram-positive bacteria, has shown synergic activity, specifically against MRSA, although having some activity against *E. coli*. The lysozyme affected the gram-positive bacteria by hydrolyzing 1,4- $\beta$ -linkages of its cell wall, due to its activity as a  $\beta$ -glucosidase. However, due to the lipopolysaccharide layer, its enzymatic effect cannot be achieved. Furthermore, SeNPs are negatively charged, being repulsed by the lipopolysaccharide gram-negative bacteria, such as *E. coli*, contributing to its lower sensitivity toward SeNP.<sup>[203]</sup> Also, Golmohammadi et al. prepared a hydrogel consisting of chitosan-cetyltrimethylammonium bromide entrapping SeNPs and mupirocin. The therapeutic combination within the hydrogel demonstrated synergic activities against mupirocin-methicillin-resistant *S. aureus* (MMRSA) inoculated in an injury created in a diabetic rat model, while improving the wound healing associated with the bacterial infection, stimulating epidermal growth, and decreasing the associated inflammation, suggesting its potential for treatment of diabetic wound infections.<sup>[204]</sup> SeNPs produced by biosynthesis using *Lactococcus lactis* had a protective effect on intestinal infection by *E. coli*, preserving the intestinal epithelial barrier due to its antioxidant and anti-inflammatory effects and by increasing occludin and claudin-1 expression.<sup>[78]</sup>

More recently, Huang et al. used a recombinant spider silk protein eADF4( $\kappa$ 16) to produce positive charged SeNPs in order to

improve SeNPs antibacterial activity against gram-negative bacteria, such as *E. coli*, comparing their activity with negative charged SeNP, produced using PVA. The eADF4( $\kappa$ 16)-SeNPs produced had a mean diameter of 46 nm and a  $\zeta$ -potential of  $+46.0 \pm 0.6 \text{ mV}$ . As a result of its small size and extremely positive charge, eADF4( $\kappa$ 16)-SeNPs showed a high antibacterial potential against *E. coli* with a minimum bacterial concentration of  $8 \pm 1 \mu\text{g mL}^{-1}$ , 50 times lower than that of negatively charged SeNPs, and a concentration not considered toxic to human cells. Therefore, the positive charge enabled a better electrostatic attraction between the SeNPs and the negatively charged bacterial cells. However, these SeNPs had a low stability in culture broth. To overcome this issue, eADF4( $\kappa$ 16)-SeNPs were immobilized in positively charged spider silk films, which retained SeNPs bactericidal activity against *E. coli*. Moreover, it was observed that the SeNPs release from the film surface was essential to exert their antibacterial effects, and that this release can be regulated by the charge of the film surface itself.<sup>[200]</sup>

El-Sayyad et al. also demonstrated the SeNPs antimicrobial potential against a wide range of pathogens involved in resistant urinary tract infections. El-Sayyad et al. produced SeNPs using both *Penicillium chrysogenum* filtrate biosynthesis and gentamicin (CN) drug as stabilizer agent and gamma radiation as reducing agent. While the biogenic SeNPs had a cubic crystalline structure and a size ranging from 12.12 to 84.15 nm, the CN-SeNPs had an amorphous structure and a mean diameter of 33.84 nm. The CN-SeNPs demonstrated to have better antibacterial potential than the biogenic SeNPs, inhibiting both gram-positive bacteria (*S. aureus* and *Bacillus subtilis*) and gram-negative (*E. coli* and *P. aeruginosa*), with the exception of *Klebsilla pneumoniae*, with minimum inhibitory concentrations (MICs) ranging from 3.950 to 0.245  $\mu\text{g mL}^{-1}$ . CN-SeNPs also inhibited the formation of *E. coli* biofilms, by provoking cell wall hardness and distortion, inducing bacterial lysis. Therefore, CN and SeNPs developed a synergic impact that translated into a higher antibacterial effect towards most bacterial strains studied.<sup>[114]</sup>

SeNPs were also studied for tuberculosis therapy. Their loading with Isoniazid, a medicine already used against tuberculosis, and manipulation with mannose, resulted in synergic effects, inducing not only antibacterial effects, mainly through ROS stress, but also targeting the phagocytic macrophages through their mannose receptors, releasing the Isoniazid in their acidic lysosomes. Therefore, this nanosystem promotes not only the destruction of the *M. tuberculosis* bacillus that infected the macrophages and escaped the phagolysosome, but also the autophagy and apoptosis of the infected macrophages, by ROS stress and PI3K/AKT/mTOR signaling pathways.<sup>[158]</sup> Furthermore, more recently, Estevez et al. demonstrated that chitosan-SeNPs by themselves have antibacterial properties against both *Mycobacterium smegmatis* and *M. tuberculosis* with MIC values of 0.400 and 0.195  $\mu\text{g mL}^{-1}$ , respectively.<sup>[205]</sup>

Other pathogenic agents that have acquired resistances against their treatment are fungi, making the development of new antifungal therapeutic agents crucial.<sup>[206,207]</sup> Since Se compounds have been used as antifungal agents, there have been several studies regarding SeNPs antifungal potential.<sup>[206–208]</sup> Initial studies demonstrated that biogenic SeNPs show antifungal potential against *C. albicans* and *Aspergillus fumigatus* at MICs of 70 and 100  $\mu\text{g mL}^{-1}$ , respectively.<sup>[206]</sup> Further studies

demonstrated SeNPs potential to reduce the expression of CDR1 and ERG11 genes in *C. albicans*, decreasing its resistance to antifungal drugs.<sup>[207]</sup> More recent studies used Chitosan-SeNPs prepared by PLA. In this study, despite bare SeNPs exhibiting an  $IC_{50}$  of 21.7 ppm for *C. albicans*, the  $IC_{50}$  of chitosan-SeNPs was 3.5 ppm, which indicates a synergic effect between SeNPs and Chitosan, that alone show some degree inhibition against *C. albicans* biofilms.<sup>[208]</sup> Also, SeNPs have shown potential against seborrheic dermatitis, a fungal infection caused by *Malassezia furfur* that occurs in the skin regions rich in oil glands. SeNPs and ketoconazole nanoparticles were integrated into a HA hydrogel using cross-linking methodology. This formulation was shown to have improved antifungal activity when compared to SeNPs and ketoconazole, with a zone of inhibition of  $35 \pm 1.67$  mm, probably due to the combined therapy of ketoconazole, that inhibit the production of ergosterol, and SeNPs, which kill fungal cells by provoking ROS stress. The hydrogel also had anti-inflammatory properties in vivo and the use of NPs was shown to increase the skin permeability to the therapeutic compounds.<sup>[132]</sup>

SeNPs also show antiviral activity, especially against H1N1, a virus responsible for a very infectious respiratory disease responsible for 8768 deaths in 207 countries in 2009.<sup>[209,210]</sup> In an initial study, functionalized SeNPs with oseltamivir demonstrated synergic antiviral activity against H1N1, increasing the viability of infected cells and viral destruction at a MIC of  $0.3 \times 10^{-9}$  M. The mechanisms behind this antiviral activity are: 1) inhibition of hemagglutinin and neuraminidase activities, glycoproteins important for virus transport into host cells; 2) caspase-3 and ROS stress inhibition in host cells, probably by modulation of the p53- and AKT-signaling pathways (p53 activation and AKT phosphorylation).<sup>[209]</sup> Other studies using SeNPs also demonstrated their synergic antiviral activity when loaded with amantadine and ribavirin.<sup>[210,211]</sup> SeNPs functionalized with amantadine had a MIC of  $0.1 \times 10^{-6}$  M, and showed similar antiviral pathways as SeNPs functionalized with oseltamivir, diminishing neuraminidase activity, ROS stress, mitochondrial dysfunction and caspase-3 activation, besides activating the phosphorylation of AKT, thus preventing cell apoptosis.<sup>[210]</sup> In vivo studies also demonstrated the potential of SeNPs functionalized with ribavirin for the protection of lung alveoli from H1N1 infection, besides bringing new information about the mechanisms behind the antiviral activity exhibited. In fact, SeNPs inhibited the upregulation of cleaved Poly-ADP-ribose polymerase (PARP), caspase-8, Bax, p38, JNK and p53 induced by H1N1, protecting the lung cells from apoptosis.<sup>[211]</sup> Interestingly, SeNPs functionalized with oseltamivir also exhibited antiviral activity against hand-foot-mouth disease, also by decreasing the activity of caspase-3, enhancing mitochondrial potential and inhibiting ROS generation, avoiding the apoptosis of host cells.<sup>[212]</sup>

Lin et al. also studied the potential of SeNPs against Enterovirus 71, which is responsible for several neuronal, hand, foot, and mouth diseases. SeNPs were capped with PEI and loaded with siRNA targeting the enterovirus 71 VP1 gene, producing PEI-SeNPs@siRNA-VP1 with the size of 80 nm, with antiviral potential towards Enterovirus 71. PEI-SeNPs@siRNA-VP1 was able to reduce VP1 expression and inhibit the proliferation of Enterovirus 71, increasing the cellular viability of SK-N-SH cells (nerve cell line) by inhibiting the Bax signaling pathway, and reducing the number of cells arrested at sub-G1 phase.<sup>[213]</sup>

More recently, SeNPs were used for production of a detection test for the severe acute respiratory syndrome coronavirus 2 (SARS-CoV-2), based on the IgM and IgG in human serum and blood. Based on the fact that SeNPs have higher levels of sensitivity and stability, besides being cheaper, than colloidal gold in qualitative lateral flow immunoassays, Wang et al. developed a 10 min kit test based on SeNPs produced by chemical reduction with SDS and PEG as templates. The tests developed demonstrated a limit of detection of  $20 \text{ ng L}^{-1}$  and  $5 \text{ ng mL}^{-1}$  for IgM and IgG, respectively, without false positives in human serum. Also, the tests have shown sensitivity and specificity values of 93.33% and 97.34%, respectively, and positive and negative predictive values of 92.31% and 97.71%, respectively.<sup>[214]</sup>

Furthermore, SeNPs have shown antiparasitic properties against chronic toxoplasmosis. The biogenic SeNPs produced using *Bacillus* sp. were demonstrated to have antiparasitic properties, especially at higher concentrations and when administered concomitantly with atovaquone. Oral administration of  $10 \text{ mg Kg}^{-1}$  SeNPs with atovaquone  $100 \text{ mg kg}^{-1}$  in male BALB/c mice infected with *Toxoplasma gondii* demonstrated to completely eliminate all tissue cysts, without presenting any toxicity. SeNPs also increased the level of the immune mediator compounds IFN- $\gamma$ , TNF- $\alpha$ , IL-12, and iNO, while reducing IL-10 levels. Thereby, it was proposed that the stimulation of the immune system was the main therapeutic effect by which the SeNPs induce their antiparasitic activity.<sup>[215]</sup>

#### 4.5. Cancer Treatment and Theragnostic Applications

Cancer is still one of the most problematic and deadly diseases worldwide<sup>[216]</sup> and, although the most common therapeutic strategies are surgery after chemotherapy, radiation, or combination of both, their side effects can be very severe for the patient.<sup>[136,133]</sup> Nanotechnology has presented advantages compared to current chemotherapy,<sup>[133,216]</sup> and SeNPs are promising therapeutic agents, due to their high bioavailability and lower toxicity when compared to organic and inorganic Se, besides having demonstrated to have stronger anticancer activity, stimulating selenoproteins and triggering cell apoptosis in cancer cells, while protecting the healthy cells, preventing ROS stress and DNA damage.<sup>[13,36,144]</sup> However, in spite of SeNPs exhibiting more antiproliferative properties towards cancer cells than the healthy ones, some normal cells, such as prostate cells and hepatocytes seems to be more sensitive than their cancer counterparts, being necessary to functionalize the SeNPs with specific compounds that enable the targeted delivery towards cancer cells.<sup>[217]</sup> Several bioconjugations and functionalizations were attempted for SeNPs, and their physical and therapeutic characteristics seem to depend on the type of functionalization and cancer cell used in the study.<sup>[36]</sup> Several molecules have been used to provide target selectivity to SeNPs, such as FA,<sup>[100]</sup> RGD-peptide<sup>[36]</sup> and TfR,<sup>[121]</sup> and, according to the molecule and the type of cancer studied, SeNPs are internalized and destroy malign cells through several molecular pathways, the most common being the production of ROS and activation of the intrinsic pathway of apoptosis.<sup>[36]</sup> Also, when loaded with chemotherapeutic drugs, SeNPs were able to protect the healthy organs from their toxic effects, while also avoiding clearance through macrophage phagocytosis.<sup>[13]</sup>

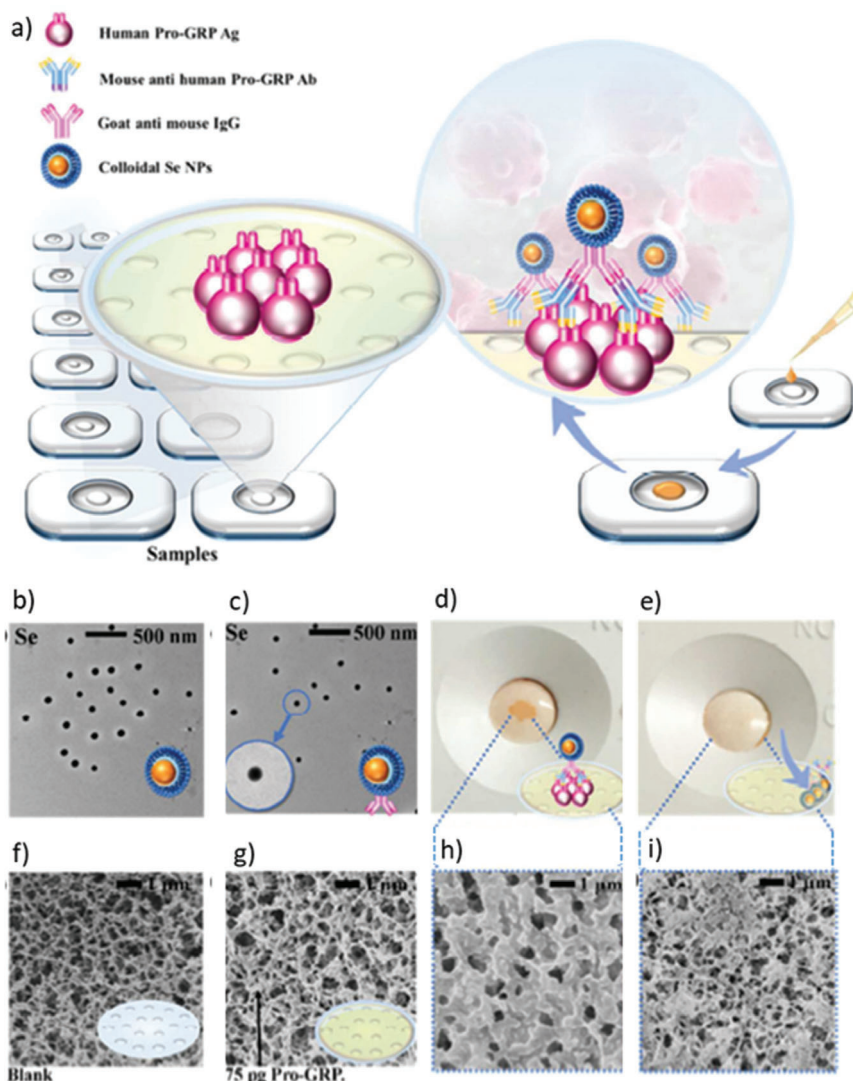


**Figure 22.** Schematic figure of the principle behind SeNPs dot-blot immunoassays tests. a) Scheme of the detection of human Pro-GRP by colloidal SeNPs. b) TEM images of colloidal SeNPs. c) TEM images of Se@Goat antimouse IgG. d,e) Result after serum test (3 min) for 100 and 0 pg mL<sup>-1</sup> goat anti-mouse IgG, respectively (concentration of pro-GRP was 25 pg mL<sup>-1</sup>). SEM images of blank nitrocellulose membrane—f) blocked nitrocellulose membrane and g) nitrocellulose membrane after h,i) dot-blot immunoassays. Reproduced with permission.<sup>[223]</sup> Copyright 2018, Royal Society of Chemistry.

Additionally, the size of SeNPs also demonstrated to inversely influence their antitumor activity, since smaller SeNPs were associated with elevated ROS production, having more antiproliferation activity towards cancer cells.<sup>[104]</sup> SeNPs have demonstrated anticancer potential against liver,<sup>[30,31]</sup> prostate,<sup>[35,218,219]</sup> bone,<sup>[133]</sup> breast<sup>[219,220]</sup> and lung cancer,<sup>[219]</sup> Dalton's lymphoma,<sup>[101,221]</sup> glioma,<sup>[222]</sup> and cell lines, among others.<sup>[36]</sup>

SeNPs have also demonstrated potential to be incorporated into endoprosthesis implants to combat osteosarcoma. Stolzoff et al. demonstrated the possibility of precipitated SeNPs in an engineering material used for orthopedic applications, PLLA, wherein SeNPs prevented bacterial adhesion and attacked cancer tissue while they enhanced the renewal of bone tissue.<sup>[133]</sup> SeNPs also exhibited prophylactic properties against peritoneal carcinomatosis, a major complication of abdominally located cancers re-

lated to surgical complications. After injection of H22 cells into Kunming mice, their weight started to increase as a result of the large amount of ascitic fluid provoked by the malignant cells and, after 14 days, the mice died. However, the intraperitoneally administration of SeNPs at a dose of 4.5 mg Se per kg body weight at 1 h after H22 inoculation resulted in the survival of all mice. Interestingly, the administration of 6 mg Se per kg body weight resulted in 33% mouse death within a week, which suggests the existence of a therapeutic window between SeNPs beneficial and toxic effects.<sup>[217]</sup>

SeNPs were also studied for cancer diagnosis. SeNPs produced by TiO<sub>2</sub> photocatalysis self-assembly on imprinting sites of zeolite-chitosan-TiO<sub>2</sub> microspheres were successfully used in dot-blot sandwich enzyme immunoassays to detect antigens typical of human lung cancer, such as Pro-GRP (Figure 22), using a

**Table 4.** Mechanisms behind SeNPs antitumor activity against several types of cancer.

Cancer cell type	Biochemical mechanism	Effects	Refs.
Breast Cancer	↓ERα ↑pp38, Bax and cytochrome c	Apoptosis	[220]
Dalton's lymphoma	↑ROS stress, ↓mitochondria membrane potential in tumor cells ↑F-actin activity, CD54 (ICAM-1) expression, CD47 and CD172a receptors in tumor activated macrophages	DNA fragmentation, cell cycle arrest at G0/G1 and apoptosis of tumor cells. ↑ Phagocytosis of tumor cells	[221]
Glioma cancer	↑ROS stress and caspase-3 activity ↓ glycolysis	Apoptosis	[222]
Hepatocellular carcinoma	↑ ROS stress and mitochondria dysfunction	Apoptosis and cell cycle arrest at sub-G1	[112]
Ovarian cancer	According to the cancer cell line: • SKOV: increased stiffness and surface roughness • OVCAR: decreased surface roughness	Apoptosis	[225]
Cervical Cancer	–	↓ Cellular viability, migration and neovascularization	[95]
Prostate cancer	↓ Androgen receptor and PSA ↑ Caspase activity ↑ROS stress, ↓mitochondria membrane potential ↑TNF and ERF1 mRNA, RIP1 kinase ↓ PSA ↑ Caspase-3, Bax and p21 mRNA ↑ miR-16 → ↓ Bcl-2, cyclin D1	Apoptosis  Necroptosis RIP1 kinase dependent  Apoptosis and cell cycle arrest	[219]  [35,218]  [159]

nitrocellulose membrane to set up the position of the hole. This serodiagnosis technique took 5 min and its sensitivity was 75 pg mL<sup>-1</sup>.<sup>[223]</sup> Also, Korany et al. studied the use of SeNPs radiolabelled with <sup>99m</sup>Tc, producing <sup>99m</sup>Tc-GSH/SeNPs with liver cancer theragnosis potential in male Swiss albino mice. The nanosystem produced presented the size range (21 ± 5 nm) indicated for passive targeting through the enhanced permeability and retention (EPR) effect, and a great antioxidant potential, that would increase their uptake and retention by tumor cells, thereby increasing the <sup>99m</sup>Tc-GSH/SeNPs amount in the solid tumor transplanted into the mice.<sup>[224]</sup>

#### 4.5.1. Antitumor Mechanisms

SeNPs have demonstrated to have antiproliferative properties towards a variety of cancer cell lines, however the pathway behind its antitumor activity seems to be dependent on the possible functionalization directed to a specific target or on if the SeNPs are loaded with another compound. Overall, SeNPs seem to exercise their activity in a dose-dependent way,<sup>[36]</sup> mainly by being reduced by both the glutaredoxin and thioredoxin antioxidant systems, with production of HSe, oxidation of nicotinamide adenine dinucleotide phosphate (NADPH) and oxygen to its radical forms.<sup>[17]</sup> Thereby, by enhancing the ROS production and the stress associated, SeNPs induce cell cycle arrest and apoptosis, while being much less cytotoxic for healthy cells (Table 4).<sup>[17,36]</sup>

Initial studies have demonstrated that SeNPs have better antiproliferative properties for MCF-7 cells (IC<sub>50</sub> value of 25 µg mL<sup>-1</sup>) than MDA-MB-231, reflecting their antitumor potential

for early-stage breast cancer (estrogen receptor α (ERα) positive) than late-stage breast (ERα negative) cancer treatment. SeNPs decreased the ERα expression, while increasing the expression of pp38, Bax and cytochrome c, both proteins that are involved in apoptosis. In vivo assays shown that administration of 0.4 mg/kg/day significantly reduced tumor growth, which suggests that the antiproliferative activity of SeNPs in breast cancer is related to ERα levels. Se can also decrease procarcinogen activation and metabolism, by preventing phase I enzymes activity and stimulating phase II enzymes, being that, while phase I enzymes are members of the cytochrome P450 that concert chemical carcinogens into reactive adducts that attack DNA, while phase II enzymes are detoxifying enzymes, and their activation represents the mechanism behind SeNPs tumor suppression.<sup>[220]</sup>

SeNPs also show antitumor potential towards Dalton's lymphoma, by enhancing ROS stress and decreasing mitochondria membrane potential, which ultimately led to DNA fragmentation, cell cycle arrest at G0/G1 and apoptosis. However, in tumor-associated macrophages, SeNPs decrease ROS levels, increase polarization of F-actin, the expression of CD54 (ICAM-1), and the number of CD47 and CD172a receptors, which translated into increased ability to adhere and phagocyte the tumor cells.<sup>[221]</sup>

Another study concerning SeNPs potential against glioma cancer shown that they had antiproliferative properties against glioma cells resistant to several chemotherapeutic-approved agents, such as adriamycin, carmustine, cisplatin, pirarubicin, and teniposide. SeNPs enhanced ROS stress, thereby increasing caspase-3 activity, while decreasing the levels of hexokinase 2 and pyruvate kinase, which resulted in reduced glucose uptake, lactase production, and ATP levels, decreasing cell energy

and ultimately leading to apoptosis of cancer cells, indicating that SeNPs decrease the glucose metabolism through an increase of ROS.<sup>[222]</sup>

SeNPs also demonstrated suppressive effects against androgen-dependent prostate cancer cell lines. SeNPs reduced the levels of androgen receptor, a protein associated with cancer cell survival, at both a transcriptional and translational level. On the one hand, mRNA levels of both androgen receptor and prostate-specific antigen (PSA) were downregulated. On the other hand, SeNPs induced androgen receptor and Mdm2 phosphorylation by AKT, which led to the ubiquitination and proteolysis of the androgen receptor by proteasomes, increased levels of caspase-3, caspase-8, and caspase-9 levels, as well as their substrate PARP, which result in the inhibition of prostate cancer cells growth and apoptosis.<sup>[219]</sup>

A further study concerning the antiproliferative activity of SeNPs against prostate cancer showed that biogenic SeNPs produced using *Bacillus licheniformis* JS2 at a concentration of 2  $\mu\text{g Se mL}^{-1}$  enhanced ROS production and diminished mitochondrial membrane potential, which led to a decrease in ATP levels. Curiously, these SeNPs enhanced the levels of TNF and ERF1 mRNA, which suggests the death of tumor cells by necroptosis, modulated by RIP1 kinase, but independent of RIP3 and MLKL.<sup>[218]</sup> Sonkusre et al. also studied the potential of biogenic SeNPs for prostate cancer therapy. SeNPs produced using *Bacillus licheniformis* biosynthesis induced necroptosis of cancer cells by the same biochemical mechanisms, while reducing the expression of PSA. However, the caspase activity was reduced, which suggests that the antitumor effect of SeNPs was independent of any caspase pathway. In vivo studies also demonstrated that SeNPs are less toxic compared to L-SeMet, causing less liver damage.<sup>[35]</sup> More recently, Liao et al. also study the anticancer application of biogenic SeNPs prepared using *E. coli* towards several cancer cells lines. These SeNPs displayed antiproliferative potential against colon, liver, cervical, breast, melanoma, and prostate cancer cells, both androgen-dependent and androgen-independent prostate cancer cells, by increasing the expression of p21 and Bax mRNA and enhancing caspase-3 activity. SeNPs also demonstrated to upregulate miR-16, which, therefore bound to cyclin D1 and Bcl-2 genes at a GCUGCU sequence site, inhibiting the expression of these anti-apoptotic proteins, thereby inducing cell cycle arrest and apoptosis of cancer cells.<sup>[159]</sup> More recently, Rajkumar et al. studied the anticancer potential of biogenic SeNPs produced by *P. stutzeri* using 8% banana peel extract with  $0.25 \times 10^{-3}$  M tryptophan as medium culture. The resultant biogenic SeNPs inhibited HeLa (cervical cancer cell line) cells viability at low concentration such as  $5 \mu\text{g mL}^{-1}$ , while also showing anti-angiogenic potential, decreasing the cancer cells migration/invasiveness and neovascularization, without showing toxicity towards normal cells, even at high concentrations.<sup>[95]</sup>

PEG-SeNPs produced by dissolving gray Se power in PEG solution at 210–220 °C under magnetic stirring also shown antiproliferative properties against HepG2 cells (hepatocarcinoma cell lines) with an  $\text{IC}_{50}$  value of  $3.27 \mu\text{g mL}^{-1}$ , while a mixture of PEG200 and SeNPs demonstrated a lower anticancer effect ( $\text{IC}_{50}$  value:  $38.2 \mu\text{g mL}^{-1}$ ). Also, HK-2 cells (human kidney cell lines) were much less affected by PEG-SeNPs, suggesting a therapeutic window for its use as anticancer agents. PEG-SeNPs increased ROS levels, decreasing the mitochondrial membrane potential,

which led to a loss of cell-to-cell contact, cell shrinkage, and ultimately apoptosis and cell cycle arrest at sub-G1.<sup>[112]</sup>

SeNPs stabilized with Val, Asp, and Lys were also studied against several cancer cell lines. These SeNPs also increased ROS overproduction and caspase-activation, inducing both intrinsic and extrinsic apoptosis pathways, with  $\text{IC}_{50}$  values from  $5.0 \times 10^{-6}$  to  $9.6 \times 10^{-6}$  M, being that the Lys-SeNPs shown better anticancer activity, followed by Val-SeNPs and the irregular shaped Asp-SeNPs shown the weakest anticancer activity.<sup>[23]</sup>

More recently, Toubhans et al. compared the potential of SeNPs stabilized by BSA (negative charged) and chitosan (positive charged) with selenite for two types of ovarian cancer cell lines, OVCAR-3 and SKOV-3, concluding that although OVCAR-3 cells were more sensitive to SeNPs, selenite was more effective in SKOV-3 cellular inhibition, which suggests that the cell lines are differently affected to each Se treatment. However, upon treatment with SeNPs, the SKOV-3 cells presented an increased surface roughness and cellular stiffness, therefore reducing their elasticity and migratory ability to create metastasis, which was not identified in selenite treatment. Though, both selenite and SeNPs treatment decreased OVCAR-3 cell surface roughness.<sup>[225]</sup>

Since SeNPs demonstrated to have anticancer effects, several studies used specific compounds whose receptors are overexpressed in tumor cells to specifically target them (Table 5).<sup>[36]</sup> For example, Zhang et al. functionalized SeNPs with ATP, by adsorption via an Se–N bond. ATP, once decorating SeNPs, specifically target P2 receptor in the plasma membrane of hepatocellular carcinoma cell lines. Upon inside the tumor cells, ATP-SeNPs induce PAPR cleavage and caspase-3, caspase-8 and caspase-9 activation, through ROS overproduction and mitochondria stress, which leads to cell arrest at sub-G1 phase, DNA fragmentation and apoptosis through both extrinsic and intrinsic pathways.<sup>[226]</sup>

Also, several studies reported the anticancer potential of SeNPs when stabilized with mushroom polysaccharides.<sup>[28]</sup> Zeng et al. studied the antitumor potential of SeNPs stabilized with polysaccharides from the fungi species PTR, *Polyporus rhinoceros*, *Coriolus versicolor*, and *Ganoderma lucidum*. The SeNPs produced entered the cells by endocytosis, inducing intrinsic mitochondria-mediated apoptosis, by increasing the activity of caspases-3/7/9, Bad, Bax, Bim, Bid, Puma, and Bak, while decreasing the activity of the antiapoptotic proteins Bcl-2 and Bcl-XL, resulting in DNA fragmentation and cell arrest at sub-G1 in gastric adenocarcinoma AGS cells. In vivo assays demonstrated the inhibition of Ki67 cells and downregulation of VEGFR2, which is deeply involved in angiogenesis, without presenting noticeable toxicity to normal organs.<sup>[28]</sup> Following this study, Huang et al. conjugated SeNPs with PTR polysaccharide–protein complexes and apply them against colorectal cancer cell lines. PTR-SeNPs entered the cells through energy-dependent caveolae-mediated endocytosis toward Golgi apparatus and clathrin-mediated into the lysosome. Then, PTR-SeNPs activated the Bcl-2 family (proapoptotic proteins Bax and Bak) and down-regulate cyclin D1 and D3, and cyclin-dependent protein kinase (CDK) 2/4/6, all regulators of G1/S phase, leading to DNA fragmentation, apoptosis, and cell arrest at G2/M phase arrest. Afterward, by using a pEGFP-LC3 plasmid transfection model, PTR-SeNPs upregulated the autophagy initiator Beclin 1 and decreased p62 levels, promoting autophagy. The relation between autophagy and apoptosis was established by

**Table 5.** Mechanisms behind functionalized SeNPs antitumor activity against several types of cancer.

Functionalization	Cancer cell type	Endocytosis mechanism	Biochemical mechanism	Effects	Refs.
ATP-SeNPs	Hepatocellular carcinoma	–	ROS stress, mitochondria dysfunction, PARP cleavage ↑ caspases 3,8 and 9	Cell cycle arrest at sub-G1 phase Apoptosis	[226]
FA-SeNPs		Nystatin-dependent lipid raft-mediated and clathrin-mediated	↓ ABC family proteins ↑ ROS stress, p53 phosphorylation, caspase 8/9 and PARP cleavage	Cell cycle arrest at sub-G1 phase Apoptosis	[130]
Fer-SeNPs		-	↑ ROS and mitochondria disruption, cytochrome c release and caspase -3/9 activation DNA-binding properties	Apoptosis	[31]
Ru-SeNPs		-	↓ FGFR1, E and AKT phosphorylation Dysfunction of bFGF	Apoptosis ↓ Angiogenesis	[230]
Ru-Se		-	↑ ROS and mitochondria dysfunction, Bax, Ca <sup>2+</sup> , caspase-3/9 ↓ Bcl-2	Cell cycle arrest at Sub-G1 and apoptosis theragnostic agent	[231]
Ru-MUA@SeNPs		Clathrin-mediated endocytosis	↑ ROS and mitochondria dysfunction Preferential in vivo accumulation at tumor sites, with inhibitory effects towards formation and motility of cancer-related blood vessels, by VEGF suppression	Anticancer, antiangiogenic and fluorescence imaging properties	[104]
Laminarin-SeNPs		-	↑ Bax and caspase-9 ↓ of Bcl-2 ↑ LC3-II, ↓ P62	Apoptosis, Inhibition of late phase of autophagy (self-protection mechanism)	[139]
SeHAN		-	↓ Ki-67, VEGF and MMP-9 Formation of calcium deposits ↑ ROS stress	Cell cycle arrest at S-G2/M phase, necrosis, and apoptosis	[228]
	Bone Cancer	-	↑ ROS stress, mitochondria dysfunction and cytochrome c, caspase-3/8/9 and truncated Bid	Apoptosis	[229]
BFP-Se,	Acute myeloid leukemia		↑ Mitochondria dysfunction ↑ GSH ↓ c-Jun activation domain-binding protein 1 ↓ thioredoxin 1	Apoptosis and cell arrest at G1 phase in U937 cells and at S phase in HL60 cells	[147]
Mushroom polysaccharides	Gastric adenocarcinoma	–	↑ capping-3/7/9, Bad, Bax, Bim, Bid, Puma, and Bak, ↓ Bcl-2 and Bcl-xL ↓ VEGFR2	DNA fragmentation, apoptosis, and cell cycle arrest at sub-G1 phase ↓ Angiogenesis	[28]
PUP-SENPs	Hepatocellular carcinoma, colorectal, cervix and especially breast adenocarcinoma		↑ ROS stress, PARP cleavage, Bax, caspase-3,8,9	Cellular dysfunctions, intrinsic and extrinsic apoptosis	[144]
Lentinan-SeNPs	Malignant ascites	Caveolae-mediated, mediated by TLR4 and caveolin 1	↑ ROS and mitochondria dysfunction ↑ caspase-3 ↓ ATP levels and inflammatory cytokines	In vitro: cell apoptosis In vivo: ↓ body weight, ascites volume and derived hemorrhage	[227]
PTR-SeNP/EGFP-LC3 plasmid	Colorectal cancer	Caveolae and clathrin-mediated	↑ Bax and Bak, ↓ cyclin D1 and 3, CDK 2/4/6 ↑ Beclin 1	Apoptosis and cell cycle arrest at G2/M phase Autophagy	[141]

(Continued)



**Table 5.** (Continued).

Functionalization	Cancer cell type	Endocytosis mechanism	Biochemical mechanism	Effects	Refs.
FA-SeNPs	Breast cancer	Folate receptor-mediated	↑ ROS production, Ca <sup>2+</sup> intracellular concentration and mitochondria dysfunction, ↑ caspases-3/9 activity Dysfunction of DNA synthesis and chromatin condensation F-actin structure interference	Changes in cell morphology, Apoptosis and cell cycle arrest at S phase	[29,30]
IONP			Initial studies: Se:IONPs shown antiproliferative activity against breast cancer cells, reducing their viability to 40.5% in Se:IONPs concentration of 1 μg mL <sup>-1</sup> . However, these results point to the use of SeNPs functionalized with IONPs to magnetically target cancer cells		[232]
TPP	Cervical cancer	–	↑ ROS stress, mitochondria dysfunction	Apoptosis	[233]
1,6-α-D-glucan stabilized SeNPs		–	↑ ROS production and mitochondria dysfunction ↑ caspase-3	Apoptosis and cell cycle arrest at S phase	[148]

Beclin 1 connection to Bcl-2, promoting the activation of Bax and Bak.<sup>[141]</sup> SeNPs stabilized with laminarin, the active substance from the *Laminaria digitata*, also showed antiproliferative properties against HepG2 cells (IC<sub>50</sub> value of 23.4 ± 2.7 × 10<sup>-6</sup> M) though increased expression of Bax and cleavage of caspase-9, and decrease of Bcl-2, thereby inducing the mitochondria intrinsic apoptosis pathway. Moreover, treatment with laminarin-SeNPs enhanced the levels of LC3-II, indicating initial autophagy, while decreasing P62 and inducing lysosomes alkalinization, thereby inhibiting the late phase of autophagy and disabled the self-protection mechanism of cancer cells.<sup>[139]</sup> SeNPs stabilized with 1,6-α-D-glucan from *Castanea mollissima* also shown anticancer properties against HeLa cells (cervical cancer cell line), inducing apoptosis by mitochondria intrinsic pathway and possible cell arrest at S phase, by increasing ROS production, decreasing the mitochondrial membrane potential and activating caspase-3 activity.<sup>[148]</sup> More recently, Jin et al. studied the anticancer potential of BFP-Se against acute myeloid leukemia, using both U937, HL60, and Molm-13 cell lines. BFP-Se strongly inhibited the proliferation of all malignant cell lines, demonstrating an IC<sub>50</sub> value of 118.3 μg mL<sup>-1</sup> for U937 cells, without presenting major toxicity towards normal cells such as hematopoietic stem cells and T cells. BFP-Se mechanism of action was based on decreasing the mitochondrial membrane potential, promoting apoptosis and cell arrest at G1 phase in U937 cells and at S phase in HL60 cells. In vivo studies using B-NSG mice also demonstrated the anticancer properties of BFP-Se when administered at low dosages (0.05 mg kg<sup>-1</sup>), decreasing the number of leukemia cells, and improving mice survival rate. Also, BFP-Se increased the GSH levels, preventing oxidative stress common in relapses of leukemia patients, while decreasing the expression of c-Jun activation domain-binding protein 1 and thioredoxin 1, two proteins overexpressed in leukemia cells, with a role in tumorigenesis promotion and progression.<sup>[147]</sup> Also, Liu et al. functionalized SeNPs with lentinan, a β-glucan obtained from *Lentinus edode* used in China for treatment of malignant ascites, producing lentinan-SeNPs with the size of 53.8 nm and with antiproliferative potential towards OVCAR-3 (ovary adenocarcinoma) and EAC cells (ascites tumor). In vivo studies in mice demonstrated

that lentinan-SeNPs decreased the body weight and volume of ascites provoked by the malignant cells, reducing the associated hemorrhage. The functionalization with lentinan improves the SeNPs uptake efficiency by caveolae-mediated endocytosis, by targeting TLR4 and caveolin 1, inducing cell membrane invaginations responsible for SeNPs uptake. Afterward, it was observed that the endocytic vesicles formed by lentinan-SeNPs and TLR4/caveolin 1 enter the mitochondria by membrane fusion mediated by a protein complex composed by TLR4, TNF receptor-associated factor 3 and mitofusin-1. Lentinan-SeNPs act by enhancing ROS and decreasing the mitochondrial membrane potential, thereby inducing caspase-3 expression and reduction of ATP levels, while decreasing the expression of several inflammatory cytokines (IL-1β, IL-6, and TNF-α), which led to cell shrinkage and formation of apoptotic bodies.<sup>[227]</sup> The anticancer properties of SeNPs stabilized with another fungus polysaccharide, PUP, were also studied. PUP-SENPs successfully inhibited several cancer cell lines (HT29, HeLa, HepG2, and MDA-MB-231) proliferation in a dose-dependent manner, with no apparent toxicity towards normal cells. PUP-SENPs exhibited the highest cytotoxic properties toward MDA-MB-231 (breast cancer cell line), with an IC<sub>50</sub> of 6.27 × 10<sup>-6</sup> M. PUP-SENPs enhanced ROS stress, leading to Bax upregulation, PARP cleavage and induction of caspases 3, 8, and 9, suggesting activation of both intrinsic and extrinsic apoptosis pathways, which resulted in morphologic cellular dysfunctions, such as loss of intercellular contact and cell shrinkage, with increased early and late apoptosis.<sup>[144]</sup>

SeNPs conjugated with HA also shown in vivo antiproliferative assays against hepatocellular cancer cells. 4.32 mg kg<sup>-1</sup> HA-SeNPs show antitumor effects, while preventing the side-effects demonstrated with 5-Fu treatment, such as leukopenia and increased AST and ALT activities, by stabilizing the levels of SOD in the liver and reducing the formation of MDA.<sup>[30]</sup>

FA-SeNPs have been shown to inhibit MCF-7 breast cancer cells at an inhibitory concentration (IC<sub>50</sub>) of 2.47 μg mL<sup>-1</sup>, while presenting an IC<sub>50</sub> of 22.52 μg mL<sup>-1</sup> for normal cells. After FA-SeNPs entered the cancer cells by endocytosis mediated by the folate receptor, they were incorporated into endocytic vesicles, whose acidic environment protonated the carboxyl groups of the

folate receptor, promoting the release of FA-SeNPs from endocytic vesicles into the cytoplasm. Here, the NPs were incorporated into the mitochondria, causing its disruption via ROS production, and then were transported into the nucleus, causing interference on the DNA synthesis and chromatin condensation. Therefore, FA-SeNPs induced mitochondria-mediated apoptosis by inducing caspase-3/9 activities, increasing the intracellular  $\text{Ca}^{2+}$  concentration and therefore changing the cancer cells morphology by interfering with F-actin structure, causing cell arrest at S phase and apoptosis.<sup>[131]</sup> FA-SeNPs have also shown anticancer properties against 4T1 breast cancer cells, drastically decreasing the mortality of mice injected with this type of cancer cell, while reducing the tumor volume.<sup>[100]</sup> FA-SeNPs were also tested against hepatocellular cancer, inhibiting the expression of ABC family proteins, and thereby overcoming the multidrug resistance effect.

Liu et al. studied the use of FA-SeNPs for delivery of Ru polypyridyl (RuPOP) against multidrug resistance hepatic cancer cells (R-HepG2). FA-SeNPs@RuPO entered the cancer cells via nystatin-dependent lipid raft-mediated and clathrin-mediated pathways and decreased the expression levels of ABC family proteins, overcoming the multidrug resistance cancer, and having better an antiproliferative effect for drug-resistant HepG2 ( $\text{IC}_{50}$  of  $0.24 \pm 0.02 \times 10^{-6}$  M) than HepG2 ( $0.33 \pm 0.02 \times 10^{-6}$  M). FA-SeNPs enhanced ROS production, increasing the expression and phosphorylation at Ser 15 site of p53. Also, p-ATM, p-BRCA1 and phosphorylated histone H2A.X were also elevated, which suggested that FA-SeNPs induced apoptosis by ROS-modulated p53 phosphorylation. The levels of caspase-8/9 and PARP cleavage were also enhanced, which indicated apoptosis through extrinsic and intrinsic pathways, and cell cycle arrest at sub-G1 phase cycle. In vivo studies have also shown that FA-SeNPs had fewer liver side-effects than SeMet and selenite treatment, presenting much higher  $\text{LD}_{50}$  values ( $1000.3 \pm 52.0$  vs  $30.5 \pm 3.0$  and  $31.1 \pm 4.3$  mg Se  $\text{kg}^{-1}$ , respectively). FA-SeNPs also have less influence on ALT, AST and LDH levels and diminish liver hypertrophy and fatty degeneration.<sup>[130]</sup>

Functionalization of SeNPs with ferulic acid (Fer) was performed by Cui et al. Fer-SeNPs had an  $\text{IC}_{50}$  value of  $11.5 \pm 3.6$   $\mu\text{g mL}^{-1}$  against HepG-2 cells. Fer-SeNPs act by enhancing ROS stress and decreasing mitochondrial membrane potential, which contributed to cytochrome c release and activation of caspases-3/9, resulting in apoptosis through the intrinsic pathway. Fer-SeNPs have also shown potential to bind to DNA.<sup>[31]</sup>

Yanhua et al. demonstrated the potential of Se incorporated into hydroxyapatite (HAT) lattice, through phosphate ion exchange against hepatocellular carcinoma. HAT is the most common inorganic mineral in the hard tissues of animals and HAT-NPs demonstrated antitumor properties. Se substituted HATNPs (SeHATNPs) downregulated the expression of Ki-67, vascular endothelial growth factor (VEGF), and matrix metalloproteinase 9 (MMP-9), proteins associated with malignant behavior, vessel formation (angiogenesis), and development of metastases, respectively. SeHATNPs also caused calcium deposition in cancer cells, activating calpain protein and increasing ROS stress causing cell arrest at S-G2/M phase, inducing both necrosis and apoptosis of malignant cells. In vivo studies show that SeHATNPs not only had the capability of destroying tumor cells, but also protected the heart, liver, and kidney.<sup>[228]</sup> Wang et al. also studied the poten-

tial of SeHATNPs against bone tumor, one of the most prevalent cancers among children and adolescents. SeHATNPs enhanced ROS stress, causing mitochondria dysfunction and cytochrome c release, activating caspase-3 and intrinsic apoptosis pathway as well. Also, SeHATNPs enhanced caspase-8/9 and truncated Bid (cleaved by caspase-8), indicating that apoptosis also occurred through the extrinsic pathway. Therefore, in vivo assays show reduced tumor volume, while protecting healthy tissues and filling the bone defect generated from bone tumor removal.<sup>[229]</sup>

Other studies reveal SeNPs also inhibit tumor-associated vasculature. Since Ru have already been shown to inhibit the proliferation of endothelial cells, Sun et al. studied the antiangiogenic properties of Ru-SeNPs. Ru-SeNPs stabilized by gallic acid not only induced cancer cells and vein endothelial cells apoptosis but also inhibited the phosphorylation and activation of FGFR1 and its downstream molecules, ERK and AKT, that are correlated to tumor growth and angiogenesis. Therefore, Ru-SeNPs show synergic activity when inducing conformational changes in basic fibroblast growth factor (bFGF), a pathologic angiogenic activator, demonstrating in vitro inhibitory activity against tube formation of endothelial cells and inhibiting their migration.<sup>[230]</sup> Another study showed that the introduction of Se into Ru complexes (Se-Ru) may be a potential tool for cancer theragnosis since Ru is a luminescent metal. Ru conjugates containing Se shown to protonate under tumor acid environment and turns into its activated product. Activated Ru-Se induced ROS and mitochondrial dysfunction, leading to Bax upregulation, Bcl-2 downregulation, and increase of cytoplasmic  $\text{Ca}^{2+}$  from endoplasmic reticulum (ER), initiating the intrinsic apoptosis pathway and cell arrest at Sub-G1 phase and DNA fragmentation. Also, RuSe exhibited florescent signals in vivo, making the visualization of Ru-Se complexes biodistribution and its use as a theragnostic agent possible.<sup>[231]</sup> Also, Sun et al. produced Ru-thiol protected SeNPs (Ru-MUA@SeNPs), with not only anticancer and antiangiogenic properties, but also with fluorescence imaging properties in vivo and ex vivo. These NPs entered into HepG2 cells (hepatocarcinoma cell line) through clathrin-mediated endocytosis, and eventually escaped the lysosomes, developing a damage in several organelles, such as the nuclear envelope, besides enhancing the production of ROS, decreasing the mitochondria membrane potential, leading to apoptosis. In vivo fluorescence studies showed that Ru-MUA@SeNPs mostly accumulate in the tumor, liver, and kidneys in the first 4 h after injection, developing an inhibitory effect toward tumor growth and the formation and motility of surrounding blood vessels, by suppressing VEGF.<sup>[104]</sup>

Hauksdóttir et al. recently studied the antitumor potential of SeNPs combined with iron oxide NPs (IONPs) that due to their magnetic properties, can specifically target tumor areas using magnets and can be also applied on magnetic resonance imaging (MRI). The most promising Se:IONPs consisted of IONPs, produced by thermal decomposition followed by a silane ligand exchange, coated with chitosan and Se, wherein Se aggregation and precipitation onto IONP's surface was promoted by the Chitosan positive charge. These Se:IONPs had a size of 5–9 nm in diameter, a  $\zeta$ -potential of 29.59 mV, and magnetic properties of 35.932 emu  $\text{g}^{-1}$ . Se:IONPs reduced the viability of breast cancer cells, however the study itself did not clarify the mechanisms behind the antitumor activity.<sup>[232]</sup>

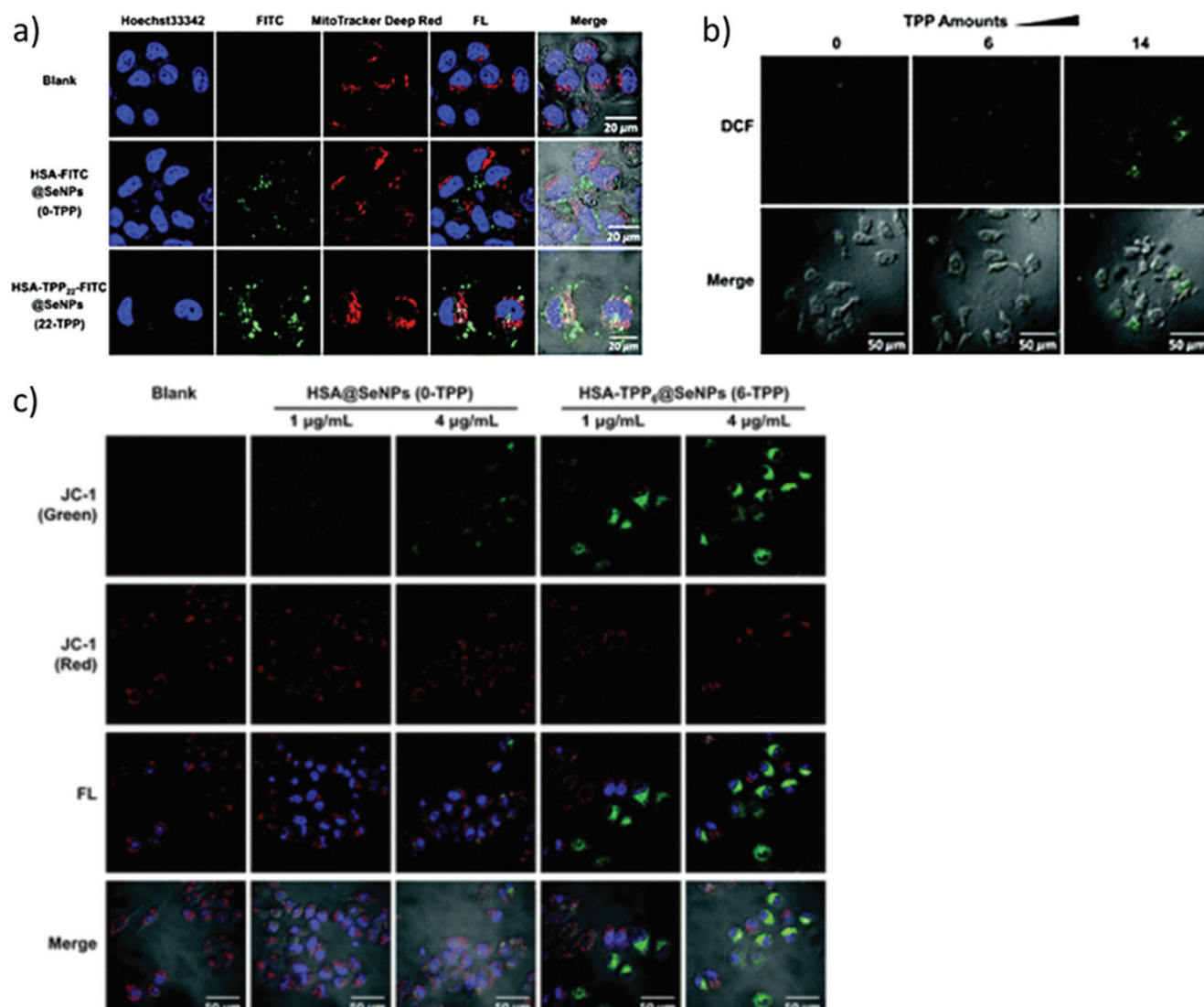


**Figure 23.** TPP-SeNPs presents antiproliferative properties against HeLa cells by increasing ROS production and inducing mitochondria dysfunction: a) HSA@SeNPs or HSA-TPP22@SeNPs labeled with fluorescein isothiocyanate isomer I (FITC) (green) were introduced to HeLa cells and the fluorescent labels MitoTracker Deep Red (red)—mitochondria—and Hoechst 33342 (blue)—nuclei were added. It was observed that, although SeNPs@FITC (green) exhibited no overlap with the mitochondria (red), incubation with TPP-SeNPs@FITC presented 34.7% colocalization signals between green (TPP-SeNPs@FITC) and red (mitochondria) channels, with the presence of a yellow color in the “combined” channel, proving that TPP increased the mitochondria-targeting ability of SeNPs. b) HeLa cells were incubated with both SeNPs and TPP-SeNPs and stained with 2',7'-dichlorofluorescein diacetate (DCFH-DA) to detect ROS. It was observed that increasing the amount of TPP groups enhanced the ROS production. c) 5,5',6,6'-tetrachloro-1,1',3,3'-tetraethylbenzimidazole carbocyanide iodide (JC-1) (green and red) probe was used to analyze the mitochondrial damage induced by SeNPs and TPP-SeNPs. It was observed that blank cells without SeNPs treatment only presented a red color, typical of healthy mitochondria. Although SeNPs presented some dose-dependent intensity of the green emission, correspondent to damaged mitochondria, treatment with TPP-SeNPs highly increased green emission and therefore could induce mitochondrial damage more effectively, with enhanced cytotoxicity effect. Reproduced with permission.<sup>[233]</sup> Copyright 2020, Royal Society of Chemistry.

More recently, Zhuang et al. functionalized SeNPs with triphenylphosphine (TPP) groups, an organic compound that specifically target mitochondria, and analyzed its antiproliferative potential against cervical carcinoma cells. TPP-SeNPs demonstrated their ability to specifically target the cancer cells mitochondria (Figure 23a), inducing ROS generation (Figure 23b) and mitochondria dysfunction (Figure 23c), having better anticancer properties than nonfunctionalized SeNPs. However, normal and cancer cells demonstrated the same cellular uptake

level, being that the in vitro SeNPs anticancer effect was explained by the overproduction of ROS and by the fact that the mitochondria transmembrane potential in cancer cells is higher than in normal cells, making them more susceptible to TPP-SeNPs cytotoxic effect. Also, Zhuang et al. argued that due to the EPR effect, TPP-SeNPs will be more prone to accumulate in tumor environments and that the SeNPs existing within healthy tissues could serve as a long-term chemopreventive supplement.<sup>[233]</sup>

SeNPs supplementation also demonstrated *in vivo* to be beneficial when conjugated with aerobic physical exercise.<sup>[234,235]</sup> SeNPs, when conjugated with physical exercise, increase T-helper 1 (Th1)-like cell production in splenocytes in mice carrying the 4T1 mammary cancer. The mechanism behind is linked to the activation of TNF- $\alpha$  and oncostatin, both anticancer cytokines, by physical exercise and the increase of interferon-gamma levels by SeNPs. Since Th cells are responsible for starting an antitumor response, the combination of SeNPs supplemented by aerobic physical exercise may be a promising approach to decrease the tumor volume.<sup>[234]</sup> Moreover, SeNPs and aerobic physical exercise demonstrated a synergic effect to reduce cachexia symptoms and muscle degeneration in 4T1 breast cancer mice, while decreasing inflammation and enhancing TNF- $\alpha$ , IL-10, and IL-15 expression, which results in immune stimulation towards cancer cells.<sup>[235]</sup>

#### 4.5.2. Combination Therapy

In addition to the functionalization of SeNPs, several other studies demonstrated that SeNPs have synergic and protective properties when loaded with already approved chemotherapeutic drugs (Table 6).<sup>[36,175]</sup> For example, Liu et al. used PEG-SeNPs for the delivery of sesamol that although it has antioxidant, anti-inflammatory, and anticancer properties, its low stability and oral bioavailability, and fast elimination limits its use. Sesamol was conjugated onto the PEG-SeNPs surface by stirring at room temperature for 48 h. Spherical PEG-SeNPs@Sesamol was shown to have antitumor activity against HepG2 cells with an  $IC_{50}$  value of  $68.7 \mu\text{g mL}^{-1}$ , six times lower than PEG-SeNPs, indicating a synergic potential between sesamol and PEG-SeNPs. PEG-SeNPs@Sesamol triggered ROS stress in cancer cells and mitochondria dysfunction, initiating the intrinsic apoptosis pathway, by activating caspases-3/9, decreasing Bcl-2 expression, and upregulating Bax and PARP, which led to chromatin condensation, DNA fragmentation, and apoptosis.<sup>[134]</sup> Mary et al. have also demonstrated the synergic anticancer properties of PEG-SeNPs carrying Crocin, a substance known by its antioxidant, anxiolytic, neuroprotective, and antitumor effects, against lung cancer. PEG-SeNPs@Crocin induced apoptosis in A549 cells, with an  $IC_{50}$  value of  $18.6 \times 10^{-6} \text{ M}$  for 24 h and  $7.9 \times 10^{-6} \text{ M}$  for 48 h, by activating the intrinsic mitochondrial apoptosis pathway, reducing the tumor volume and weight in mice without present significant side effects.<sup>[137]</sup> Also, concomitant administration of stabilized SeNPs and N-Acetyl-L-cysteine (NAC) has shown advantages in the treatment of peritoneal carcinomatosis. NAC is a ROS scavenger and a precursor for GSH biosynthesis, which can have both antioxidant properties or can boost SeNPs oxidant and anticancer properties. Therefore, although *in vivo* studies demonstrated that SeNPs had potential anticancer properties against H22 cancer cells (hepatocellular carcinoma cell line), decreasing the cancer cells proliferation and the mice body weight, with a longer survival time than cisplatin, NAC increased SeNPs-induced ROS production and, thereby, increased the SeNPs anticancer potential in both *in vitro* and *in vivo* studies. It was proposed that NAC enable intracellular GSH biosynthesis, by increasing the supply of thiols in the form of a cysteine sulfhydryl group, the main GSH component. GSH has an important role in SeNPs biotransforma-

tion and consequent ROS overproduction in cancer cells, leading to apoptosis and higher proliferation inhibition of cancer cells. Also, NAC thiol groups can also directly enhance redox cycling of SeNPs, with increased ROS production. While SeNPs administration at the dosages of 5 or 6  $\text{mg kg}^{-1}$  led to 25 or 50% survival in healthy animals, coadministration with NAC ( $250 \text{ mg kg}^{-1}$ ) enhanced the survival to 87.5 or 100%, indicating that NAC reduced SeNPs lethality as well.<sup>[236]</sup> Bidkar et al. showed that SeNPs stabilized with pluronic F-127 and loaded with paclitaxel (PTX) inhibit the growth of A549, HeLa, HT29 and MCF7 cells with  $IC_{50}$  values of  $13.8 \times 10^{-6}$ ,  $8.7 \times 10^{-6}$ ,  $4.8 \times 10^{-6}$ , and  $5.4 \times 10^{-6} \text{ M}$ , respectively, which represents an improved antitumor activity when compared with unloaded SeNPs. SeNPs@PTX induced apoptosis by two main mechanisms. The first one, related to SeNPs, consists in the production of ROS and destabilization of the mitochondrial membrane, causing a release of Cytochrome C into cytoplasm and activation of caspase-3, inducing the intrinsic apoptosis pathway. The other mechanism, associated with PTX, consists in its binding to the microtubulin  $\beta$ -subunit, causing cycle arrest at G2/M phases. However, SeNPs@PTX inhibited the proliferation of both normal and cancer cells, thereby it would need an improved functionalization to specifically target these nanoparticles toward cancer cells.<sup>[237]</sup> Further studies on PTX-SeNPs functionalized with HA (HA-SeNPs@PTX). HA-SeNPs@PTX show inhibition activity against lung cancer cells, being taken up into A549 cells through clathrin-mediated endocytosis, and triggering Sub-G1 cell arrest and apoptosis, by enhancing the intrinsic apoptosis pathway (activation of caspase-3 and cleavage of PARP). Moreover, HA-SeNPs@PTX also inhibited the migration and invasion of cancer cells. On top of that, HA-SeNPs@PTX was demonstrated to be biocompatible, not being toxic to the heart, liver, spleen, lung, and kidney of mice.<sup>[29]</sup>

Also, SeNPs loading DOX were also studied in several articles.<sup>[36]</sup> For example, HA-Se@DOX exhibits antitumor activity against cervical carcinoma cells. HA-Se@DOX targeted the cancer cells via CD44 and were internalized by clathrin-mediated endocytosis (Figure 24-I). Once inside tumor cells, HA-Se@DOX enhanced ROS stress (Figure 24-II) and caspase-3 activation, leading to the activation of pro-apoptotic proteins Bim, Bak, Bad, and Bax, and downregulating the anti-apoptotic Bcl-2 and ki67 that are linked to cancer cell growth (Figure 24-III). HA-Se@DOX was demonstrated to have better antitumor activity than SeNPs@DOX and DOX, probably due to the enhanced cellular uptake provided by HA-specific connection to CD44. *In vivo* assays also show that DOX side effects were reduced and that the body weight of mice treated with HA-Se@DOX slightly increased.<sup>[120]</sup> Xia et al. demonstrated SeNPs@DOX antitumor effects against lung cancer cells, when functionalized with the cycle peptide RGDfC. RGDfC-SeNPs@DOX were internalized into cancer cells by clathrin-mediated endocytosis, inducing cell arrest at sub-G1 phase, apoptosis and inhibiting the motility and migration of cancer cells, showing better anticancer properties than DOX alone.<sup>[152]</sup> Similar to RGDfC, RGD functionalization of SeNPs@Dox was also studied as an anticancer nanosystem. RGD bound to the integrin expressed in vein endothelial cells, thereby improving the cellular uptake of RGD-SeNPs@Dox and preventing angiogenesis. RGD-SeNPs@Dox demonstrated antiproliferative properties against breast cancer, by enhancing ROS stress. The levels of PARP cleavage increased and

**Table 6.** Mechanisms behind SeNPs antitumor activity when loaded with other approved chemotherapeutic agents.

Functionalization	Cancer cell type	Endocytosis mechanism	Biochemical mechanism	Effects	Refs.
Paclitaxel Pluronic F-127	Breast cancer	–	↑ ROS stress, mitochondria dysfunction, caspase-3 Microtubulin stabilization against depolymerization	Apoptosis and cell cycle arrest at G2/M phase	[237]
HA	Lung cancer	Clathrin-mediated	↑ Caspase-3 and PARP cleavage	Apoptosis and cell cycle arrest at sub-G1 phase	[29]
Irinotecan -	Ileocecal colorectal adenocarcinoma	–	↑ caspase-7/8/9, PARP cleavage and p53 ↓ Nrf2, Prx1	DNA fragmentation, apoptosis ↓ Cytoprotection, drug resistance	[39]
5-Fluorouracil -	Melanoma	Clathrin- and caveolae mediated	↑ ROS stress, mitochondria dysfunction, cytochrome c, caspase-3/8/9	Apoptosis and cell cycle arrest at sub-G1 phase	[37]
Cetuximab, DTSSP, Gd, PAMAM Anisomycin -	Nasopharyngeal carcinoma Hepatocarcinoma	Dynamin-related lipid raft-mediated Macropinocytosis and clathrin-mediated	Potential theragnostic agent ↑ phosphorylation of p21, p27, p53 and p73; caspase-3/8/9 ↓ CDK2 and ICBP90	[239] Apoptosis and cell cycle arrest at sub-G1 phase	[240]
Cisplatin MUN	Kidney	–	↓ ROS stress, mitochondria dysfunction, caspase-3 activity	↓ DNA fragmentation, cell cycle arrest at sub-G1 phase, apoptosis ↑ protection against cisplatin renal side effects	[241]
Cyclophosphamide -	Liver and bone	–	↓ ROS stress and lipid peroxidation ↑ SOD, CAT, and GPx	↓ Hepatotoxicity and genotoxicity	[243]
-	Ascites carcinoma	-	↑ ROS stress	Apoptosis ↓ Neovascularization and MMP-9 ↓ Tumor volume	
Oridonin GE11	Esophageal carcinoma	Dynamin-mediated and clathrin-mediated	↑ ROS stress and mitochondria dysfunction, caspases -3/9, Bax ↓ Bcl-2 ↓ PI3K/AKT and Ras-Raf-MEK-ERK pathways, EGFR, CD31, ↑ IL-2 and TNF-α	Apoptosis and cell cycle arrest at S phase F-actin and nuclei degradation ↓ Angiogenesis Immunostimulation	[150]
Doxorubicin HA	Cervical cancer	Clathrin mediated	↑ ROS stress and caspase-3 ↑ Bim, Bak, Bad and Bax, ↓ Bcl-2, Ki67	Apoptosis ↓ Side effects compared with DOX treatment	[120]
RGDFC	Lung cancer	Clathrin mediated	–	Apoptosis and cell cycle arrest at sub-G1 phase ↑ Motility and migration of cancer cells	[152]

(Continued)

**Table 6.** (Continued).

Functionalization	Cancer cell type	Endocytosis mechanism	Biochemical mechanism	Effects	Refs.
SeLPs		Clathrin-mediated and micropinocytosis	-	Apoptosis ↓ Cardiotoxicity ↑ Pharmacokinetics	[238]
RGD	Breast cancer	-	↑ ROS stress, PARP cleavage and caspase-3/8/9 ↑ Phosphorylation of ATM, ATR and p53 ↓ Cyclin A and CDK2 ↓ VEGF-VEGFR2-ERK/AKT signaling axis	DNA fragmentation, chromatin condensation, cell cycle arrest at sub-G1 and S phases, Apoptosis	[24]
GA	Hepatocellular carcinoma	Clathrin-mediated	↑ caspase-3 and pp53, Bad and Bax ↓ Bcl-xL	Apoptosis and cell cycle arrest at sub-G1 phase	[146]
FA-chitosan	Ovarian cancer (sensitive and resistant to DOX)	-	↑ Caspase-3 and PARP	Apoptosis and drug resistance reversion	[41]
HSA-MSe	Breast cancer	Micropinocytosis and clathrin-mediated	-	Apoptosis	[154]
Tf-chitosan	Breast cancer Liver cancer Melanoma	Dynamin-dependent lipid raft-mediated and clathrin-mediated	↑ ROS stress, mitochondria dysfunction, Bad, PARP, caspase-3/8/9, Bid and p53 and p38 ↓ Bcl-xl and ERK	Apoptosis and cell cycle arrest at sub-G1 phases	[119]

caspase-3/8/9 were upregulated, leading to DNA fragmentation, chromatin condensation, and apoptosis through both intrinsic and extrinsic pathways. Also, phosphorylation of the cell cycle regulators ATM, ATR, and p53 was also observed, indicating that RGD-SeNPs@Dox effectively caused DNA damage. On the other hand, cyclin A and CDK2 were downregulated, inducing cell cycle arrest at S phase, and VEGF-VEGFR2-ERK/AKT signaling axis was also inhibited, indicating a successful decrease in cell migration and angiogenesis. In vivo studies also demonstrated that this nanosystem reduced DOX cardiotoxicity and hepatotoxicity, while this prolonged its blood circulation.<sup>[24]</sup>

SeNPs@DOX functionalized with GA were also studied against hepatocellular carcinoma cells. GA is recognized by the asialoglycoprotein receptors on cancer cells, enhancing the SeNPs uptake by clathrin-associated endocytosis. After GA-SeNPs@DOX enters the lysosomes, DOX is released due to the acidic environment. GA-SeNPs@DOX escaped lysosomes to cytoplasm and acted by enhancing caspase-3 and phosphorylated p53 (pp53) activity, therefore downregulating Bcl-xL and upregulating Bad and Bax. Therefore, GA-SeNPs@DOX induced DNA fragmentation, cycle arrest at sub-G1 phase and apoptosis, while presenting insignificant side effects in the heart, liver, spleen, lung, and kidney in vivo.<sup>[146]</sup> SeNPs@Dox were also studied against ovarian cancer. SeNPs@Dox functionalized with FA and chitosan show antitumor properties against both DOX-sensitive and resistant ovarian cancer cells. FA-Chitosan-SeNPs@DOX were internalized in tumor cells by folate-receptor mediated endocytosis and induced caspase-3 and PARP activation, leading to changes in the cellular shape and adherence, which ultimately led to apoptosis. FA-chitosan-SeNPs@Dox demonstrated to have

higher IC<sub>50</sub> toward DOX-sensitive cancer cells ( $1.0 \times 10^{-6}$  M) than the resistant ones ( $0.89 \times 10^{-6}$  M), which indicates that FA-Chitosan-SeNPs@Dox could overcome the drug resistance.<sup>[41]</sup> Also, Zhao et al. show the synergic antiproliferative activity of mesoporous Se (MSe) when loaded with DOX in its framework and stabilized with human serum albumin (HSA) (HSA-MSe@DOX) against MCF-7 cells (breast cancer cell line). HSA interacted with SPARC, a protein overexpressed in several types of cancer, and enabled the entry of HSA-MSe@DOX into cancer cells via micropinocytosis and clathrin-mediated endocytosis, and, after escaped the lysosome, was partly found in the nucleus, causing cancer cells apoptosis. HSA-MSe@DOX presented lower IC<sub>50</sub> values ( $2.1 \pm 0.3 \times 10^{-6}$  M) than MSe ( $14.8 \pm 0.2 \times 10^{-6}$  M), HSA-MSe ( $9.9 \pm 0.3 \times 10^{-6}$  M), DOX ( $5.9 \pm 0.4 \times 10^{-6}$  M) and MSe@DOX ( $4.6 \pm 0.2 \times 10^{-6}$  M), which suggested a probable antitumor synergic activity. Also, in vivo imaging using tumor-bearing mouse demonstrated that HSA-MSe@DOX presented the highest DOX fluorescence in tumor sites and the lowest DOX accumulation in the liver and kidneys, compared to free DOX and MSe@DOX, probably due to the HSA targeting effect, demonstrating also the highest reducing effect in tumor weight.<sup>[154]</sup>

Functionalization of SeNPs@DOX with chitosan and Tf were also studied. Since Tf receptors are mainly overexpressed in cancer cells, Tf-chitosan-SeNPs@DOX shows higher antiproliferative assays toward the cancer cells studied (A375, HepG2, and MCF-7) than endothelial cells. Tf-chitosan-SeNPs@DOX uptake was performed by both dynamin-dependent lipid raft-mediated and clathrin-mediated endocytosis. When inside the lysosome, the acid environment protonated the amino groups of the chitosan, leading to its dissolution and DOX release.

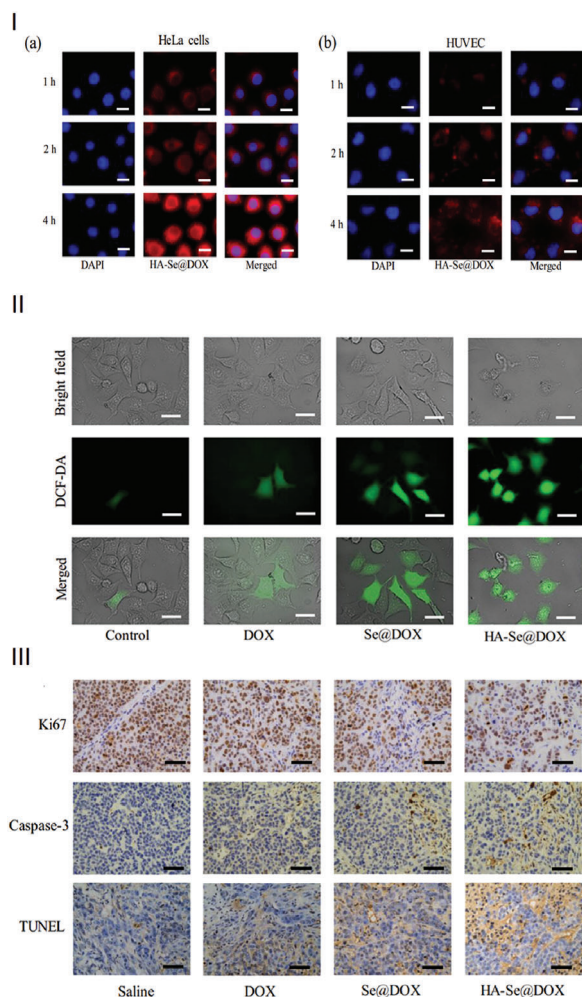


**Figure 24.** Antiproliferative properties of HA-Se@DOX: (I) Using fluorescence microscopy, it was possible to observe that HA-Se@DOX uptake was highly increased in a) HeLa cells compared to b) HUVEC, probably due to the CD44-mediated specific targeting performed by HA. (II) Using DCFH-DA staining, it is possible to observe that HA-Se@DOX incubation induced the highest ROS production in HeLa cells when compared to Se@DOX and DOX. (III) Immunohistochemistry studies indicate that HA-Se@DOX were the most effective in diminishing Ki67-positive cancer cells, while enhancing caspase-3 activity, compared to Se@DOX and DOX, thereby demonstrating greater antitumor properties compared with DOX or Se@DOX. Reproduced with permission.<sup>[120]</sup> Copyright 2020, Elsevier.

Tf-chitosan-SeNPs synergistically enhanced ROS stress, thus causing mitochondria dysfunction and activation of apoptosis-induced proteins such as Bad, PARP, caspase-3/8/9, Bid, p53 and p38 and downregulating the expression of Bcl-xl and ERK, without affecting the expression of Bax and Bcl-2, suggesting that apoptosis occurred via both extrinsic and intrinsic pathways, by activation of p53 and MAPK pathways, causing cell arrest at sub-G1 phases.<sup>[119]</sup> Another study concerning the antitumor activity of Se-functionalized liposomes (LPs) for DOX delivery (SeLPs@DOX) into tumor cells, showed that this delivery strategy had synergic activity towards lung adenocarcinoma cells, with an  $IC_{50}$  value of  $0.92 \pm 0.16 \mu\text{g mL}^{-1}$ . SeLPs@DOX entered into the cells via clathrin-mediated endocytosis and micropinocytosis

and induced apoptosis. SeLPs@DOX were shown to reduce the DOX cardiotoxicity and to improve its pharmacokinetics properties *in vivo*.<sup>[238]</sup>

Gao et al. studied SeNPs antitumor potential when loaded with irinotecan against HCT-8 cells (ileocecal colorectal adenocarcinoma). These two compounds show synergic antitumor activities, activating caspase-7/8/9 and their substrate PARP and upregulating p53, resulting in DNA fragmentation and apoptosis. Also, their conjugation reduced irinotecan toxicity, including weight loss, hepatic damage, neutropenia, anemia, and thrombocytopenia, while reducing the tumor growth in mice, due to Se protective properties. Se inactivated Nrf2 and downregulated Prx1 in tumor tissues while enhancing their expression in normal cells. Since activated Nrf2 translocates into the nucleus and activates the expression of cytoprotective phase II detoxifying enzymes and antioxidants, and Prx1 is linked to resistance to several chemotherapeutic drugs, Se not only protected normal cells from irinotecan toxicity, but also enhanced its activity towards tumor cells.<sup>[39]</sup>

The synergism between 5-Fu and SeNPs was studied against melanoma. 5-Fu capped SeNPs through Se–O and Se–N bonds and physical adsorption, which stabilized SeNPs, and prevented their aggregation and precipitation. 5-Fu also increased cellular uptake of SeNPs by A375 (melanoma) cells, via both clathrin and caveolae-mediated pathways. Once inside the cells, 5-Fu-SeNPs escaped the lysosomes and were released into the cytoplasm, inducing mitochondria dysfunction via ROS stress, cytochrome c release and, therefore, activation of caspase-3/8/9, leading to DNA fragmentation and nuclear condensation, cell arrest at sub-G1 and initiating both extrinsic and intrinsic apoptosis pathways. Fu-SeNPs not only inhibited A375 cell lines, but also MCF-7, HepG2, Colo201, and PC-3 cancer cells with  $IC_{50}$  values varying from  $6.2 \times 10^{-6}$  to  $14.4 \times 10^{-6}$  M.<sup>[37]</sup> A further study indicated that 5Fu-SeNPs had higher cytotoxic effects against MCF7 (hormone-dependent breast cancer cell line) and Caco-2 (colon adenocarcinoma) than MDA-MB-231 (hormone-independent breast cancer cell line) and HCT 116 (colon cancer cell line) cancer cells. 5Fu-SeNPs inhibited the glucose transporters, thus decreasing the intracellular glucose. Se increased ROS levels and also influenced zinc concentration, thereby inducing apoptosis in breast and colorectal cancer cells.<sup>[102]</sup> Furthermore, SeNPs loaded with 5-Fu, and functionalized with cetuximab, to target epidermal growth factor receptor (EGFR) in cancer cells, polyamidoamine (PAMAM) and 3,3'-dithiobis (sulfosuccinimidyl propionate) (DTSSP) as intratumoral GSH response agents, and gadolinium (Gd) chelate as the MRI agent, were developed, using tween-80 as stabilizer, due to its steric properties and hydrogen bond effect. PAMAM enabled the NPs to be pH-sensitive. Gd, the magnetic contrast agent, and 5-Fu, an antitumor drug, were linked to SeNPs by electrostatic interaction, and Se–O and Se–N bonds. These nanoplatforms had a size of 71.4 nm and demonstrated stability in fetal bovine serum and Dulbecco's modified Eagle medium within 84 h. The NPs were shown to be safe, not causing any alteration in the morphology of erythrocytes, and to have powerful anticancer activity against nasopharyngeal carcinoma cells, by preventing their proliferation, migration, and invasion. The nanoplatforms produced by Huang et al. entered into the cancer cells by dynamin-related lipid raft-mediated endocytosis. Once inside the cell, the

disulfide bond in DTSSP and the PAMAM protonated under the GSH acidic environment, inducing SeNPs release, demonstrating a dual pH-sensitive activity. Also, using MRI analysis in mice intravenously administered with these Se nanoplateforms, it was possible to observe a considerable brightening phenomenon, especially in the tumor region, demonstrating their theragnostic potential, as promising contrast agents for MRI.<sup>[239]</sup>

Xia et al. demonstrated the synergic effects in loading anisomycin (Am) into SeNPs (SeNPs@Am) against hepatocarcinoma cells. SeNPs@Am uptake into cancer cells was size-correlated and occurred via macropinocytosis and clathrin-mediated endocytosis pathways. Once inside lysosomes, Am molecules were protonated and released from SeNPs. Phosphorylation of p21, p27, p53, and p73 were all elevated, which resulted in CDK2 inhibition, and ICBP90 degradation through a ubiquitination-dependent protease. Since both CDK2 and ICBP90 control cell cycle progression, their inhibition resulted in cell cycle arrest at sub-G1 phase. Also, SeNPs@Am enhanced the cleavage and activation of caspase-3/8/9, leading to apoptosis. SeNPs@Am exhibited more antitumor potential than SeNPs and Am alone, which suggests the existence of synergy between these two compounds.<sup>[240]</sup>

SeNPs demonstrated not only synergic effects, but also protective properties against chemotherapy drugs' side effects. For example, SeNPs are shown to reduce cell death caused by cisplatin in HK-2 proximal tubular cells. SeNPs were functionalized with 1-mercapto-1-undecanol (MUN), a thiol compound with antioxidant properties, producing spherical MUN-SeNPs through formation of a Se—S bond. MUN-SeNPs were shown better physical and antioxidant properties than bare SeNPs, decreasing the ROS stress caused by cisplatin treatment, decreasing mitochondria dysfunction and caspase-3 activation, which translated into less DNA damage, nucleus damage, and apoptosis of noncancer cells. The percentage of cell arrest at sub-G1 phase and cytoplasmic shrinkage decreased, which demonstrated the antagonist effect of the MUN-SeNPs against cisplatin-induced renal injury through ROS scavenging.<sup>[241]</sup> More recently, Barbanente et al. developed a nanosystem consisting of selenite-doped HANPs loaded with a cytotoxic platinum complex, which demonstrated to have an acidic-induced release of selenite. This nanocomplex has shown antiproliferative properties against both human prostate and breast cancer cells, without compromising the proliferation of bone marrow stem cells, when the Pt/Se ratio was higher than 2, while lower rate numbers demonstrated to result in high toxicity towards bone marrow stem cells. However, the adsorption of the platin complex was reduced by the amount of selenite incorporated into the HA matrix.<sup>[242]</sup>

In vivo studies also demonstrated that SeNPs were able to prevent the side effects of cyclophosphamide treatment, such as liver damage and bone marrow dysfunction. Concomitant administration of SeNPs with cyclophosphamide is shown to decrease ROS levels and lipid peroxidation in hepatocytes and bone marrow cells, which indicated that SeNPs diminished cyclophosphamide hepatotoxicity and immunotoxicity, which was verified by the diminution of ALT and AST levels and improvement of hemoglobin, white blood cells count and red cell distribution width values. SeNPs also diminished DNA fragmentation and chromosomal aberration caused by cyclophosphamide. Moreover, SeNPs enhanced the activity of SOD, CAT, and GPx,

which are involved in ROS scavenging. Interestingly, cyclophosphamide antitumor activity was enhanced when administered concomitantly with SeNPs: ROS stress and consequent apoptosis of cancer cells increased, and tumor-associated neovascularization and MMP-9 decreased. Consequently, the concomitant administration decreased the tumor volume in mice, increasing the mean survival time. Therefore, SeNPs enhanced the antitumor effect of cyclophosphamide at the same time that diminished its side effects, such as hepatotoxicity and genotoxicity.<sup>[243]</sup>

SeNPs also displayed potential for oridonin loading and targeted delivery for esophageal carcinoma, using GE11 as functionalizing agent. GE11-SeNPs@Oridonin had high positive charge, enhancing its cellular uptake into KYSE-150 cells by dynamin mediated lipid raft endocytosis and clathrin-mediated endocytosis, and, after escaping the lysosomes, this nanosystem enhanced ROS stress and decreased mitochondria membrane potential, reducing Bcl-2 expression and activating caspases-3/9 and Bax, causing F-actin and nuclei disruption, which led to cell arrest at S phase and apoptosis. GE11-SeNPs@Oridonin also downregulated PI3K/AKT and Ras-Raf-MEK-ERK pathways, decreasing EGFR levels, and reduced CD31, thereby inhibiting angiogenesis. In vivo studies in mice also showed that GE11-SeNPs@Oridonin increased cellular uptake in cancer cells and significantly reduced the tumor growth, without affecting the body weight and vital organs. The treatment with GE11-SeNPs@Oridonin also increased both IL-2 and TNF- $\alpha$  production, signaling the immune system toward the tumor cells.<sup>[150]</sup>

SeNPs have been also studied in chemoradiotherapy, showing synergic effects when used concomitantly with radiation, in order to reduce treatment cycles, cancer recurrences, and the side effects characteristic of radiation.<sup>[244–247]</sup> Recently, Tian et al. analyzed the potential of SeNPs combined with radiotherapy against lung cancer cell lines, concluding that the combined therapy resulted in increased the apoptosis of cancer cells, while preventing their migration and invasion, by inhibiting CCND1, c-myc, MMP2 and MMP9, proteins associated with cancer cell proliferation and invasion. Moreover, the expression of proapoptosis proteins, such as caspases-3/9, was enhanced.<sup>[247]</sup>

Also, PEG-SeNPs were demonstrated to potentiate lung cancer cells' sensitivity to X-rays. The combination of PEG-SeNPs with radiotherapy showed synergic effects, increasing dramatically the ROS stress and the activation of caspase-3, leading to higher apoptosis rate of cancer cells.<sup>[244]</sup> Another study demonstrated the synergic potential of concomitant application of FA-SeNPs and radioactive <sup>125</sup>I seeds. FA-SeNPs demonstrated to sensitive breast cancer cells to this radioisotope, increasing ROS generation, thereby inducing the phosphorylation of MAPK proteins, such as p-p38, p-JNK, and decreasing the expression of p-ERK. PARP phosphorylation was also upregulated, leading to cell cycle arrest at G2/M phases. Therefore, concomitant used of FA-SeNPs and <sup>125</sup>I seeds resulted in higher anticancer effects than FA@SeNPs and <sup>125</sup>I seeds used separately. In vivo assays show that this combined therapy decreased tumor growth and volume, without presenting side effects in the main organs, or changes in blood urea nitrogen, LDH, AST and albumin values.<sup>[245]</sup>

SeNPs were also studied for photothermal therapy (PTT), which uses light energy for anticancer applications and is usually used for the treatment of superficial and small tumors.<sup>[248]</sup>



SeNPs functionalized with PG-6 and RC-12, a derivative of RGD and a cell-penetrating peptide (CPP) that recognizes integrin receptor overexpressed in cancer cells. PG-6 is identified by MM2 and MM9 in the cancer microenvironment. This nanosystem was shown to produce heat and release DOX when irradiated with near infrared (NIR) light. Under NIR radiation, RC-PG-SeNPs@DOX shown morphologic changes, such as decreased size from 116 to 51.2 nm and structure collapse, which triggered the release of DOX. The temperature of RC-PG-SeNPs@DOX was mainly positively influenced by their concentration and the density of light radiated. RC-PG-SeNPs@DOX also shown to have more toxicity towards hepatic cancer cells ( $IC_{50}$  value of  $10.7 \times 10^{-6}$  M) than healthy cells ( $IC_{50}$  value of  $24.4 \times 10^{-6}$  M). RC-PG-SeNPs@DOX entered into the cancer cells by dynamin-mediated lipid raft endocytosis and clathrin-mediated endocytosis pathways and quickly overproduce ROS species, thereby causing apoptosis and inhibiting cell migration.<sup>[125]</sup> Wang et al. produced a Se-nanosystem consisting of ultrasmall Se particles@porous-silica-folic acid-copper sulfide nanocomposites loading DOX (Se@SiO<sub>2</sub>-FA-CuS/DOX) for synergic photothermal therapy and chemotherapy. This nanosystem presented a low release profile at physiologic pH while under acidic conditions, similar to the cancer environment, the release was much faster, especially under NIR laser exposure. In vitro assays demonstrated that this nanosystem, particularly when under laser irradiation, showed antiproliferative activity toward cancer cell lines, in concentrations nontoxic to endothelial cells, protecting them from DOX toxicity. Also, in vivo assays demonstrated that administration of Se@SiO<sub>2</sub>-FA-CuS/DOX and concomitant treatment with NIR induced a more remarkable anticancer activity than DOX and Se@SiO<sub>2</sub>-FA-CuS/DOX with or without NIR, being the only treatment to not only completely eliminate the tumor, but also induce mice weight gain, without side effects in major organs.<sup>[249]</sup> More recently, Chen et al. used tellurium (Te) and Se salts to produce 2D TeSe-based lateral heterojunction and study the photothermal properties of this nanosystem against hepatocellular carcinoma, using 808 nm light of the near-infrared region. After Se doping, uniform and biocompatible TeSeNPs were produced, with less toxicity compared to Te nanomaterials, while they demonstrated more stability, since Te nanowires were degraded after 2 d preparation, where TeSeNPs at a Se:Te ratio of 1:1 was stable for 1 month without degradation. This Se:Te ratio was also considered the optimal for anticancer applications, since the resultant TeSeNPs exhibited the highest accumulating efficiency and cytotoxic effect toward cancer cells, compared to the other ratios studied, without presenting any signs of toxicity in mice at the dose of 6.0 mg kg<sup>-1</sup>. Also, this TeSeNPs was found to have the highest photothermal efficiency, generating PTT of 60 °C and fully eliminating the tumor cells, while TeSeNPs produced using ratios Se:Te of 2:1 reached 50 °C, and only partially decreased the tumor, which quickly rebounded. The TeSeNPs (1:1) decreased, not only Ki67+ tumor cells, but also the neovascularization, promoting hypoxia in the tumor tissues. Therefore, Chen et al. suggested the use of these nanosystems in monotherapy or combined with radiotherapy or other chemotherapeutic agents.<sup>[248]</sup> Recently, Mohammadi et al. compared the combined therapy of phototherapy and sonotherapy with Cur-SeNPs administration for melanoma treatment. Although Cu-SeNPs reduced cell viability in a concentration-dependent manner, the

cells treated with only laser light showed a 7% cell viability reduction and the treatment with only ultrasonic waves resulted in a 23% decrease in cell viability. However, the combined treatment of 100 µg mL<sup>-1</sup> of Cur-SeNPs with laser light or ultrasound waves resulted in decreased cell viability of 33.9 and 22.9%, respectively. This increased antiproliferative effect is explained by the fact that Cur-SeNPs acted as a NIR light and ultrasound absorbing agent, and therefore the use of laser radiation increased Cur-SeNPs-induced ROS overproduction along with sonotherapy in melanoma cancer cells.<sup>[250]</sup>

Also, Zheng et al. produced a biocompatible nanocomposite constituted by Se and bismuth and a silica shell (Se@SiO<sub>2</sub>@Bi NCs), with anticancer properties, especially when in synergy with radiotherapy and photothermal therapy. Se@SiO<sub>2</sub>@Bi NCs were not only mainly accumulated at the tumor site, with pH-dependent release, but also strongly absorbed NIR light and converted it to heat, raising the temperature to 54 °C in vivo, which could effectively kill the cancer cells, while also showing optimal radiation sensitization for cancer cells, and protecting the healthy cells from X-ray's damage. Therefore, the combined therapy of Se@SiO<sub>2</sub>@Bi NCs with PTT and radiotherapy totally eliminated the cancer cells in mice after 14 d of treatment, without major side effects, while also presenting computed tomography imaging properties.<sup>[251]</sup>

Liu et al. also studied the potential of SeNPs for photothermal/photodynamic synergistic therapy. Photodynamic therapy uses photosensitizers to induce ROS overproduction and cancer cell apoptosis. Liu et al. produced a nanosystem composed by molybdenum selenide nanoparticles loaded by the photosensitizer Indocyanine green (ICG), and functionalized by the active targeting agent HA and a pH-responsive release molecule polydopamine (PDA) (MoSe<sub>2</sub>@ICG-PDA-HA). The nanosystem enhanced ICG stability and cellular uptake and, under laser irradiation, presented a better photothermal effect (around 62 °C) than both ICG and MoSe<sub>2</sub>NPs, which indicates a possible photothermal synergy between ICG and MoSe<sub>2</sub>NPs. MoSe<sub>2</sub>@ICG-PDA-HA presented anticancer properties against 4T1 mouse breast cancer cells, by enhancing ROS production by up to three times that of free ICG under laser irradiation, inducing also photocytotoxicity. In vivo assays also demonstrated that MoSe<sub>2</sub>@ICG-PDA-HA were the most effective in inhibiting 4T1 cancer cells, while presenting the least liver and kidney accumulation, when compared to MoSe<sub>2</sub>@ICG-PDA and ICG, with increased nuclear dissolution and fragmentation, and reduction of ki-67<sup>[252]</sup>

On the other hand, Xiao et al. studied the SeNPs potential for chemodynamic therapy, by synthesizing SeNP-coated in manganese carbonate-deposited iron oxide (MCDION-Se), with a pH-sensitive release and good biocompatibility. MCDION-Se displayed theranostic properties, while promoting the production of superoxide anion radicals and decreasing the ATP levels, which resulted in cancer cell apoptosis, due to the synergic activity between Se and manganese. Therefore, in vivo studies demonstrated that MCDION-Se successfully causes cancer tissue reduction and avoids drug resistance, without systemic side effects.<sup>[253]</sup>

An Se-based nanosystem that combined immunotherapy, radiotherapy, and chemotherapy approaches was also proposed by Gao et al. This nanosystem comprised a radiation-sensitive diselenide-containing polymer backbone, the tumor-targeting

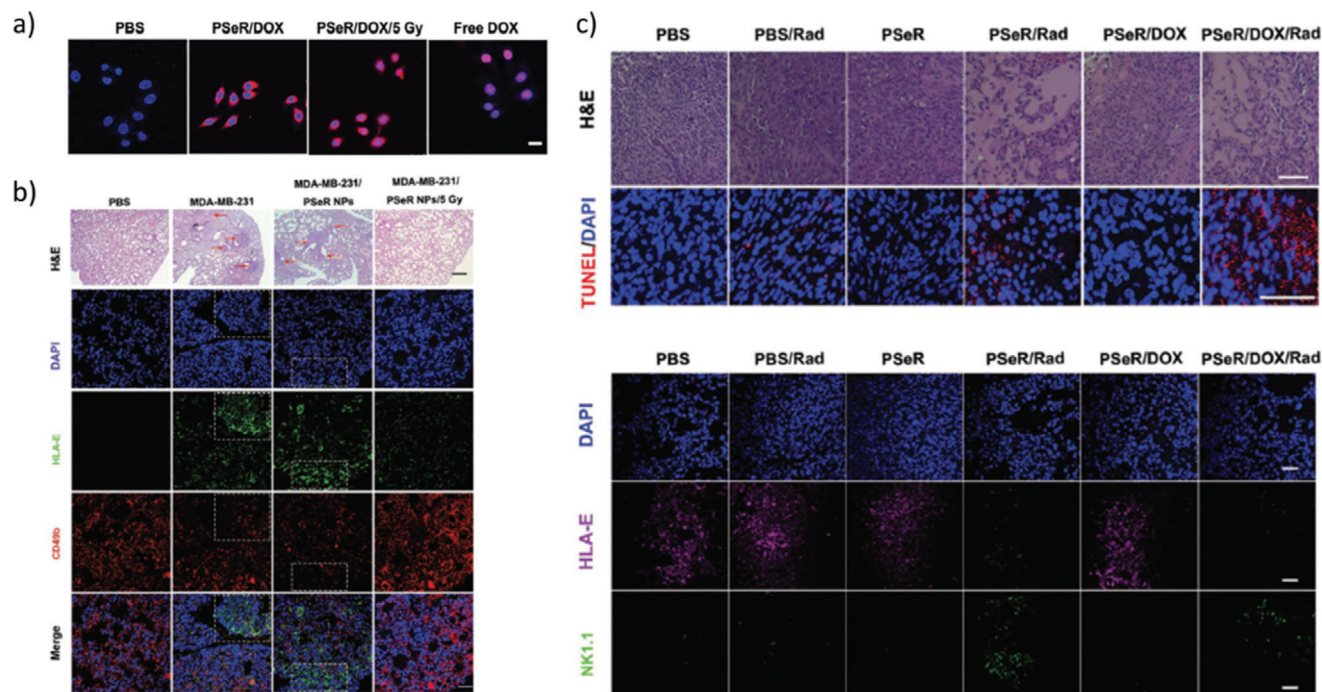


**Figure 25.** Combined therapy of PSeR/DOX and 5 Gy radiation demonstrated synergic activity towards breast cancer cell line MDA-MB-231, combining immunotherapy, radiotherapy, and chemotherapy. a) Fluorescence microscopy images demonstrated that 5 Gy radiation treatment induced a 50% DOX (red) release from PSeR/DOX NPs at 24 h, a value much higher than the nonradiation groups. Besides, although DOX released from the nanosystem was mostly accumulated in the cytoplasm, the use of radiation stimulated DOX release inside the nucleus (blue). b) Hematoxylin and eosin (H&E) and oncogene immunohistochemistry (IHC) staining demonstrate the CD49b(+) NK cell infiltration within the MDA-MB-231 lung metastasis (red arrows) in mice. Although the number of CD49b(+) NK cells was significantly decreased and an increased HLA-E expression was verified in the MDA-MB-231 lung metastasis without treatment or with PSeR treatment, combined therapy with 5 Gy radiation resulted in HLA-E downregulation and improved CD49b(+) NK cells count. c) TUNEL-DAPI assays, H&E staining and IHC staining was performed in the tumor tissues of mice, demonstrating that combined treatment of PSeR/DOX and radiation was the most effective in inducing cancer cell apoptosis, reducing HLA-E expression levels in tumor tissues and enhancing NK cells infiltration in the lung metastasis foci. Reproduced with permission.<sup>[246]</sup> Copyright 2020, Wiley-VCH GmbH.

peptide RGD modified with PEG and, as a chemotherapeutic drug, DOX (PSeR/DOX), which was also used as a therapeutic agent. A low dose of ionizing radiation (5 Gy) induced the oxidation of the diselenide bond and improved DOX release in the cancer cell nucleus (Figure 25a), with much better antiproliferative properties than 5 Gy radiation, PSeR/DOX, PSeR/5Gy, or free DOX/5Gy single treatment, suggesting the existence of synergism among the PSeR/DOX and the radiation used. Also, the combined treatment enhanced catalase levels and decreased GPx expression, with ROS overproduction. Furthermore, 5 Gy radiation and PSeR/DOX demonstrated synergic activity in suppressing human leukocyte antigen-E (HLA-E) expression in MDA-MB-231 cancer cells, thereby blocking the interaction between HLA-E and NK group 2A inhibitory checkpoint receptor and sensitizing this cancer cell line to NK cells (Figure 25b). In vivo studies also demonstrated that the combination therapy of 5 Gy radiation and PSeR/DOX ensured NK cell lung infiltration and anticancer response, with enhanced serum expression levels of Granzyme B and IFN- $\gamma$ , improved Se concentration in the tumor compared to the SeNPs average tumor concentration, and decreased DOX blood clearance, thereby decreasing MDA-MB-231 lung metastasis with much better results than radiation and PSeR/DOX single-therapies, without reducing mice weight (Figure 25c).<sup>[246]</sup>

#### 4.5.3. Delivery of Genetic Material

Small interfering RNA has been used to inhibit the expression level of the correspondent messenger RNA (mRNA), therefore downregulating the expression of tumor-related proteins,<sup>[254]</sup> being considered the best posttranscriptional gene silencing strategy so far due to its full complementarity to mRNA.<sup>[255]</sup> However, siRNA therapeutics are limited due to its negative charge and instability due to nuclease degradation, which results in incapability to reach and cross the cell membrane.<sup>[254]</sup> Recently, SeNPs have been studied as gene nanocarriers with the goal of suppressing cellular genetic transcription and inhibiting the expression of proteins associated with tumor growth, by enhancing the delivery of genetic material while decreasing its degradation (Table 7).<sup>[40,256]</sup> For example, FA-SeNPs stabilized with chitosan have shown to efficiently deliver genetic material to cancer cells, while protecting mRNA from RNase degradation.<sup>[126]</sup>

Initial studies used SeNPs conjugated with L-/D-Arg, through Se-NH bonds, and Ru (II) as a luminescent tracking vector, to load siRNA. Interestingly, while D-SeNPs demonstrated a poor capability in performing H-bonds to DNA, which resulted in low genetic material loading and delivery, Ru-L-SeNPs efficiently loaded siRNA, protecting the genetic material from

**Table 7.** Mechanisms behind SeNPs antitumor activity when loaded with siRNA.

Functionalization	siRNA	Cancer cell type	Endocytosis mechanism	Biochemical mechanism	Effects	Refs.	
Ru, L-Arg	MDR1	Lung cancer	–	↑ p53, Bax ↓ Bcl-2, MAPKs and PI3K/AKT signaling pathways ↓ P-gp	Apoptosis, DNA fragmentation and nuclear condensation Multidrug resistance inhibition	[256]	
PEI	HSP70	Hepatocellular carcinoma	–	↑ ROS stress, mitochondrial dysfunction, caspase-3, PARP cleavage and p53 ↓ AKT	DNA fragmentation and apoptosis	[254]	
HA, PEI	HES5	Hepatocellular carcinoma	Clathrin-mediated	↓ HES5 mRNA expression ↓ CD31	Apoptosis and cell cycle arrest at G0/G1 phases Angiogenesis inhibition	[121]	
RGDfC peptide	KLK12	Colorectal cancer	Clathrin-mediated ( $\alpha_v\beta_3$ integrin receptor)	↑ ROS stress, mitochondria disruption, Bak, caspase-3 and pp53	↓ KLK12 gene transcription, Ki67 cells ↓ CD31	Apoptosis and cell cycle arrest at sub-G1 cell phase ↓ Angiogenesis	[158]
	Derlin1	Cervical cancer			↓ Derlin1 gene transcription	[151]	
	MEF2	Ovarian cancer		↑ ROS stress, mitochondria disruption, ↓ MEF2 gene expression	Apoptosis and cell cycle arrest at sub-G1 cell phase In vivo Biocompatibility	[258]	

enzymatic degradation. Therefore, Ru-L-SeNPs were used to deliver a siRNA targeting the MDR1 gene, responsible for the multidrug resistance of A549R (cis-platinum resistant lung carcinoma cells). Ru-L-SeNPs@MDR1-siRNA successfully entered into cancer cells, and siRNA was released into the cytoplasm. Ru-L-SeNPs@MDR1-siRNA enhanced p53 activity, triggering apoptosis, DNA fragmentation, and nuclear condensation. Also, anti-apoptotic Bcl-2 was suppressed, while proapoptotic Bax activity was induced. Ru-L-SeNPs@MDR1-siRNA additionally inhibited MAPKs and PI3K/AKT signaling pathways. Moreover, siRNA encapsulation increased its genetic silencing efficiency, decreasing the protein levels of P-glycoprotein (P-gp), which resulted in the reversal of multidrug resistance. In vivo studies have shown that Ru-L-SeNPs@MDR1-siRNA were preferentially accumulated in cancer tissues, decreasing the tumor volume, and inhibiting the formation of blood vessels, while decreasing systemic toxicity, indicating Ru-L-SeNPs@MDR1-siRNA as a vector for siRNA delivery with synergic anticancer properties.<sup>[256]</sup>

Li et al. used PEI-SeNPs to deliver the siRNA that silence HSP70, which is overexpressed in several types of cancer, producing nanosystems that, due to their positive charge, entered easily into hepatocellular carcinoma cells. The optimal PEI-SeNPs: HSP70 siRNA ratio was 40:1, in which almost all HSP70-siRNAs were loaded, and the nanosystems produced were stable for at least 30 d. PEI-SeNPs@HSP70-siRNA escaped the lysosomes and were transported into the cytosol, inducing ROS stress and mitochondrial dysfunction, caspase-3 activity, and PARP cleavage, as well as the modulation of the AKT and p53 signaling pathways, which resulted in cytoplasmic shrinkage, loss of cellular adherence, DNA fragmentation and apoptosis, without affecting the cell cycle distribution. Moreover, the level of HSP70 mRNA expression was diminished, due to the downstream activity caused by HSP70-siRNA.<sup>[254]</sup>

PEI-SeNPs also demonstrated efficiency in loading siRNA targeting the Hairy and enhancer of split 5 (HES5), which plays a crucial role in cancer development. The HES5-siRNA was linked to PEI on SeNPs surface by electrostatic interactions and afterward PEI-SeNPs@HES5 siRNA was then functionalized with HA, which was responsible for active target its receptor CD44, overexpressed on HepG2 cells. The nanosystem produced was capable of preventing siRNA degradation from serum nucleases and entered into the cancer cells by clathrin-mediated endocytosis. HA-PEI-SeNPs@siRNA-HES5 considerably downregulated the mRNA expression of HES5 in HepG2 cells and caused cycle arrest at G0/G1 phases. Also, HA-PEI-SeNPs@siRNA-HES5 could efficiently inhibit angiogenesis, which was reflected by the decrease of CD31 levels. In vivo studies demonstrated that HA could direct the nanosystems towards tumor tissues, enhancing tumor accumulation and inhibiting its growth while preventing systemic toxicity.<sup>[121]</sup>

Also, Xia et al. functionalized SeNPs with RGDfC peptide and subsequently anionic KLK12-siRNA was loaded onto the surface of RGD-SeNPs, developing RGD-SeNPs@siRNA-KLK12. Kallikrein-related peptidase 12 (KLK12) targeting was chosen since its expression is enhanced in colorectal cancer but diminished in healthy cells, is considered a cell growth factor. Loading KLK12-siRNA onto RGDfC-SeNPs surface demonstrated to decrease its degradation and selectively deliver it to the cancer cells. RGD peptide could specifically bind to cancer cells, through  $\alpha_v\beta_3$  integrin receptor and induce clathrin-associated endocytosis of RGDfC-SeNPs@siRNA-KLK12. Once inside the cells, RGDfC-Se@siRNA-KLK12 escapes endosomes and induces ROS stress, provoking mitochondria dysfunction, and downregulate Ki67. KLK12-siRNA silence the KLK12 gene, downregulating its mRNA expression. Thus, RGDfC-SeNPs@siRNA-KLK12 induced cell arrest at sub-G1 cell phase and apoptosis. In vivo

assays demonstrate that RGDfC-SeNPs@siRNA-KLK12 also increase the proapoptotic proteins Bak, caspase-3 and pp53, reducing the tumor volume without presenting systemic toxicity in the heart, kidney, liver, lung and spleen. Besides, RGDfC-SeNPs@siRNA-KLK12 suppressed cancer cells migration, invasion, and angiogenesis, which is demonstrated by a decrease in CD31 levels.<sup>[257]</sup> Xia et al. also used RGDfC-SeNPs to deliver Derlin1 -siRNA, since Derlin1 is a protein that transports unfolded and misfolded proteins from endoplasmic reticulum lumen to cytoplasm, being overexpressed in several cancer types. Indeed, RGDfC-SeNPs@siRNA-Derlin1 shown efficiency in silence Derlin1 gene in cervical cancer cells, inhibiting their migration and invasion. RGDfC-SeNPs@siRNA-Derlin1 also generated ROS overproduction and mitochondrial dysfunction, thereby inducing apoptosis and cell cycle arrest at sub-G1. In vivo studies demonstrated that RGDfC-SeNPs@siRNA-Derlin1 were well tolerated, without signs of cytotoxicity, while inhibiting cervical cancer growth, by activating pp53, caspase-3, and Bak activities.<sup>[151]</sup>

Maiyo et al. used FA-chitosan-SeNPs to deliver Fluc-siRNA to silence luciferase gene in colorectal adenocarcinoma. Fluc-siRNA loading into the functionalized SeNPs was realized by ionic interactions, and the nanosystem produced not only was stable but also protected the Fluc-siRNA from RNAase degradation. The nanosystem entered into cancer cells by both non-specific endocytosis and folate receptor endocytosis, inducing cytotoxicity.<sup>[255]</sup>

More recently, Xia et al. studied the potential of delivering a siRNA to silence the myocyte enhancer factor 2 (MEF2), a transcription factor correlated with the occurrence and development of cancers, using RGDfC-SeNPs as a carrier. The RGDfC interacted with  $\alpha_v\beta_3$  integrin, which was overexpressed in the ovarian cancer cell line used, induced the uptake of the nanosystem by clathrin-associated endocytosis. RGDfC-SeNPs@siRNA-MEF2D silenced the expression of the MEF2D gene, while increasing the amount of cellular ROS and mitochondrial stress, inducing apoptosis with a peak at the sub-G1 phase. Further in vivo studies supported the antitumor potential of this nanosystem, while proving their biocompatibility.<sup>[258]</sup>

The loading of mRNA inside SeNPs for cancer therapy was also studied since mRNA is easily produced and does not require to be delivered inside the nucleus to function. Xia et al. study the use of SeNPs stabilized with chitosan and functionalized with FA to load and protect Fluc-mRNA, wherein FA was conjugated to chitosan through carbodiimide chemistry, resulting in nanosystems stable for two months at 4 °C. FA-Chitosan-SeNPs@RNA presented positive charge, which was essential for mRNA binding and association with the negatively charged cancer cell membranes. Also, FA-chitosan-SeNPs were able to protect mRNA from RNase A degradation activity, presenting moderate antiproliferative properties towards colorectal and colon carcinoma cells and low cytotoxicity in the human embryonic kidney, breast adenocarcinoma, and nasopharyngeal cells. Therefore, Xia et al. suggested the use of chitosan-SeNPs for tumor vaccination and immunotherapy, due their synergic activity with mRNA.<sup>[126]</sup>

## 5. Conclusion and Future Perspectives

Se is an essential element for human health, its intake depends on geographic location and the aliments consumed, although several forms of Se supplementation are currently available. In

the human body, it is used for production of selenoproteins, which usually incorporate Se in the form of selenocysteine in their active center. As a result of the selenoproteins' antioxidant, immunomodulatory and regulatory properties, Se has a crucial role in the human body, influencing the thyroid, liver, brain, and the reproduction functions, besides having antitumor and antimicrobial properties. However, since Se has a narrow therapeutic window, both deficiency and excessive Se intake can lead to severe symptoms and are correlated with several diseases.

With the objective of reducing Se toxicity and improve its therapeutic efficiency, SeNPs have been produced and study using both microorganisms, reducing agents, and physical methods, being that the biosynthesis of SeNPs offers several advantages compared to the other methods, such as the inexistence of harsh chemicals and conditions, low cost and toxicity, and the fact that SeNPs are already stabilized according to the microorganism. The SeNPs produced using other methods need to be stabilized, since bare SeNPs are usually unstable and precipitate, and can also be functionalized, according to the therapeutic application desired.

SeNPs have demonstrated excellent properties for the prevention and treatment of several diseases, such as diabetes, AD, inflammatory-related diseases, such as RA, atherosclerosis, and stroke, and antimicrobial infections. However, SeNPs are mostly studied for anticancer applications, since high Se levels are more prone to cause oxidant stress in cancer cells than in healthy ones, existing a narrow therapeutic margin for its use as for its use as a chemotherapeutic agent. SeNPs have been also functionalized with several ligands, whose receptor is preferentially expressed in cancer cells, as well as loaded with several approved chemotherapeutic drugs and genetic material, demonstrating the ability to reduce the toxicity associated with these compounds while developing a synergic activity. Overall, SeNPs enter cancer cells through clathrin-mediated endocytosis and trigger ROS overproduction and mitochondria dysfunction, thereby activating caspase-3 activity and the intrinsic apoptosis pathway. However, the anticancer mechanism of action of SeNPs also differs according to the preparation method, the targeting moieties used, and the loadings applied (**Figure 26**). Currently, the literature studies do not have the same research extension, making it difficult to compare the chemotherapeutic potential between different loadings, functionalizations, and cancer cell types. Moreover, it would be important to evaluate the properties of SeNPs prepared using the biosynthesis method, since the coating of biogenic SeNPs is specific for each microorganism.

Therefore, the main conclusions that can be taken from the literature about SeNPs are the following:

- There are several methodologies for SeNPs production, from the use of microorganisms to the use of chemical agents or physical methods, such as PLA. However, all procedures include the reduction of selenium salts into Se(0) to form SeNPs.
- Different compounds can be used for the stabilization and/or functionalization of SeNPs, conferring new therapeutic advantages toward specific diseases, such as synergic therapeutic activities or active targeting toward specific cells.
- Although SeNPs therapeutic margin is very narrow, SeNPs have better medicinal properties than selenium salts and lower toxicity.

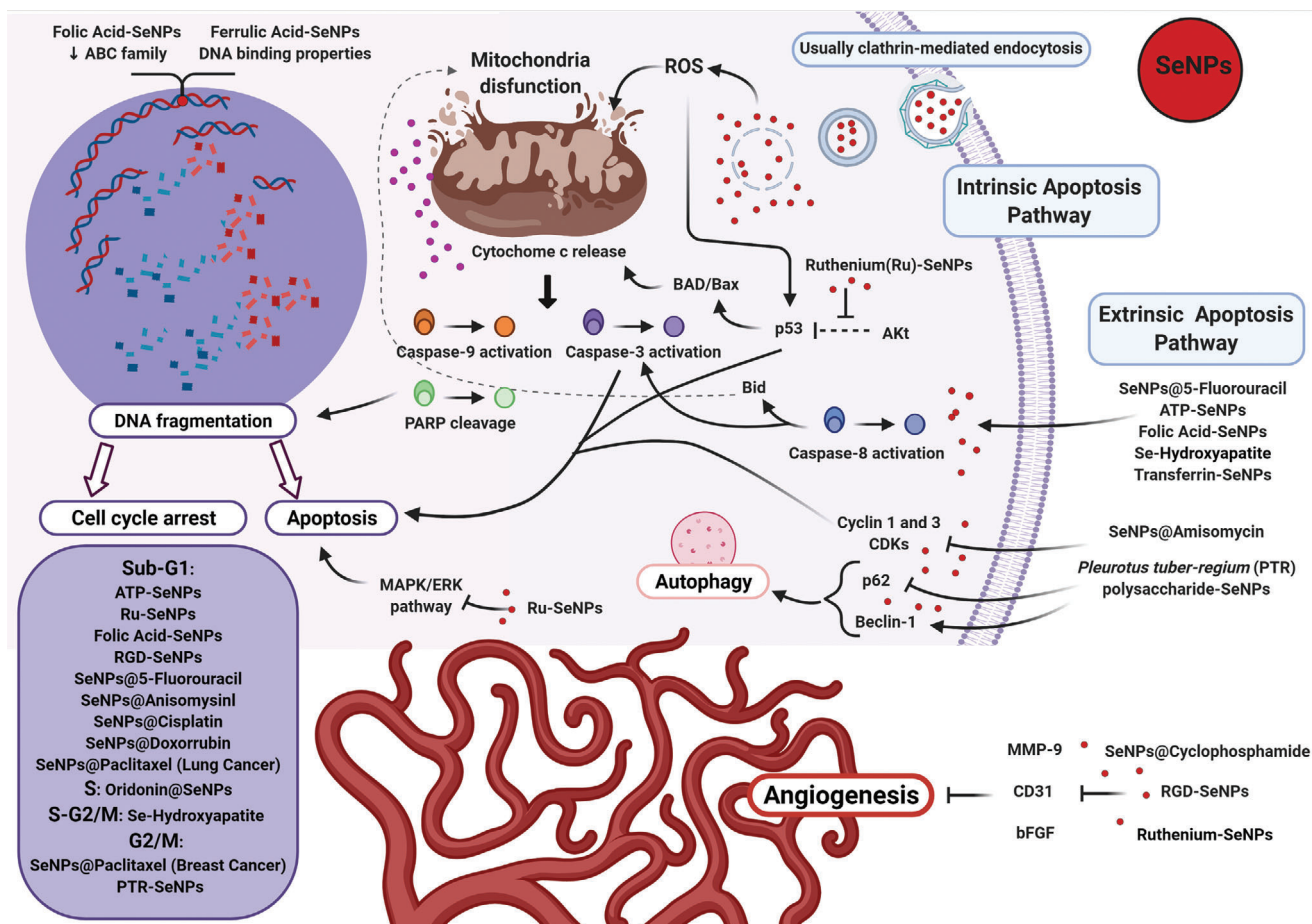


Figure 26. Antitumor mechanisms of action of SeNPs according to their coating/functionalization and loading. Figure created with Biorender.

- SeNPs potential therapeutic applications comprise AD, diabetes, inflammatory-based diseases/conditions, such as RA and liver fibrosis, bacterial, fungal and viral infections.
- The most studied SeNPs medical application is cancer therapy, due to the fact that cancer cells are more sensitive to the oxidative stress caused by high levels of Se than the normal cells.
- Also, SeNPs can be functionalized toward cancer cells, inducing ROS overproduction, mitochondria dysfunction, and caspase-3 activation and activation of the intrinsic pathway of apoptosis.
- Furthermore, SeNPs can be loaded with approved chemotherapeutic drugs, decreasing their side effects, while acting in synergy against cancer cells, with potential to induce both intrinsic and extrinsic apoptosis pathways, depending on the chemotherapeutic drug used.
- SeNPs have been also studied for the delivery of specific siRNA that inhibit the expression of proteins associated with tumor growth and invasion.
- Novel studies have also reported SeNPs potential for PTT, photodynamic and chemodynamic therapy, immunotherapy and radiotherapy synergism.

However, for their clinical translation, it is still necessary to undertake extensive studies regarding their safety, due to their narrow therapeutic window, and clarification of their synergic activities with other therapeutic compounds to gain better management and understanding of how their properties can vary according to their loading and functionalization.

## Acknowledgements

H.A.S. acknowledges the financial support from the HiLIFE Research Funds, the Sigrid Jusélius Foundation, and the Academy of Finland (Grant no. 317042). C.F. and H.F.F. are supported by Fundação para a Ciência e a Tecnologia, Ministério da Ciência, Tecnologia e Ensino Superior (FCT-MCTES) (PhD grant no. SFRH/BD/144851/2019, project grants no. UIDB/04138/2020 and UIDP/04138/2020). H.F. thanks the generous financial support from “La Caixa” Foundation under the framework of the Healthcare Research call 2019 (HR18-00589; NanoPanther). The authors thank Troy Faithfull for proof-reading the text.

## Conflict of interest

The authors declare no conflict of interest.

## Keywords

biomedicine, cancer, reactive oxidative species, selenium nanoparticles

Received: March 29, 2021

Revised: May 16, 2021

Published online:

- [1] K. Brown, J. Arthur, *Public Health Nutr.* **2001**, *4*, 593.
- [2] M. Kielczykowska, J. Kocot, M. Pazdzior, I. Musik, *Adv. Clin. Exp. Med.* **2018**, *27*, 245.
- [3] S. Hariharan, S. Dharmaraj, *Inflammopharmacology* **2020**, *28*, 667.
- [4] R. F. Burk, K. E. Hill, *Annu. Rev. Nutr.* **2015**, *35*, 109.
- [5] A. P. Fernandes, V. Gandin, *Biochim. Biophys. Acta, Gen. Subj.* **2015**, *1850*, 1642.
- [6] L. A. Daniels, *Biol. Trace Elem. Res.* **1996**, *54*, 185.
- [7] M. P. Rayman, *Hormones* **2020**, *19*, 9.
- [8] R. Muecke, L. Schomburg, J. Buentzel, K. Kisters, O. Micke, *Integr. Cancer Ther.* **2010**, *9*, 136.
- [9] M. P. Rayman, *Lancet* **2000**, *356*, 233.
- [10] M. Roman, P. Jitaru, C. Barbante, *Metallomics* **2014**, *6*, 25.
- [11] M. Vinceti, T. Filippini, L. A. Wise, *Curr. Environ. Health Rep.* **2018**, *5*, 464.
- [12] M. Bodnar, M. Szczygłowska, P. Konieczka, J. Namiesnik, *Crit. Rev. Food Sci. Nutr.* **2016**, *56*, 36.
- [13] A. Khurana, S. Tekula, M. A. Saifi, P. Venkatesh, C. Godugu, *Biomed. Pharmacother.* **2019**, *111*, 802.
- [14] S. A. Wadhvani, U. U. Shedbalkar, R. Singh, B. A. Chopade, *Appl. Microbiol. Biotechnol.* **2016**, *100*, 2555.
- [15] K. Bai, B. Hong, J. He, Z. Hong, R. Tan, *Int. J. Nanomed.* **2017**, *12*, 4527.
- [16] B. Hosnedlova, M. Kepinska, S. Skalickova, F. Fernandez, B. Ruttkay-Nedecky, Q. Peng, M. Baron, M. Melcova, R. Opatrilova, J. Zidkova, G. Bjørklund, J. Sochor, R. Kizek, *Int. J. Nanomed.* **2018**, *13*, 2107.
- [17] G. Zhao, X. Wu, P. Chen, L. Zhang, C. S. Yang, J. Zhang, *Free Radicals Biol. Med.* **2018**, *126*, 55.
- [18] A. Kumar, I. Sevonkaev, D. V. Goia, *J. Colloid Interface Sci.* **2014**, *416*, 119.
- [19] P. Nonsuwan, S. Puthong, T. Palaga, N. Muangsin, *Carbohydr. Polym.* **2018**, *184*, 9.
- [20] S. Skalickova, V. Milosavljevic, K. Cihalova, P. Horky, L. Richtera, V. Adam, *Nutrition* **2017**, *33*, 83.
- [21] X. Song, Y. Chen, G. Zhao, H. Sun, H. Che, X. Leng, *Carbohydr. Polym.* **2020**, *231*, 115689.
- [22] B. Yu, Y. Zhang, W. Zheng, C. Fan, T. Chen, *Inorg. Chem.* **2012**, *51*, 8956.
- [23] Y. Feng, J. Su, Z. Zhao, W. Zheng, H. Wu, Y. Zhang, T. Chen, *Dalton Trans.* **2014**, *43*, 1854.
- [24] X. Fu, Y. Yang, X. Li, H. Lai, Y. Huang, L. He, W. Zheng, T. Chen, *Nanomedicine* **2016**, *12*, 1627.
- [25] J. Zhang, Z. Teng, Y. Yuan, Q. Z. Zeng, Z. Lou, S. H. Lee, Q. Wang, *Int. J. Biol. Macromol.* **2018**, *107*, 1406.
- [26] K. Bai, B. Hong, Z. Hong, J. Sun, C. Wang, *J. Nanobiotechnol.* **2017**, *15*, 92.
- [27] W. Chen, L. Yue, Q. Jiang, W. Xia, *IET Nanobiotechnol.* **2019**, *13*, 30.
- [28] D. Zeng, J. Zhao, K. H. Luk, S. T. Cheung, K. H. Wong, T. Chen, *J. Agric. Food Chem.* **2019**, *67*, 2865.
- [29] J. Zou, S. Su, Z. Chen, F. Liang, Y. Zeng, W. Cen, X. Zhang, Y. Xia, D. Huang, *Artif. Cells, Nanomed. Biotechnol.* **2019**, *47*, 3456.
- [30] Y. Ren, T. Zhao, G. Mao, M. Zhang, F. Li, Y. Zou, L. Yang, X. Wu, *Int. J. Biol. Macromol.* **2013**, *57*, 57.
- [31] D. Cui, C. Yan, J. Miao, X. Zhang, J. Chen, L. Sun, L. Meng, T. Liang, Q. Li, *Mater. Sci. Eng.: C* **2018**, *90*, 104.
- [32] J. Gupta, M. T. Fatima, Z. Islam, R. H. Khan, V. N. Uversky, P. Salahuddin, *Int. J. Biol. Macromol.* **2019**, *130*, 515.
- [33] S. X. Ren, B. Zhang, Y. Lin, D. S. Ma, H. Yan, *Med. Sci. Monit.* **2019**, *25*, 991.
- [34] P. Srivastava, M. Kowshik, *Enzyme Microb. Technol.* **2016**, *95*, 192.
- [35] P. Sonkusre, *Front. Oncol.* **2020**, *9*, 1541.
- [36] S. Menon, S. D. KS, R. Santhiya, S. Rajeshkumar, V. K. S., *Colloids Surf., B* **2018**, *170*, 280.
- [37] W. Liu, X. Li, Y. S. Wong, W. Zheng, Y. Zhang, W. Cao, T. Chen, *ACS Nano* **2012**, *6*, 6578.
- [38] O. M. Abd El-Moneim, A. H. Abd El-Rahim, N. A. Hafiz, *Toxicol. Rep.* **2018**, *5*, 771.
- [39] F. Gao, Q. Yuan, L. Gao, P. Cai, H. Zhu, R. Liu, Y. Wang, Y. Wei, G. Huang, J. Liang, X. Gao, *Biomaterials* **2014**, *35*, 8854.
- [40] F. Maiyo, M. Singh, *Nanomedicine* **2017**, *12*, 1075.
- [41] U. Luesakul, S. Puthong, N. Neamati, N. Muangsin, *Carbohydr. Polym.* **2018**, *181*, 841.
- [42] M. Navarro-Alarcon, C. Cabrera-Vique, *Sci. Total Environ.* **2008**, *400*, 115.
- [43] D. Constantinescu-Aruxandei, R. M. Frîncu, L. Capră, F. Oancea, *Nutrients* **2018**, *10*, 1466.
- [44] B. A. Zachara, *Adv. Clin. Chem.* **2018**, *86*, 157.
- [45] H. Steinbrenner, S. Al-Quraishy, M. A. Dkhil, F. Wunderlich, H. Sies, *Adv. Nutr.* **2015**, *6*, 73.
- [46] K. H. Winther, M. P. Rayman, S. J. Bonnema, L. Hegedüs, *Nat. Rev. Endocrinol.* **2020**, *16*, 165.
- [47] J. C. Avery, P. R. Hoffmann, *Nutrients* **2018**, *10*, 1203.
- [48] C. Liao, B. A. Carlson, R. F. Paulson, S. Prabhu, *Free Radical Biol. Med.* **2018**, *127*, 165.
- [49] L. Kuršvītienė, A. Mongirdienė, J. Bernatienė, J. Šulinskienė, I. Stanevičienė, *Antioxidants* **2020**, *9*, 80.
- [50] O. Micke, L. Schomburg, J. Buentzel, K. Kisters, R. Muecke, *Molecules* **2009**, *14*, 3975.
- [51] J. Moreda-Piñeiro, A. Moreda-Piñeiro, P. Bermejo-Barrera, *Crit. Rev. Food Sci. Nutr.* **2017**, *57*, 805.
- [52] K. Pyrzyńska, *Mikrochim. Acta* **2002**, *140*, 55.
- [53] A. Sentkowska, *Importance of Selenium in the Environment and Human Health*, IntechOpen, London **2019**.
- [54] B. Kamer, W. Wąsowicz, K. Pyziak, A. Kamer-Bartosńska, J. Gro-madzińska, R. Pasowska, *Arch. Med. Sci.* **2012**, *8*, 1083.
- [55] J. E. Spallholz, *Methods Mol. Biol.* **2019**, *1866*, 199.
- [56] H. W. Tan, H. Mo, A. T. Y. Lau, *Int. J. Mol. Sci.* **2018**, *20*, 75.
- [57] A. P. Kipp, *Hormones* **2020**, *19*, 41.
- [58] O. M. Guillin, C. Vindry, T. Ohlmann, L. Chavatte, *Nutrients* **2019**, *11*, 2101.
- [59] D. P. Ingles, J. B. Cruz Rodriguez, H. Garcia, *Curr. Cardiol. Rep.* **2020**, *22*, 22.
- [60] L. N. Kohler, J. Foote, C. P. Kelley, A. Florea, C. Shelly, H. H. S. Chow, P. Hsu, K. Batai, N. Ellis, K. Saboda, P. Lance, E. T. Jacobs, *Nutrients* **2018**, *10*, 1924.
- [61] M. Vinceti, T. Filippini, K. J. Rothman, *Eur. J. Epidemiol.* **2018**, *33*, 789.
- [62] A. Valea, C. E. Georgescu, *Hormones* **2018**, *17*, 183.
- [63] M. P. Rayman, *Proc. Nutr. Soc.* **2019**, *78*, 34.
- [64] D. Vicente-zurdo, I. Romero-sánchez, N. Rosales-conrado, M. E. León-gonzález, *Anal. Bioanal. Chem.* **2020**, *412*, 6485.
- [65] N. Solovyev, *Hormones* **2020**, *19*, 73.
- [66] N. Solovyev, E. Drobyshev, G. Bjørklund, Y. Dubrovskii, R. Lysiuk, M. P. Rayman, *Free Radical Biol. Med.* **2018**, *127*, 124.
- [67] X. Zhang, R. Liu, W. Cheng, J. Zhu, *Mech. Ageing Dev.* **2019**, *180*, 89.
- [68] J. H. Ellwanger, S. I. R. Franke, D. L. Bordin, D. Prá, J. A. P. Henriques, *An. Acad. Bras. Cienc.* **2016**, *88*, 1655.

- [69] I. H. Qazi, C. Angel, H. Yang, B. Pan, E. Zoidis, C. J. Zeng, H. Han, G. B. Zhou, *Molecules* **2018**, *23*, 3053.
- [70] I. H. Qazi, C. Angel, H. Yang, E. Zoidis, B. Pan, Z. Wu, Z. Ming, C. J. Zeng, Q. Meng, H. Han, G. Zhou, *Antioxidants* **2019**, *8*, 268.
- [71] R. F. Burk, K. E. Hill, *Biochim. Biophys. Acta, Gen. Subj.* **2009**, *1790*, 1441.
- [72] R. Asadpour, M. H. Aliyoldashi, A. Saberivand, G. Hamidian, M. Hejazi, *Andrologia* **2020**, *52*, e13824.
- [73] S. Shoeibi, P. Mozdziak, A. Golkar-Narenji, *Top. Curr. Chem.* **2017**, *375*, 88.
- [74] L. Gunti, R. S. Dass, N. K. Kalagatur, *Front. Microbiol.* **2019**, *10*, 931.
- [75] M. Ashengroph, S.-R. Hosseini, *Int. Microbiol.* **2021**, *24*, 103.
- [76] A. J. Kora, L. Rastogi, *IET Nanobiotechnol.* **2017**, *11*, 179.
- [77] A. V. Tugarova, A. A. Kamnev, *Talanta* **2017**, *174*, 539.
- [78] C. Xu, L. Qiao, L. Ma, S. Yan, Y. Guo, X. Dou, B. Zhang, A. Roman, *Front. Microbiol.* **2019**, *10*, 1632..
- [79] I. Mates, I. Antoniac, V. Laslo, S. Vicas, M. Brocks, L. Fritea, C. Milea, A. Mohan, S. Cavalu, *UPB Sci. Bull. Ser. B: Chem. Mater. Sci.* **2019**, *81*, 206.
- [80] A. Presentato, E. Piacenza, M. Anikovskiy, M. Cappelletti, D. Zannoni, R. J. Turner, *New Biotechnol.* **2018**, *41*, 1.
- [81] S. Faramarzi, Y. Anzabi, H. Jafarizadeh-Malmiri, *Arch. Microbiol.* **2020**, *20*, 1.
- [82] Y. H. Cui, L. L. Li, N. Q. Zhou, J. H. Liu, Q. Huang, H. J. Wang, J. Tian, H. Q. Yu, *Enzyme Microb. Technol.* **2016**, *95*, 185.
- [83] G. Sharma, A. R. Sharma, R. Bhavesh, J. Park, B. Ganbold, J. S. Nam, S. S. Lee, *Molecules* **2014**, *19*, 2761.
- [84] S. Li, Y. Shen, A. Xie, X. Yu, X. Zhang, L. Yang, C. Li, *Nanotechnology* **2007**, *18*, 405101.
- [85] R. Avendaño, N. Chaves, P. Fuentes, E. Sánchez, J. I. Jiménez, M. Chavarría, *Sci. Rep.* **2016**, *6*, 1.
- [86] E. Cremonini, E. Zonaro, M. Donini, S. Lampis, M. Boaretti, S. Dusi, P. Melotti, M. M. Lleo, G. Vallini, *Microb. Biotechnol.* **2016**, *9*, 758.
- [87] S. Shoeibi, M. Mashreghi, *J. Trace Elem. Med. Biol.* **2017**, *39*, 135.
- [88] N. Srivastava, M. Mukhopadhyay, *Bioprocess Biosyst. Eng.* **2015**, *38*, 1723.
- [89] S. A. Wadhvani, M. Gorain, P. Banerjee, U. U. Shedbalkar, R. Singh, G. C. Kundu, B. A. Chopade, *Int. J. Nanomed.* **2017**, *12*, 6841.
- [90] K. S. Prasad, J. V. Vaghasiya, S. S. Soni, J. Patel, R. Patel, M. Kumari, F. Jasmani, K. Selvaraj, *Appl. Biochem. Biotechnol.* **2015**, *177*, 1386.
- [91] A. V. Tugarova, P. V. Mamchenkova, V. A. Khanadeev, A. A. Kamnev, *New Biotechnol.* **2020**, *58*, 17.
- [92] H. Fernández-Llamas, L. Castro, M. L. Blázquez, E. Díaz, M. Carmona, *Sci. Rep.* **2017**, *7*, 1.
- [93] W. Zhang, Z. Chen, H. Liu, L. Zhang, P. Gao, D. Li, *Colloids Surf., B* **2011**, *88*, 196.
- [94] Y. Wang, X. Shu, Q. Zhou, T. Fan, T. Wang, X. Chen, M. Li, Y. Ma, J. Ni, J. Hou, W. Zhao, R. Li, S. Huang, L. Wu, *Int. J. Mol. Sci.* **2018**, *19*, 2799.
- [95] K. Rajkumar, S. Koganti, S. Burgula, *Int. J. Nanomed.* **2020**, *15*, 4523.
- [96] N. Qamar, P. John, A. Bhatti, *Int. J. Nanomed.* **2020**, *15*, 3497.
- [97] S. Chung, R. Zhou, T. J. Webster, *Int. J. Nanomed.* **2020**, *15*, 115.
- [98] J. F. Ramos, T. J. Webster, *Int. J. Nanomed.* **2012**, *7*, 3907.
- [99] C. Zhang, X. Zhai, G. Zhao, F. Ren, X. Leng, *Carbohydr. Polym.* **2015**, *134*, 158.
- [100] A. R. Shahverdi, F. Shahverdi, E. Faghfuri, M. Reza khoshayand, F. Mavandadnejad, M. H. Yazdi, M. Amini, *Arch. Med. Res.* **2018**, *49*, 10.
- [101] S. Kumar, M. S. Tomar, A. Acharya, *Colloids Surf., B* **2015**, *126*, 546.
- [102] A. A. Abd-Rabou, A. B. Shalby, H. H. Ahmed, *Biol. Trace Elem. Res.* **2019**, *187*, 80.
- [103] Y. Wang, P. Chen, G. Zhao, K. Sun, D. Li, X. Wan, J. Zhang, *Food Chem. Toxicol.* **2015**, *85*, 71.
- [104] D. Sun, Y. Liu, Q. Yu, X. Qin, L. Yang, Y. Zhou, L. Chen, J. Liu, *Bio-materials* **2014**, *35*, 1572.
- [105] X. Huang, X. Chen, Q. Chen, Q. Yu, D. Sun, J. Liu, *Acta Biomater.* **2016**, *30*, 397.
- [106] H. Kong, J. Yang, Y. Zhang, Y. Fang, K. Nishinari, G. O. Phillips, *Int. J. Biol. Macromol.* **2014**, *65*, 155.
- [107] S. Zeng, Y. Ke, Y. Liu, Y. Shen, L. Zhang, C. Li, A. Liu, L. Shen, X. Hu, H. Wu, W. Wu, Y. Liua, *Colloids Surf., B* **2018**, *170*, 115.
- [108] Y. Huang, Y. Fu, M. Li, D. Jiang, C. J. Kutyreff, J. W. Engle, X. Lan, T. Chen, *Angew. Chem., Int. Ed. Engl.* **2020**, *59*, 4406.
- [109] N. Ma, Y. Li, H. Xu, Z. Wang, X. Zhang, *J. Am. Chem. Soc.* **2010**, *132*, 442.
- [110] M. Panahi-Kalamuei, M. Salavati-Niasari, S. M. Hosseinpour-Mashkani, *J. Alloys Compd.* **2014**, *617*, 627.
- [111] C. Mellinas, A. Jiménez, M. D. C. Garrigós, *Molecules* **2019**, *24*, 4048.
- [112] S. Zheng, X. Li, Y. Zhang, Q. Xie, Y. S. Wong, W. Zheng, T. Chen, *Int. J. Nanomed.* **2012**, *7*, 3939.
- [113] A. I. El-Batal, F. M. Mosallam, M. M. Ghorab, A. Hanora, M. Gobara, A. Baraka, M. A. Elsayed, K. Pal, R. M. Fathy, M. A. Elkodous, G. S. El-Sayyad, *Int. J. Biol. Macromol.* **2020**, *156*, 1584.
- [114] G. S. El-Sayyad, H. S. El-Bastawisy, M. Gobara, A. I. El-Batal, *Biol. Trace Elem. Res.* **2020**, *195*, 323.
- [115] L. D. Geoffrion, T. Hesabizadeh, D. Medina-Cruz, M. Kusper, P. Taylor, A. Vernet-Crua, J. Chen, A. Ajo, T. J. Webster, G. Guisbiers, *ACS Omega* **2020**, *5*, 2660.
- [116] G. Guisbiers, Q. Wang, E. Khachatryan, L. Mimun, R. Mendoza-Cruz, T. Webster, K. Nash, *Int. J. Nanomed.* **2016**, *11*, 3731.
- [117] X. Zhang, H. Yan, L. Ma, H. Zhang, *J. Food Biochem.* **2020**, *44*, e13363.
- [118] M. F. Attia, N. Anton, J. Wallyn, Z. Omran, T. F. Vandamme, *J. Pharm. Pharmacol.* **2019**, *71*, 1185.
- [119] Y. Huang, L. He, W. Liu, C. Fan, W. Zheng, Y. S. Wong, T. Chen, *Bio-materials* **2013**, *34*, 7106.
- [120] Y. Xia, M. Xiao, M. Zhao, T. Xu, M. Guo, C. Wang, Y. Li, B. Zhu, H. Liu, *Mater. Sci. Eng., C* **2020**, *106*, 110100.
- [121] Y. Xia, M. Guo, T. T. Xu, Y. H. Li, C. B. Wang, Z. F. Lin, M. Q. Zhao, B. Zhu, *Int. J. Nanomed.* **2018**, *13*, 1539.
- [122] X. Zhai, C. Zhang, G. Zhao, S. Stoll, F. Ren, X. Leng, *J. Nanobiotechnol.* **2017**, *15*, 4.
- [123] K. Bai, B. Hong, W. Huang, J. He, *Pharmaceutics* **2020**, *12*, 43.
- [124] X. Song, Y. Chen, H. Sun, X. Liu, X. Leng, *Food Chem.* **2020**, *331*, 127378.
- [125] X. Fang, C. Li, L. Zheng, F. Yang, T. Chen, *Chem. - Asian J.* **2018**, *13*, 996.
- [126] F. Maiyo, M. Singh, *Pharmaceutics* **2019**, *12*, 164.
- [127] K. Kalishwaralal, S. Jeyabharathi, K. Sundar, S. Selvamani, M. Prasanna, A. Muthukumar, *Mater. Sci. Eng., C* **2018**, *92*, 151.
- [128] K. Bai, B. Hong, J. He, W. Huang, *Nutrients* **2020**, *12*, 857.
- [129] Y. Xia, T. Xu, M. Zhao, L. Hua, Y. Chen, C. Wang, Y. Tang, B. Zhu, *Int. J. Mol. Sci.* **2018**, *19*, 3582.
- [130] T. Liu, L. Zeng, W. Jiang, Y. Fu, W. Zheng, T. Chen, *Nanomed. Nanotechnol., Biol. Med.* **2015**, *11*, 947.
- [131] J. Pi, H. Jin, R. Liu, B. Song, Q. Wu, L. Liu, J. Jiang, F. Yang, H. Cai, J. Cai, *Appl. Microbiol. Biotechnol.* **2013**, *97*, 1051.
- [132] A. Garg, C. Singh, D. Pradhan, G. Ghosh, G. Rath, *Pharm. Dev. Technol.* **2020**, *25*, 748.
- [133] M. Stolzoff, T. J. Webster, *J. Biomed. Mater. Res., Part A* **2016**, *104*, 476.
- [134] F. Liu, H. Liu, R. Liu, C. Xiao, X. Duan, D. J. McClements, X. Liu, *J. Agric. Food Chem.* **2019**, *67*, 2991.
- [135] H. Amani, R. Habibey, F. Shokri, S. J. Hajmiresmail, O. Akhavan, A. Mashaghi, H. Pazoki-Toroudi, *Sci. Rep.* **2019**, *9*, 6044.
- [136] S. H. Jalalian, M. Ramezani, K. Abnous, S. M. Taghdisi, *Cancer Lett.* **2018**, *416*, 87.

- [137] T. A. Mary, K. Shanthy, K. Vimala, K. Soundarapandian, *RSC Adv.* **2016**, *6*, 22936.
- [138] A. Selmani, L. Ulm, K. Kasemets, I. Kurvet, I. Erceg, R. Barbir, B. Pem, P. Santini, I. D. Marion, T. Vinković, A. Krivohlavek, M. D. Sikirić, A. Kahru, I. V. Vrčec, *Chemosphere* **2020**, *250*, 126265.
- [139] D. Cui, J. Ma, T. Liang, L. Sun, L. Meng, T. Liang, Q. Li, *Int. J. Biol. Macromol.* **2019**, *137*, 829.
- [140] W. Cai, T. Hu, A. M. Bakry, Z. Zheng, Y. Xiao, Q. Huang, *Ultrason. Sonochem.* **2018**, *42*, 823.
- [141] G. Huang, Z. Liu, L. He, K. H. Luk, S. T. Cheung, K. H. Wong, T. Chen, *Biomater. Sci.* **2018**, *6*, 2508.
- [142] Y. Liu, S. Zeng, Y. Liu, W. Wu, Y. Shen, L. Zhang, C. Li, H. Chen, A. Liu, L. Shen, B. Hu, C. Wang, *Int. J. Biol. Macromol.* **2018**, *114*, 632.
- [143] Y. Xiao, Q. Huang, Z. Zheng, H. Guan, S. Liu, *Int. J. Biol. Macromol.* **2017**, *99*, 483.
- [144] X. Gao, X. Li, J. Mu, C. Ho, J. Su, Y. Zhang, X. Lin, Z. Chen, B. Li, Y. Xie, *Int. J. Biol. Macromol.* **2020**, *152*, 605.
- [145] W. Y. Qiu, Y. Y. Wang, M. Wang, J. K. Yan, *Colloids Surf., B* **2018**, *170*, 692.
- [146] Y. Xia, J. Zhong, M. Zhao, Y. Tang, N. Han, L. Hua, T. Xu, C. Wang, B. Zhu, *Drug Delivery* **2019**, *26*, 1.
- [147] Y. Jin, L. Cai, Q. Yang, Z. Luo, L. Liang, Y. Liang, B. Wu, L. Ding, D. Zhang, X. Xu, L. Zhang, F. Zhou, *Carbohydr. Polym.* **2020**, *240*, 116329.
- [148] H. Li, D. Liu, S. Li, C. Xue, *Int. J. Biol. Macromol.* **2019**, *129*, 818.
- [149] A. Nasrolahi Shirazi, R. K. Tiwari, D. Oh, B. Sullivan, A. Kumar, Y. A. Beni, K. Parang, *Mol. Pharmaceutics* **2014**, *11*, 3631.
- [150] J. Pi, J. Jiang, H. Cai, F. Yang, H. Jin, P. Yang, J. Cai, Z. W. Chen, *Drug Delivery* **2017**, *24*, 1549.
- [151] Y. Xia, G. Tang, C. Wang, J. Zhong, Y. Chen, L. Hua, Y. Li, H. Liu, B. Zhu, *Drug Delivery* **2020**, *27*, 15.
- [152] Y. Xia, Y. Chen, L. Hua, M. Zhao, T. Xu, C. Wang, Y. Li, B. Zhu, *Int. J. Nanomed.* **2018**, *13*, 6929.
- [153] K. Kalishwaralal, S. Jayabharathi, K. Sundar, A. Muthukumar, *Artif. Cells, Nanomed. Biotechnol.* **2014**, *44*, 471.
- [154] S. Zhao, Q. Yu, J. Pan, Y. Zhou, C. Cao, J. M. Ouyang, J. Liu, *Acta Biomater.* **2017**, *54*, 294.
- [155] J. Chen, Y. Wei, X. Yang, S. Ni, F. Hong, S. Ni, *Colloids Surf., B* **2020**, *190*, 110910.
- [156] S. Chaudhary, P. Chauhan, R. Kumar, K. K. Bhasin, *Sci. Total Environ.* **2018**, *643*, 1265.
- [157] P. A. Tran, N. O'Brien-Simpson, E. C. Reynolds, N. Pantarat, D. P. Biswas, A. J. O'Connor, *Nanotechnology* **2015**, *27*, 045101.
- [158] J. Pi, L. Shen, E. Yang, H. Shen, D. Huang, R. Wang, C. Hu, H. Jin, H. Cai, J. Cai, G. Zeng, Z. W. Chen, *Angew. Chem., Int. Ed.* **2020**, *59*, 3226.
- [159] G. Liao, J. Tang, D. Wang, H. Zuo, Q. Zhang, Y. Liu, H. Xiong, *World J. Surg. Oncol.* **2020**, *18*, 81.
- [160] F. K. Tareq, M. Fayzunnisa, S. Kabir, M. Nuzat, *Microb. Pathog.* **2018**, *115*, 68.
- [161] P. Srivastava, J. M. Braganca, M. Kowshik, *Biotechnol. Prog.* **2014**, *30*, 1480.
- [162] F. Jiang, W. Cai, G. Tan, *Nanoscale Res. Lett.* **2017**, *12*, 401.
- [163] H. Yin, Z. Xu, A. H. Bao, J. Bai, Y. Zheng, *Chemistry Letters*. **2005**, *34*, 122.
- [164] M. Steichen, P. Dale, *Electrochem. Commun.* **2011**, *13*, 865.
- [165] B. X. Cao, Y. Xie, S. Zhang, *Adv. Mater.* **2004**, *16*, 649.
- [166] H. Chen, D. Shin, J. Nam, K. Kwon, J. Yoo, *Mater. Res. Bull.* **2010**, *45*, 699.
- [167] D. Sun, W. Zhang, Q. Yu, X. Chen, M. Xu, Y. Zhou, J. Liu, *J. Colloid Interface Sci.* **2017**, *505*, 1001.
- [168] P. A. Tran, T. J. Webster, *Int. J. Nanomed.* **2013**, *8*, 2001.
- [169] U. Luesakul, S. Komenek, S. Puthong, N. Muangsinsin, *Carbohydr. Polym.* **2016**, *153*, 435.
- [170] S. P. W. Hageman, R. D. Van Der Weijden, J. M. Alfons, C. J. N. Buisman, *Int. J. Miner. Process* **2017**, *169*, 7.
- [171] S. Sotoodehnia-korani, A. Iranbakhsh, M. Ebadi, A. Majid, Z. O. Ardebili, *Environ. Pollut.* **2020**, *265*, 114727.
- [172] L. Rena, Z. Wua, Y. Maa, W. Jianp, H. Xiong, L. Zhoua, *J. Sci. Food Agric.* **2021**, *101*, 476.
- [173] K. Loeschner, N. Hadrup, M. Hansen, S. A. Pereira, B. Gammelgaard, L. H. Møller, A. Mortensen, H. R. Lam, E. H. Larsen, *Metalomics* **2014**, *6*, 330.
- [174] Y. He, S. Chen, Z. Liu, C. Cheng, H. Li, M. Wang, *Life Sci.* **2014**, *115*, 44.
- [175] A. Khurana, S. Tekula, M. Aslam, P. Venkatesh, C. Godugu, *Biomed. Pharmacother.* **2019**, *111*, 802.
- [176] W. Cong, R. Bai, Y. F. Li, L. Wang, C. Chen, *ACS Appl. Mater. Interfaces* **2019**, *11*, 34725.
- [177] S. A. Abdulmalek, M. Balbaa, *PLoS One* **2019**, *14*, e0220779.
- [178] O. M. El-borady, M. S. Othman, H. H. Atallah, A. E. Abdel, *Heliyon* **2020**, *6*, e04045.
- [179] N. E. Eleraky, A. Allam, S. B. Hassan, M. M. Omar, *Pharmaceutics* **2020**, *12*, 142.
- [180] S. Kirwale, V. Pooladanda, S. Thatikonda, S. Murugappan, A. Khurana, C. Godugu, *Nanomedicine* **2019**, *14*, 1991.
- [181] W. Deng, H. Wang, B. Wu, X. Zhang, *Acta Pharm. Sin. B* **2019**, *9*, 74.
- [182] L. Wang, C. Li, Q. Huang, X. Fu, *Food Funct.* **2019**, *10*, 539.
- [183] A. A.-R. Mohamed, S. I. Khater, A. H. Arisha, M. M. M. Metwally, G. Mostafa-Hedeab, E. S. El-Shetry, *Gene* **2021**, *768*, 145288.
- [184] X. Huo, Y. Zhang, X. Jin, Y. Li, L. Zhang, *J. Photochem. Photobiol., B* **2019**, *190*, 98.
- [185] L. Yang, N. Wang, G. Zheng, *Nanoscale Res. Lett.* **2018**, *13*, 303.
- [186] F. Paquin, J. Rivnay, A. Salleo, N. Stingelin, C. Silva, *J. Mater. Chem. C* **2017**, *5*, 5954.
- [187] M. Naziroğlu, S. Muhamad, L. Pecze, *Expert Rev. Clin. Pharmacol.* **2017**, *10*, 773.
- [188] L. Yang, W. Wang, J. Chen, N. Wang, G. Zheng, *J. Biomed. Mater. Res., Part A* **2018**, *106*, 3034.
- [189] F. Gao, J. Zhao, P. Liu, D. Ji, L. Zhang, M. Zhang, Y. Li, Y. Xiao, *Int. J. Biol. Macromol.* **2020**, *142*, 265.
- [190] K. Y. Lu, P. Y. Lin, E. Y. Chuang, C. M. Shih, T. M. Cheng, T. Y. Lin, H. W. Sung, F. L. Mi, *ACS Appl. Mater. Interfaces* **2017**, *9*, 5158.
- [191] M. A. El-Ghazaly, N. A. Fadel, E. R. Rashed, A. I. El-Batal, S. A. Kewanay, *Can. J. Physiol. Pharmacol.* **2017**, *95*, 101.
- [192] F. H. Ali, N. M. El-sayed, M. Dina, A. A. M. Ahmed, P. A. Hanna, Y. M. A. Moustafa, *Ecotoxicol. Environ. Saf.* **2020**, *195*, 110479.
- [193] S. Malhotra, M. N. Welling, S. B. Mantri, K. Desai, *J. Biomed. Mater. Res., Part B* **2016**, *104*, 993.
- [194] S. Zhu, C. Luo, W. Feng, Y. Li, M. Zhu, S. Sun, X. Zhang, *Int. J. Pharm.* **2020**, *578*, 119104.
- [195] L. Guo, J. Xiao, H. Liu, H. Liu, *Metalomics* **2020**, *12*, 204.
- [196] M. Luo, S. Huang, J. Zhang, L. Zhang, K. Mehmood, J. Jiang, N. Zhang, D. Zhou, *Environ. Sci. Pollut. Res.* **2019**, *26*, 21828.
- [197] R. Shahabi, A. Anissian, S. A. Javadmoosavi, F. Nasirinezhad, *Drug Chem. Toxicol.* **2021**, *44*, 92.
- [198] M. Lesnichaya, E. Karpova, B. Sukhov, *Colloids Surf., B* **2021**, *197*, 111381.
- [199] T. Huang, J. A. Holden, D. E. Heath, N. M. O'Brien-Simpson, A. J. O'Connor, *Nanoscale* **2019**, *11*, 14937.
- [200] T. Huang, S. Kumari, H. Herold, H. Bargel, T. B. Aigner, D. E. Heath, N. M. O'Brien-Simpson, A. J. O'Connor, T. Scheibel, *Int. J. Nanomed.* **2020**, *15*, 4275.
- [201] P. Sonkusre, S. Singh Cameotra, *Colloids Surf., B* **2015**, *136*, 1051.
- [202] A. Lin, Y. Liu, X. Zhu, X. Chen, J. Liu, Y. Zhou, X. Qin, J. Liu, *ACS Nano* **2019**, *13*, 13965.
- [203] M. Vahdati, T. T. Moghadam, *Sci. Rep.* **2020**, *10*, 510.



- [204] R. Golmohammadi, S. Najjar-peerayeh, T. T. Moghadam, *Sci. Rep.* **2020**, *10*, 2854.
- [205] H. Estevez, A. Palacios, D. Gil, J. Anguita, M. Vallet-regi, B. González, R. Prados-rosales, J. L. Luque-garcia, R. Prados-rosales, *Front. Microbiol.* **2020**, *11*, 800.
- [206] M. Shakibaie, N. S. Mohazab, S. A. Ayatollahi Mousavi, *Jundishapur J. Microbiol.* **2015**, *8*, e26381.
- [207] N. Parsamehr, S. Rezaie, S. Khodavaisy, S. Salari, S. Hadizadeh, M. Kord, S. A. Ayatollahi Mousavi, *Curr. Med. Mycol.* **2017**, *3*, 16.
- [208] H. H. Lara, G. Guisbiers, J. Mendoza, L. C. Mimun, B. A. Vincent, J. L. Lopez-Ribot, K. L. Nash, *Int. J. Nanomed.* **2018**, *13*, 2697.
- [209] Y. Li, Z. Lin, M. Guo, Y. Xia, M. Zhao, C. Wang, T. Xu, T. Chen, B. Zhu, *Int. J. Nanomed.* **2017**, *12*, 5733.
- [210] Y. Li, Z. Lin, M. Guo, M. Zhao, Y. Xia, C. Wang, T. Xu, B. Zhu, *Int. J. Nanomed.* **2018**, *13*, 2005.
- [211] Z. Lin, Y. Li, G. Gong, Y. Xia, C. Wang, Y. Chen, L. Hua, J. Zhong, Y. Tang, X. Liu, B. Zhu, *Int. J. Nanomed.* **2018**, *13*, 5787.
- [212] J. Zhong, Y. Xia, L. Hua, X. Liu, M. Xiao, T. Xu, B. Zhu, H. Cao, *Artif. Cells, Nanomed. Biotechnol.* **2019**, *47*, 3485.
- [213] Z. Lin, Y. Li, T. Xu, M. Guo, C. Wang, M. Zhao, H. Chen, J. Kuang, W. Li, Y. Zhang, T. Lin, Y. Chen, H. Chen, B. Zhu, *ACS Omega* **2020**, *5*, 12495.
- [214] Z. Wang, Z. Zheng, H. Hu, Q. Zhou, W. Liu, X. Li, Z. Liu, Y. Wang, Y. Ma, *Lab Chip* **2020**, *20*, 4255.
- [215] A. Keyhani, N. Ziaali, M. Shakibaie, A. T. Kareshk, S. Shojaee, M. A. Shekaari, *J. Med. Microbiol.* **2020**, *69*, 104.
- [216] X. Montané, A. Bajek, K. Roszkowski, J. M. Montornés, M. Giamberini, S. Roszkowski, O. Kowalczyk, R. Garcia-Valls, B. Tylkowski, *Molecules* **2020**, *25*, 1605.
- [217] X. Wang, K. Sun, Y. Tan, S. Wu, J. Zhang, *Free Radical Biol. Med.* **2014**, *72*, 1.
- [218] P. Sonkusre, S. S. Cameotra, *J. Nanobiotechnol.* **2017**, *15*, 43.
- [219] L. Kong, Q. Yuan, H. Zhu, Y. Li, Q. Guo, Q. Wang, X. Bi, X. Gao, *Biomaterials* **2011**, *32*, 6515.
- [220] K. K. Vekariya, J. Kaur, K. Tikoo, *Nanomed. Nanotechnol. Biol. Med.* **2012**, *8*, 1125.
- [221] P. K. Gautam, S. Kumar, M. S. Tomar, R. K. Singh, A. Acharya, S. Kumar, B. Ram, *Biochem. Biophys. Rep.* **2017**, *12*, 172.
- [222] B. Xu, Q. Zhang, X. Luo, X. Ning, J. Luo, J. Guo, Q. Liu, G. Ling, N. Zhou, *NeuroReport* **2020**, *31*, 226.
- [223] Y. Zhao, Q. Sun, X. Zhang, J. Baeyens, H. Su, *Soft Matter* **2018**, *14*, 481.
- [224] M. Korany, F. Marzook, B. Mahmoud, S. A. Ahmed, S. M. Ayoub, *Bioorg. Chem.* **2020**, *100*, 103910.
- [225] B. Toubhans, S. A. Gazze, C. Bissardon, S. Bohic, A. T. Gourlan, D. Gonzalez, L. Charlet, R. S. Conlan, L. W. Francis, *Nanomed.: Nanotechnol., Biol., Med.* **2020**, *29*, 102258.
- [226] Y. Zhang, X. Li, Z. Huang, W. Zheng, C. Fan, T. Chen, *Nanomed.: Nanotechnol., Biol. Med.* **2013**, *9*, 74.
- [227] H. Liu, Y. Qin, Z. Zhao, Y. Zhang, J. Yang, D. Zhai, *Theranostics* **2020**, *10*, 9083.
- [228] W. Yanhua, H. Hao, Y. Li, S. Zhang, *Colloids Surf., B* **2016**, *140*, 297.
- [229] Y. Wang, J. Wang, H. Hao, M. Cai, S. Wang, J. Ma, Y. Li, C. Mao, S. Zhang, *ACS Nano* **2016**, *10*, 9927.
- [230] D. Sun, Y. Liu, Q. Yu, Y. Zhou, R. Zhang, X. Chen, A. Hong, J. Liu, *Biomaterials* **2013**, *34*, 171.
- [231] Z. Zhao, P. Gao, Y. You, T. Chen, *Chem. - Eur. J.* **2018**, *24*, 3289.
- [232] H. L. Hauksdóttir, T. J. Webster, *J. Biomed. Nanotechnol.* **2018**, *14*, 510.
- [233] Y. Zhuang, L. Li, L. Feng, S. Wang, H. Su, H. Liu, H. Liu, Y. Wu, *Nanoscale* **2020**, *12*, 1389.
- [234] M. Molanouri Shamsi, S. Chekachak, S. Soudi, R. Gharakhanlou, L. B. S. Quinn, K. Ranjbar, S. Rezaei, F. J. Shirazi, B. Allahmoradi, M. H. Yazdi, M. Mahdavi, F. A. Voltarelli, *Nutrition* **2019**, *57*, 141.
- [235] M. Molanouri Shamsi, S. Chekachak, S. Soudi, L. S. Quinn, K. Ranjbar, J. Chenari, M. H. Yazdi, M. Mahdavi, *Cytokine* **2017**, *90*, 100.
- [236] G. Zhao, R. Dong, J. Teng, L. Yang, T. Liu, X. Wu, Y. He, Z. Wang, H. Pu, Y. Wang, *ACS Omega* **2020**, *12*, 20.
- [237] A. P. Bidkar, P. Sanpui, S. S. Ghosh, *Nanomedicine* **2017**, *12*, 2641.
- [238] Q. Xie, W. Deng, X. Yuan, H. Wang, Z. Ma, B. Wu, X. Zhang, *Eur. J. Pharm. Biopharm.* **2018**, *122*, 87.
- [239] J. Huang, W. Huang, Z. Zhang, X. Lin, H. Lin, L. Peng, T. Chen, *ACS Appl. Mater. Interfaces* **2019**, *11*, 11177.
- [240] Y. Xia, P. You, F. Xu, J. Liu, F. Xing, *Nanoscale Res. Lett.* **2015**, *10*, 349.
- [241] Y. Li, X. Li, Y. S. Wong, T. Chen, H. Zhang, C. Liu, W. Zheng, *Biomaterials* **2011**, *32*, 9068.
- [242] A. Barbanente, R. A. Nadar, L. D. Esposti, B. Palazzo, M. Iafisco, J. J. P. van den Beucken, S. C. G. Leeuwenburgh, N. Margiotta, *J. Mater. Chem. B* **2020**, *8*, 2792.
- [243] A. Bhattacharjee, A. Basu, J. Biswas, T. Sen, S. Bhattacharya, *Mol. Cell. Biochem.* **2017**, *424*, 13.
- [244] H. Zhang, Q. Sun, L. Tong, Y. Hao, T. Yu, *Biomed. Pharmacother.* **2018**, *107*, 1135.
- [245] Y. Yang, Q. Xie, Z. Zhao, L. He, L. Chan, Y. Liu, Y. Chen, M. Bai, T. Pan, Y. Qu, L. Ling, T. Chen, *ACS Appl. Mater. Interfaces* **2017**, *9*, 25857.
- [246] S. Gao, T. Li, Y. Guo, C. Sun, B. Xianyu, H. Xu, *Adv. Mater.* **2020**, *32*, 1907568.
- [247] J. Tian, X. Wei, W. Zhang, A. Xu, *Front. Bioeng. Biotechnol.* **2020**, *16*, 598997.
- [248] L. Liu, H. Zhang, Y. Cao, *Sci. Adv.* **2020**, *6*, eaay6825
- [249] Y. Wang, X. Liu, G. Deng, J. Sun, H. Yuan, Q. Li, Q. Wang, J. Lu, *Nanoscale* **2018**, *10*, 2866.
- [250] S. Mohammadi, E. Soratjiahromi, R. Dehdari Vais, N. Sattarahmady, *J. Biomed. Phys. Eng.* **2020**, *10*, 597.
- [251] N. Zheng, Q. Wang, C. Li, X. Wang, X. Liu, X. Wang, G. Deng, J. Wang, L. Zhao, J. Lu, *Adv. Healthcare Mater.* **2021**, *10*, 2002024.
- [252] Y. Liu, C. Wei, A. Lin, J. Pan, X. Chen, X. Zhu, Y. Gong, G. Yuan, L. Chen, J. Liu, Z. Luo, *Colloids Surf., B* **2020**, *189*, 110820.
- [253] J. Xiao, G. Zhang, R. Xu, H. Chen, H. Wang, G. Tian, B. Wang, C. Yang, G. Bai, Z. Zhang, H. Yang, K. Zhong, D. Zou, Z. Wu, *Biomaterials* **2019**, *216*, 119254.
- [254] Y. Li, Z. Lin, M. Zhao, T. Xu, C. Wang, H. Xia, H. Wang, B. Zhu, *Int. J. Nanomed.* **2016**, *11*, 3065.
- [255] F. Maiyo, M. Singh, *Biomedicines* **2020**, *8*, 76.
- [256] Q. Chen, Q. Yu, Y. Liu, D. Bhavsar, L. Yang, X. Ren, D. Sun, W. Zheng, J. Liu, L. mei Chen, *Nanomed.: Nanotechnol., Biol., Med.* **2015**, *11*, 1773.
- [257] Y. Xia, G. Tang, M. Guo, T. Xu, H. Chen, Z. Lin, Y. Li, Y. Chen, B. Zhu, H. Liu, J. Cao, *Mater. Sci. Eng., C* **2020**, *110*, 110594.
- [258] C. Wang, Y. Xia, S. Huo, D. Shou, Q. Mei, W. Tang, Y. Li, H. Liu, Y. Zhou, B. Zhu, *Int. J. Nanomed.* **2020**, *15*, 9759.



**Cláudio Ferro** graduated in pharmaceutical sciences from the Faculty of Pharmacy of University of Lisbon in 2017. Currently, as a Ph.D. student under the supervision of Prof. Helena Florindo and Prof. Hélder A. Santos. He is working in the development of selenium nanoparticles encapsulated by viral membranes as a promising anticancer therapy system.



**Helena F. Florindo** graduated in pharmaceutical sciences in 2003 (University of Lisbon) and obtained her Ph.D. degree in pharmaceutical technology in 2008 (University of Lisbon), in collaboration with the University of London. She is an associate professor with tenure and habilitation at the Faculty of Pharmacy, University of Lisbon. Since 2015, she is the head of the BioNanoSciences – Drug Delivery & Immunotherapy Research Group, at the Research Institute for Medicines, University of Lisbon. Both nanotechnology and immune-oncology fields have motivated her multidisciplinary research focused on the development of functionalized nanobiomaterials as novel technologies for immune modulation against cancer and infectious diseases.



**Hélder A. Santos** obtained his Doctor of Science in technology (chemical engineering) in 2007 from the Helsinki University of Technology. Currently, he is a full professor in pharmaceutical nanotechnology at the Faculty of Pharmacy, University of Helsinki, and Head of the Nanomedicines and Biomedical Engineering Lab. His scientific expertise lies in the development of nanoparticles/nanomedicines for biomedical applications, particularly inorganic and polymeric-based nanomaterials for simultaneous controlled drug delivery, diagnostic, and therapy for cancer, diabetes, and cardiovascular diseases.